MODELING KINETICS AND INHIBITION OF CHLOROETHENE REDUCTIVE DECHLORINATION IN MIXED CULTURE

A Thesis

Presented to the Faculty of the Graduate School

of Cornell University

In Partial Fulfillment of the Requirements for the Degree of

Master of Science

by

Qi Meng

August 2014

ABSTRACT

Chlorinated ethenes such as tetrachloroethene (PCE) and trichloloethene (TCE) are among the most prevalent contaminants in soil, sediments and groundwaters. Currently, *In-situ* bioremediation via anaerobic reductive dechlorination has become a widely used technology for groundwater contaminated with chlorinated ethenes. To better understand the reductive dechlorination remediation process and the inter-relationships among the complex microbial communities that comprise it, a comprehensive biokinetic model was recently developed at Cornell University by Gretchen Heavner, a modification of an earlier Cornell model developed by Donna Fennell. The Heavner model uses specific biomasses based on quantitative PCR-based population data, and under some conditions can accurately predict kinetics of dechlorination, fermentation of electron donors, and competition for electron donors between dechlorinators and methanogens, and generation of methane. However, the platform used to run the model — STELLA® (High Performance Systems) — is cumbersome for simulation of long time-spans, limiting the model's utility. Furthermore, the model uses an empirical, "mRNA-tuning" technique to improve data fits at high PCE-loadings, which makes the model descriptive, rather than predictive, in such cases. Additionally, electron donor fermentation is not predicted well at high electron-donor feeding rates.

The overall purpose of this thesis research was to address some of the limitations of the Heavner model. The STELLA® model was successfully converted to run in MATLAB® using Runge-Kutta 4th-order integration. The model fits at high-PCE and high electron-donor loadings were improved by utilizing the inhibitory effects of high PCE on dechlorination and methanogenesis, and by postulating additional pathways of butyrate's fermentation and acetate's hydrogenation to storage products.

Model simulations indicate that by adding 2nd-order Haldane inhibition instead of mRNA

tuning, the model revised in this thesis research predicts the dechlorination, methanogenesis and donor fermentation well over a broad range of PCE feeding rates. Moreover, when simulating donor fermentation at high-PCE-loadings, butyrate's fermentations and acetate's hydrogenation to storage products must be considered to obtain a mass balance between butyrate consumption and product formation.

BIOGRAPHICAL SKETCH

Qi Meng was born July 18, 1989 to Mei Tao and Qingzhong Meng in Laiwu, China. She grew up in the beautiful small town in the middle of Shandong Province. The polluted air and river by the smoke and wastewater from the iron works gave her the first motivation to be an environmental engineer. After graduating from 17th Middle School in 2008, she attended Tongji University, which is one of the top 3 schools for environmental engineering in China.

During her undergraduate years at Tongji University, she became involved in research projects studying the effect of hexavalent chromium on performance of membrane bioreactors. Qi received her bachelor's degree in Water Supply and Wastewater Treatment Engineering in June 2012.

In August 2012, Qi enrolled as a Master of Science student in Civil and Environmental Engineering at Cornell University under the guidance of Prof. James M. Gossett. Her research project was to develop a kinetics model of anaerobic reductive dechlorination in mixed culture.

Based on the conversations with people from environmental consulting firms, Qi is very interested in applying the knowledge and ability she has obtained in school to the real world. She is also interested in the remediation field work and hopes to learn more about *in-situ* remediation remedies. Therefore, after completing her M.S., Qi is planning to work in an environmental consulting firm in the U.S..

To my family

Qi

ACKNOWLEDGEMENTS

First and foremost, I would love to thank my thesis advisor, Professor James M. Gossett for his guidance, support, and patience in the past two years. During the difficult times of my research, his invaluable advice, as well as his encouragement and confidence in me gave me the strength to move on. His disciplined approach to research and consideration for people will be an excellent example for me to strive for in my career and in my life.

I would also like to thank my minor advisor, Professor Ruth E. Richardson, for her excellent advice and her support in my work. She helped me understand Gretchen Heavner's model and experiments thoroughly and helped me develop my background in molecular biology. Her comments were very helpful and resulted in a more understandable thesis.

I would like to thank Qiuyun Felicia Teng and Stephanie A. H. Divo for offering me the opportunity to work as a teaching assistant for a Mandarin course. Special thanks to Qiuyun for all the helpful suggestions for teaching and for always being considerate and voluntarily taking my shift when I had exams or interviews.

I'm grateful to Gretchen Heavner and Donna Fennell, on whose work my research is based. They were always glad to help me when I got questions about their work despite the long time after their graduation.

I would like to thank all of the wonderful friends I made while in Ithaca. Thanks to Hui Zhi for listening to me when I needed an ear. Thanks to people from Richardson Lab and my office mates in both CEE and Deparment of Asian Studies, for friendship and the great time we had together. Thanks to people from Scott Land Yard Group for making me feel Ithaca is my second home. Thanks to my cute students for their participation and enthusiasm in my classes and making

me less nervous in teaching.

I would like to thank my parents, for their love, encouragement, and confidence in me. They've been supportive of every decisions I've made.

Finally, I would like to thank my boyfriend, Yitian Sun, for his companion and love. He was always there to cheer me up and made my days in Ithaca more wonderful and memorable. Many thanks for the good advice and standing by me when I had hard times.

TABLE OF CONTENTS

LIST OF TABLES

LIST OF FIGURES

LIST OF ABBREVIATIONS

ADF	**aerobic dynamic feeding**
BHB^-	**β-hydroxybutyrate**
DCE	**dichloroethene**
DHC	***Dehalococcoides***
DMC195	***Dehalococcoides mccartyi* strain 195**
DNAPLs	**dense non-aqueous phase liquids**
dt	**time step**
EA	**electron acceptor**
ED	**electron donor**
ETH	**ethene**
FYE	**fermented yeast extract**
MCLs	**Maximum Contaminant Levels**
MHU	***Methanospirillum***
MS	***Methanosaeta***
O&M	**operation and maintenance**
ODEs	**ordinary differential equations**
PCE	**tetrachloroethene**
PHB	**poly-β-hydroxybutyrate**
PON	**particulate organic nitrogen**
ppb	**parts-per-billion**
RK4	**Runge-Kutta 4^{th} integration method**
TCE	**trichloloethene**

U.S. EPA	**United States Environmental Protection Agency**
VC	**chloroethene**
VFAs	**volatile fatty acids**
VSS	**volatile suspended solids**
YE	**yeast extract**

CHAPTER ONE — INTRODUCTION

1.A Context

Chlorinated ethenes have been extensively used as cleaning and degreasing solvents because they are non-flammable and chemically stable. Their frequent use, their careless handling and storage, and the lack of regulations over decades led to the chlorinated ethenes being among the most commonly detected subsurface contaminants. Owing to their toxicity and risk of cancer, chlorinated ethenes in drinking water are regulated to very low concentrations.

In-situ bioremediation via anaerobic reductive dechlorination has become a promising approach for remediating groundwaters contaminated with chlorinated ethenes. The only organisms able to convert tetrachloroethene (PCE) and/or trichloloethene (TCE) to non-toxic ethene and inorganic chloride are various species and strains of the bacterium *Dehalococcoides* (DHC). It is commonly observed in both environmental systems and in laboratory cultures that DHC grow most robustly in mixed communities containing fermenters and methanogens. In the laboratory mixed culture on which this study is based, the only DHC present is *Dehalococcoides mccartyi* strain 195, which uses chlorinated ethenes as electron acceptors, hydrogen as electron donor, and acetate as carbon source. Hydrogen and acetate are provided via dehydrogenation of butyrate by fermentative bacteria. Other important constituents of the culture are methanogens – both acetotrophic and hydrogenotrophic – which, while apparently competing with DHC, also produce important growth factors for the dechlorinators.

Several models have been developed to describe reductive dechlorination of chlorinated ethenes over a broad concentration range. Fennell and Gossett (1998) simulated both fermentation of electron donors and the competition between dechlorination and methanogenesis. Their model

incorporated real-time calculation of thermodynamic H_2 ceilings for fermentation reactions, as well as H_2 thresholds for dechlorination reactions. The Fennell & Gossett model was limited to batch-fed or semi-continuous-fed conditions and did not include competitive inhibition among the chlorinated-ethene substrates.

Many modeling studies (Yu & Semprini, 2004; Cupples et al., 2004) reported that competitive inhibition existed among chloroethenes. Yu and Semprini (2004) incorporated both competitive inhibition and self-inhibition to predict reductive dechlorination and showed that a model with both kinds of inhibition achieved improved agreement with experimental data.

Recently, a comprehensive biokinetic model was developed by Heavner et al. (2013) for the conversion of the chlorinated ethenes in mixed culture. This model was modified from that of Fennell and Gossett (1998) to include molecular biological data for individual biomass-types, continuous-fed conditions, and competitive inhibition among chloroethene substrates. To improve model fits at high-PCE-loading conditions, Heavner also incorporated "mRNA tuning" adjustment in both the models for dechlorination and acetoclastic methanogenesis. This model predicted the kinetics of dechlorination, fermentation of electron donors, competition for hydrogen between dechlorinators and methanogens, generation of methane, and biomass growth fairly well. However, the platform used to run the model — STELLA® (High Performance Systems) — is cumbersome for simulation of long time-spans, limiting the model's utility. Furthermore, the "mRNA tuning" adjustment made the model strictly empirical rather than predictive in *in-situ* application. Additionally, electron donor (butyrate) fermentation was not captured well at high electron-donor feeding rates — butyrate disappearance was not accounted-for in the appearance of expected products (acetate and methane), and acetate concentrations were far lower than expected, based upon butyrate consumption and methane production.

1.B Objectives

The purpose of this thesis research was to address some of the limitations of the Heavner model described in the preceding paragraph. Specific objectives were as follows:

1) Convert the Heavner model to run in MATLAB®, a superior software platform for simulation;
2) Eliminate the empirical mRNA-tuning adjustment in Heavner's model (2013) and seek alternative mechanistic approaches (e.g., Haldane inhibition) to model data at high PCE concentrations;
3) Improve model fits for donor fermentation at high electron-donor loadings by inclusion of pathways for alternative products of butyrate fermentation and acetate hydrogenation.

In all of the foregoing, the experimental data from Heaver et al. (2013) were used to assess the efficacies of the changes proposed herein.

CHAPTER TWO — BACKGROUND

2.A The Chlorinated Ethenes Problem

Chlorinated ethenes such as tetrachloroethene (PCE) and trichloloethene (TCE) are among the most prevalent contaminants in soil, sediments and groundwater (Lyon & Vogel, 2013). Since the 1930s, chlorinated ethenes have been extensively used in industrial, military and household applications, especially as dry-cleaning solvents and as degreasing agents (ITRC, 2005; Aggazzotti et al., 1994). Their widespread use is based on their excellent solvent capabilities, low flammability and chemical stability (Doherty, 2000; Löffler & Edwards, 2006).

Among the chlorinated ethenes, PCE and TCE are the most frequently detected compounds in groundwater (Westrick et al., 1984; Russell et al., 1992; Bradley, 2003). These compounds, along with their daughter products, dichloroethenes (DCEs) and chloroethene (vinyl chloride, VC), are all considered toxic to human health. VC and TCE are proven human carcinogens (IARC, 1995; WHO, 1999; Kielhorn et al., 2000; U.S. EPA, 2011). Due to the potential relation between chlorinated ethenes and human health problems including kidney dysfunction, neurological effects, dizziness, loss of consciousness, cancer, etc. (Moran, 2006), the United States Environmental Protection Agency (U.S. EPA) has set Maximum Contaminant Levels (MCLs) for chlorinated ethenes in drinking water at very low concentrations. MCLs in drinking water for PCE, TCE, *cis*-DCE and VC are 5 ppb, 5 ppb, 70 ppb and 2 ppb, respectively (U.S. EPA, 2004a).

Before the potential effects of chlorinated ethenes on human health and the environment were fully understood, the widespread use, lack of regulations and improper disposal practices of chlorinated ethenes for decades had resulted in ubiquitous subsurface contamination (ITRC, 2005; Löffler et al., 2013a). Therefore, practical methods were sought to remediate chlorinated ethenes from groundwater. Multiple technologies have been developed and applied. In the 1980s and early

1990s, pump-and-treat systems were widely used to extract contaminated groundwater by pumping from a well or trench and either replacing it with clean water or allowing uncontaminated groundwater from the surrounding area to flow towards the hydraulic depression created by pumping (Mackay & Cherry, 1989; U.S. EPA, 2007). Extracted groundwater is commonly treated by *ex situ* processes such as air stripping, ion exchange, or carbon adsorption (McCarty, 2010; U.S. EPA, 2007). However, it has been proved to be difficult for pump-and-treat to achieve complete remediation, especially when PCE or TCE form dense non-aqueous phase liquids (DNAPLs), which will act as continuing sources of contamination in groundwater (U.S. EPA, 2001; ITRC, 2005). Furthermore, at most sites, large volumes of groundwater must be extracted, even with very low concentrations of contaminants.

Other physical and chemical remedies, including *in situ* thermal treatment, *in situ* chemical oxidation/reduction and cosolvent/surfactant flushing, also have limited effectiveness and often have potential of high operation and maintenance (O&M) cost (Löffler et al., 2013a; U.S. EPA, 2004b).

2.B Anaerobic Microbial Degradation of Chlorinated Ethenes

Limitations associated with physical and chemical remedies have triggered development of bioremediation of chlorinated ethenes. Early attempt focused on aerobic degradation of chlorinated ethenes. In 1985, Wilson and Wilson (1985) reported that methane monooxygenases could initiate the cometabolic breakdown of TCE. However, efficiency of aerobic treatment decreases significantly with the increase of the number of chlorines. Moreover, chlorinated ethenes contamination typically exists in anaerobic subsurface environments. Therefore, anaerobic biological reductive dechlorination of chloroethenes has been considered a promising alternative for chlorinated ethenes remediation.

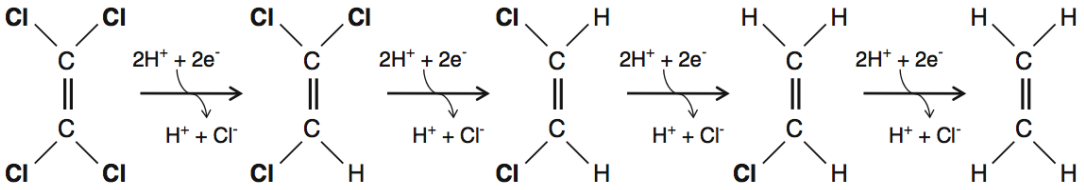

Figure 2.1 Reductive dechlorination pathway (Löffler et al., 2013a)

In anaerobic environments poly-chlorinated ethenes, such as PCE and TCE, can readily undergo reductive dechlorination reactions in which chlorine substituents are replaced by hydrogen. Figure 2.1 shows the pathway for anaerobic reductive dechlorination of PCE to ethene. PCE and TCE are reductively dechlorinated to less chlorinated ethenes (DCEs, VC, ETH) using H_2 as the electron donor – generally produced as a fermentation product of more complex donors occurring either naturally (e.g., humic substances), or as co-contaminants (e.g., petroleum constituents), or purposefully supplied to stimulate the process as part of enhanced in-situ remediation (e.g., molasses, methanol, lactate, butyrate, etc.). Reductive dechlorination of PCE and TCE was first observed in methanogenic cultures (Bouwer & McCarty, 1983; Vogel & McCarty, 1985; Fathepure et al., 1987). Unfortunately, early observations were that the process resulted in the accumulation of *cis*-DCE and VC (Gantzer & Wackett, 1991). The conversion of PCE and TCE to DCEs and VC is not useful because DCEs (like the parent compounds, PCE and TCE) pose a threat to public health and VC is a proven human carcinogen. Therefore, the complete conversion of chlorinated ethenes to benign ethenes and inorganic chloride is crucial to achieve detoxification.

In 1989, Freedman and Gossett (1989) demonstrated that anaerobic enrichment cultures were capable of reductively dechlorinating PCE to ethene, although the conversion from VC to ETH was rate-limiting. This discovery demonstrated the existence of the microbes capable of

overcoming the "DCE stall" (Löffler et al., 2013a). Further studies by DiStefano and Gossett (1991, 1992) showed that high concentrations PCE could be completely dechlorinated by anaerobic methanol-PCE enrichment cultures and hydrogen was the direct electron donor used for dechlorination. Subsequently, many organisms were isolated that were capable of reductively transforming PCE and TCE, but the conversion of PCE and TCE by these isolates stalled at *cis*-DCE (e.g. Holliger et al., 1993, 1998; Krumkolz et al., 1996; Neumann et al., 1994).

In 1997, an organism that could dechlorinate PCE to VC and ethene was successfully isolated from Freedman and Gossett's enrichment culture (Maymó-Gatell et al., 1997). This organism, *Dehalococcoides ethenogenes* strain 195 (which is now called *Dehalococcoides mccartyi* strain 195) grew with the reduction of PCE, TCE and DCE, but VC's transformation to ethene was a cometabolic process (Maymó-Gatell et al., 2001). Subsequently, some other related isolates, which were capable of growing with VC as electron acceptor, were described (He et al., 2003; Sung et al., 2006; Müller et al., 2004), and several research groups obtained *Dehalococcoides*-containing mixed cultures that dechlorinate chlorinated ethenes to ethene (e.g., Duhamel et al., 2002; Richardson et al., 2002; Vainberg et al., 2009).

2.C Mixed Community

It is commonly observed that strains of *Dehalococcoides* (DHC) grow most robustly in mixed communities containing fermenters and methanogens in both environmental systems and in laboratory cultures. Though the competition for H_2 between dechlorinators and methanogens (Fennell & Gossett, 1998) might be detrimental to the dechlorination process, the production of growth factors (e.g., vitamin B_{12}) by methanogens or other community members would promote the growth of DHC in mixed community. Furthermore, mixed cultures with the presence of oxygen-consuming microbes could provide protection for DHC against oxygen (Löffler et al.,

2013a).

Several mixed communities containing various *Dehalococcoides* strains have been studied over the years. In addition to requiring halogenated organic compounds as electron acceptors, DHC strains also require hydrogen as electron donor. Only hydrogen can be used by pure DHC cultures as an electron donor, but in mixed communities, other electron donors that could be fermented to hydrogen such as butyrate, propionate and lactate could also be used. Among these electron donors, butyrate and propionate are demonstrated to have an advantage in that their fermentation proceeds slowly and they result in less methanogenesis due to thermodynamic constraints on the ceiling of hydrogen that can be produced in their fermentation (Fennell & Gossett, 1997).

The mixed community modeled in this study is D2, maintained at Cornell University. Hydrogen is provided to *Dehalococcoides mccartyi* strain 195 (DMC195), the only DHC in this culture, by fermentation of butyrate to actetate and hydrogen. Methanogens are usually also present in *Dehalococcoides*-containing cultures or chlorinated-ethene-contaminated sites. Two kinds of methanogens in D2 are the acetoclastic methanogen *Methanosaeta* (MS) and the hydrogenotrophic methanogen *Methanospirillum* (MHU) (Rowe et al., 2008).

2.D Models of Reductive Dechlorination

Several models have been developed to describe reductive dechlorination of chlorinated ethenes and to provide better understanding of the reductive dehalogenation process. Initially, the Michaelis-Menten form of kinetics was applied to simulate the reductive dechlorination of chlorinated ethenes at low to moderate concentrations (Fennell & Gossett, 1998; Garant & Lynd, 1998; Haston and McCarty, 1999; Tandoi et al., 1994). Competitive inhibition terms then were included into the kinetics to describe the observed mutual inhibition of each step by the presence

of the other chlorinated ethenes (Tonnaer et al., 1997; Yu, 2003), as well as the competition for electron donor (H_2) between electron acceptors (Cupples et al., 2004). Yu (2003) reported that more-chlorinated ethenes competitively inhibited reductive dechlorination of the less-chlorinated ethenes, with inhibition constants equal to the K_s values, while product inhibition could be neglected.

Recently, several studies indicated substrate inhibition or toxicity to the dechlorinators at high chloroethene concentrations. Yu and Semprini (2004) included self-inhibition by TCE, DCE and VC at high PCE concentrations into their model by applying Haldane kinetics and successfully simulated the gradual decline in dechlorination rates as substrate concentration increases. However, Haldane kinetics cannot describe the abrupt stall of dechlorination activity when PCE concentrations exceed a maximum tolerable level, as observed in other studies (Amos et al., 2007; Duhamel et al., 2002; Haest et al., 2006). Based on Luong's work (1987), Amos et al. (Amos et al., 2007) included a substrate inhibition factor in the model which could make the dechlorination rate nil when chlorinated ethene concentrations approach some threshold concentration. Haest et al. (2010) simulated the inhibition of PCE and TCE by using an empirically "log-logistic dose-response model," which was frequently applied to describe a sharp decrease of degradation rate at specific concentrations in ecotoxicological studies.

This study is based on two previous models: Fennell and Gossett (1998) and Heavner et al. (2013). Details of these two models are presented below.

2.E Fennell's Model

A model was developed by Fennell and Gossett (1998) to describe the kinetics of dechlorination, donor fermentation, methanogenic use of H_2 and acetate, and the growth of all

involved microbial communities. The model was constructed and implemented using STELLA® Version 4.02 (High Performance Systems, Inc.).

2.E.1 Experimental Methods

Fennell's experimental data and methods are detailed in her previous publication (Fennell & Gossett, 1998) and PhD dissertation (1998). A culture enriched with methanol, PCE and yeast extract was used as inoculum. Semicontiuously operated experiments were conducted in 160-mL serum bottles with 100 mL diluted source culture at 35 °C. Vitamin solutions and yeast extract (YE) were added routinely as nutritional supplements. After pulse inputs of PCE and an electron donor, reactants, intermediates and products were monitored to obtain the experimental data that were used for comparison with the model.

2.E.2 Kinetics Model for Donor Fermentation

Kinetics of donor fermentation were of Michaelis-Menten form but included a thermodynamics factor (Φ) to incorporate the effects of products acetate and H_2 on the overall fermentation kinetics.

The model for the degradation of organic electron donor (leading to production of H_2) is:

$$\frac{dMt_{donor}}{dt} = \frac{k_{donor} X_{donor} S \Phi}{Ks_{donor} + S} \text{ where } \Phi = 1 - \exp\left(\frac{\Delta G_{rxn} - \Delta G_{critical}}{RT}\right) \qquad (2.1)$$

where Mt_{donor} is total amount of substrate (donor) in the bottle (μmol); k_{donor} is maximum specific rate of donor degradation (μmol/mg VSS/h); X_{donor} is donor-fermenting biomass in the serum bottle (mg VSS); K_{Sdonor} is half-velocity coefficient for the donor (μmol/L); S is substrate (donor) concentration (μmol/L); and t is time (h).

Φ is the thermodynamics factor. It represents the distance of the reaction from the point at

which free energy rises to a critical threshold value. A value of Φ approaching one means the donor fermentation is completely uninfluenced by thermodynamic constraints. A value of Φ approaching zero means that the concentrations of reactants and products have reached values where the reaction free energy (ΔG_{rxn}) is no longer more negative than some critical value for biological feasibility. $\Delta G_{critical}$ was estimated by Fennell to be -19 kJ, based on observing reactant and product concentrations at points where various donor fermentation reactions ceased, then calculating the reaction free energies at such points.

In applying the donor-fermentation model, Fennell calculated ΔG_{rxn} for each time increment using the instantaneous, aqueous concentration of each compound with the equation:

$$\Delta G_{rxn} = \Delta G^{O}_{35^{\circ}C} + RT \ln\left(\frac{[\text{products}]}{S[\text{other reactants}]}\right) \tag{2.2}$$

2.E.3 Kinetics Models for Dechlorination

The model describing the dechlorination of the chlorinated ethenes used Michaelis-Menten kinetics, with the inclusion of both chloroethene and H_2 as limiting substrates. TCE and DCEs were not detected significantly in Fennell's study, so competitive inhibition was not included in her model for dechlorination.

$$\frac{dMw_{CE}}{dt} = \frac{-k_{CE} X_{dechlor} Cw_{CE}}{Ks_{CE} + Cw_{CE}} \times \frac{(Cw_{H2} - H_2 threshold_{dechlor})}{Ks_{H2dechlor} + (Cw_{H2} - H_2 threshold_{dechlor})} \tag{2.3}$$

where Mw_{CE} is the total amount of a particular chloroethene (PCE, TCE, *cis*-1,2-DCE or VC) in the bottle (μmol); k_{CE} is the maximum specific rate of the chloroethene utilization (μmol/mg of VSS/h); $X_{dechlor}$ is the dechlorinator biomass contained in the serum bottle (mg of VSS); Cw_{CE} is the aqueous chloroethene concentration (μmol/L); Ks_{CE} is the half-velocity coefficient for

chloroethene use (μmol/L); Cw_{H2} is the aqueous concentration of H_2 (μmol/L); $H_2threshold_{dechlor}$ is the threshold for H_2 use by dechlorinators (μmol/L); and $Ks_{H2dechlor}$ is the half-velocity coefficient for H_2 use by dechlorinators.

2.E.4 Kinetics Model for Methanogenesis

There were two types of methanogenesis in the mixed culture. Acetotrophic methanogenesis was modeled using a Michaelis-Menten-type kinetics model. Hydrogenotrophic methanogenesis was also modeled using Michaelis-Menten-type kinetics model, but with inclusion of a threshold for H_2 use.

$$\frac{dMt_{CH4\,fromH2}}{dt} = \frac{1}{4} k_{H2,meth} X_{hydrogenotoph} \times \frac{(Cw_{H2} - H_2threshold_{meth})}{Ks_{H2,meth} + (Cw_{H2} - H_2threshold_{meth})} \tag{2.4}$$

where $Mt_{CH4\ from\ H2}$ is the total CH_4 produced via hydrogenotrophs (μmol); $k_{H2,meth}$ is the maximum rate of H_2 utilization (μmol/mg of VSS/h); $X_{hydrogenotroph}$ is the hydrogenotrophic methanogenic biomass contained in the bottle (mg of VSS); Cw_{H2} is the aqueous hydrogen concentration (μmol/L); $K_{SH2,meth}$ is the half-velocity coefficient for H_2 use by hydrogenotrophic methanogens (μmol/L); and $H_2threshold_{meth}$ is the threshold for H_2 use by hydrogenotrophic methanogens (μmol/L).

2.E.5 Kinetics Model for Biomass Growth

Biomass growth of involved organisms in the mixed culture — i.e., dechlorinators, donor fermenters, and methanogens — was modeled separately for each with equations of the following general form:

$$\frac{dX}{dt} = Y\left(-\frac{dMt}{dt}\right)_{utiliz} - k_d X \tag{2.5}$$

where $(dMt/dt)_{utiliz}$ is the utilization rate by the organisom of interest (μmol/h); Y is the organism yield (mg of VSS/ μmol substrate used); X is the biomass of the specific organism group being modeled (mg of VSS); and k_d is the decay coefficient for the organism group (h^{-1}).

2.E.6 Limitations

Fennell applied her model to semicontinuously operated experiments with pulse inputs of PCE and electron donors, and episodic wasting and purging events. However, there were additional limitations of Fennell's model. Firstly, total biomass content of cultures was estimated from particulate organic nitrogen (PON) and then converted to volatile suspended solids (mg VSS). Fennell estimated component biomasses from this total by applying respective yield coefficients — in essence, partitioning the total, measured biomass into various component populations. There was no direct measure of component populations. Secondly, the model mimicked the batch addition of PCE and electron donors, and not continuously fed donor or chlorinated ethenes.

2.F Heavner's Model

A subsequent researcher, Heavner (Heavner et al., 2013), modified Fennell's model (Fennell & Gossett, 1998) to describe continuously fed reactors. Also, by utilizing molecular biology techniques, Heavner reworked the previous model to include molecular biological data for estimating population densities (cells/mL) and for employing with kinetic rate constants (µmole/cell/h). Heavner's modified model encompassed the kinetics of dechlorination, donor fermentation, competition for H_2 by *Dehalococcoides mccartyi* and hydrogenotrophic methanogens, and generation of methane. Based on Fennell's model, Heavner's model used Michaelis-Menten-type kinetics, and included both H_2 thresholds and thermodynamic limitations on butyrate fermentation. The model was also simulated in STELLA®, though in Version 8 (High

Performance Systems, Inc.).

2.F.1 Experimental Methods

The experimental data and most of the experimental methods were reported in Heavner's previous publication (Heavner et al., 2013) and PhD dissertation (2013). The source culture was an enrichment culture (D2) containing *Dehalococcoides* strain 195 (DMC195) maintained on PCE and butyrate. The experiments were performed in 160-mL serum bottles with 100 mL D2 stock culture. The reactors were continuously fed with electron donors and electron acceptors — either PCE, TCE or cDCE — with different concentrations, but were not continuously wasted. Fermented yeast extract (FYE) and vitamin solution were pulse-fed periodically. To avoid dramatic change of culture volume and pressure, liquid and headspace samples were collected. Experimental parameters are described in detail in Heavner's publication (Heavner et al., 2013) and PhD dissertation (2013).

2.F.2 Model Development

The kinetics of donor fermentation, hydrogenotrophic methanogenesis, and the growth of specific biomasses of the organisms were based on Fennell's model except that the units of biomass were changed from mg VSS to 16S rRNA gene copies, and all kinetic constants in the equations were altered accordingly.

2.F.3 Competitive Inhibition Models for Dechlorination

Heavner's model for dechlorination was based on Fennell's model (Fennell & Gossett, 1998). It was of Michaelis-Menten form, wherein the rate of dechlorination was described not only by the chloroethenes concentrations but also by the H_2 concentration. And the H_2 threshold was also included in the model as Fennell described. In addition, previous study by Yu (2003) showed

that competitive inhibition existed among chlorinated ethenes. Therefore competitive inhibition kinetics were also included in Heavner's model for dechlorination.

$$\frac{dMw_{CE}}{dt} = \frac{-k_{CE} X_{DMC195} Cw_{CE}}{Ks_{CE}\left(1+\frac{S_{I,1}}{K_{I,1}}+\frac{S_{I,2}}{K_{I,2}}\right)+Cw_{CE}} \times \frac{(Cw_{H2} - H_2 threshold_{dechlor})}{Ks_{H2,DMC195} + (Cw_{H2} - H_2 threshold_{dechlor})} \quad (2.6)$$

where Mw_{CE} is the total amount of a particular chloroethene (PCE, TCE, DCE or VC) in the bottle (µmol); k_{CE} is the maximum specific rate of chloroethene utilization (µmol/cell/h); X_{DMC195} is the total DMC195 biomass contained in the serum bottle (cells); Cw_{CE} is the aqueous chloroethene concentration (µmol/L); Ks_{CE} is the half velocity constant for chloroethene use (µmol/L); Cw_{H2} is the aqueous H_2 concentration (µmol/L); $Ks_{H2,DMC195}$ is the half-velocity constant for H_2 use by DMC195 (µmol/L); $H_2threshold_{DMC195}$ is the thermodynamic threshold for H_2 use by dechlorinators (µmol/L); $S_{I,1}$ and $S_{I,2}$ are the aqueous concentrations of chloroethenes that inhibit the chloroethene of interest (µmol/L); and $K_{I,1}$ and $K_{I,2}$ are the inhibition constants of each chlorothene (µmol/L), and equal to their respective Ks_{CE} values, in accordance with standard models of competitive inhibition.

Experiments were conducted by Heavner to develop a competitive inhibition model for DMC195. Results of competitive inhibition studies are shown in Figure 3.2.

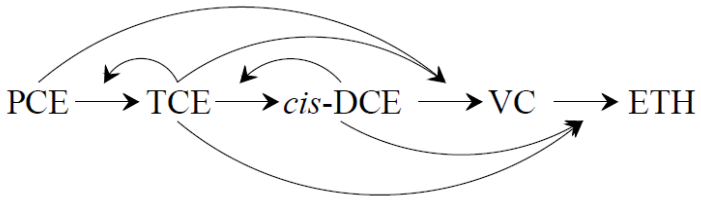

Figure 2.2. Proposed competitive inhibition model for DMC195. This Figure is modified from Figure A1.3 in Heavner's PhD dissertation (2013). Solid lines show the existence of competitive inhibition (e.g. TCE inhibits PCE dechlorination).

A previous study (Yu & Semprini, 2004) with PM and EV cultures indicated that more-chlorinated ethenes inhibit reductive dechlorination of the less-chlorinated ethenes. The different competitive inhibition findings by Heavner (2013) are likely due to strain-specific reductive dehalogenases in the D2 culture, versus the other *Dehalococcoides*-containing cultures.

2.F.4 Haldane Inhibition Model for Acetoclasitic Methanogenesis

Acetate at high concentration is inhibitory to the methanogens. Therefore, Heavner modified Fennell's model for acetoclastic methanogenesis to include Haldane inhibition. The Haldane inhibition constant (K_I) was estimated from batch experiments.

$$\frac{dMt_{CH4\,fromAcetate}}{dt} = \frac{k_{Ace,meth} X_{MS} S}{KS + S + S^2 / K_I} \tag{2.7}$$

2.F.5 Model Fits

The models were compared with results from experimental data using Pearson's chi-squared (χ^2) test for goodness of fit. Both models with and without inhibition were evaluated and their model fits were compared. The "bare bones" model (Heavner et al. 2013) was Fennell's model (Fennell & Gossett, 1998) updated to include continuous-feed conditions and molecular biological data for particular population densities — but with no inhibitions included. The "bare bones" model simulated the total amount of VC and ETH well at low feeding rates for the electron acceptors. However, as the feeding rates increased, the model fits decreased. The reason for the poor model fits at high feeding rates might be the accumulation of the more chlorinated ethenes competitively inhibiting the dechlorination of the less chlorinated ethenes. Furthermore, VC and ETH were not predicted well individually in the "bare bones" model.

The inclusion of competitive inhibition in the model improved the overall model fits for

VC and ETH individually at high feeding rates without affecting good fits at low feeding rates.

2.F.6 mRNA Biomarker Adjustment

The inclusion of microbial biological data in the model improved the model predictions of biomasses. However, the model fits of DMC195 activity and acetoclastic methanogenic activity at high feeding rates were poor. According to Heavner's study, there was a linear trend for the plot of the expression of a key gene for methanogenesis (McrA), versus methanogenesis activity. Similarly, a linear trend for the plot of the expression of HupL, a key hydrogenase representing DMC195 activity, versus chloroethene respiration rate was observed. Therefore, mRNA biomarker levels for acetoclastic methanogenesis and dechlorination were incorporated into the model (with a logic operator) to improve model fits — Heavner referred to this approach as "mRNA-tuning." The equations for the modified models are listed below.

$$\frac{dMt_{CH4\,fromAcetate}}{dt} = MIN\left[\frac{k_{Ace,meth} X_{MS} S}{Ks + S + S^2/K_I}; \left(\frac{McrA_{transcript}}{cell} \times B\right)\right] \tag{2.8}$$

$$\frac{dMw_{CE}}{dt} = MIN\left[\frac{-k_{CE} X_{dechlor} Cw_{CE}}{Ks_{CE}\left(1 + \frac{S_{I,1}}{K_{I,1}} + \frac{S_{I,2}}{K_{I,2}}\right) + Cw_{CE}} \times \frac{(Cw_{H2} - H_2 threshold_{dechlor})}{Ks_{H2dechlor} + (Cw_{H2} - H_2 threshold_{dechlor})}, \left(\frac{HupL_{transcripts}}{cell} \times D\right)\right] \tag{2.9}$$

$McrA_{transcript}$/cell or $HupL_{transcript}$/cell are the mRNA expression levels at steady state in continuous-feed experiments. B and D are the slopes in the plots of McrA expression vs. methanogenesis rate and HupL expression vs. actual respiration rate, respectively. The plots and

values can be found in Heavner's previous publication (Heavner et al. 2013) and PhD dissertation (2013). The model thus included a logic "switch" to ensure that when the mRNA expressions were lower than some maximum values at lower feeding rates, the mRNA adjustment factor didn't affect the model. After including the empirically derived mRNA adjustment factor, the model fits were greatly improved for both methanogenesis and dechlorination.

2.F.7 Limitation

The biokinetics model reworked by Heavner et al. (2013) predicted dechlorination, donor fermentation, methanogenesis and biomass growth fairly well under various conditions. It also supported utilizing quantitative molecular biomarkers to improve biokinetic model fits. However, Heavner's model has limitations. First of all, the model as extended by Heavner et al. used a strictly empirical, "mRNA-tuning" technique to improve data fits under some conditions, making the model descriptive, and not predictive. Secondly, Heavner failed to predict donor fermentation accurately at high electron donor loadings. At high electron donor feeding rates, disappearance of butyrate exceeded the appearance of the measured metabolic products (i.e. acetate, methane, and H_2). Although the observed expression of PHB synthase suggested the possibility of the storage of alkanoic acids as PHB, Heavner et al. (2013) didn't include butyrate's fermentation to products other than acetate or acetate's fermentation to products other than methane in the model. Neither butyrate concentration nor acetate concentration was predicted well at high electron donor loadings.

2.G Limitations of STELLA®

STELLA® (High Performance Systems) is an icon-based software platform for constructing finite-difference dynamic models. Its intuitive graphical interface simplifies the management and interaction with complex models. However, STELLA® has many limitations. The total of time steps allowed in one simulation in STELLA® is limited, so the smaller the time

step (dt) is, the shorter the maximum simulation time may be. Both Fennell and Gossett (Fennell and Gossett, 1998) and Heavner et al. (2013) found that rather small dt values were required to capture accurately the dynamics of high-turnover in some constituents (e.g., H_2) — dt values ≤ 0.03125 h. For this dt, the maximum simulation time was 1021 hr or 42 days. Thus, long-span runs, for example 100 days, of the model have to be simulated by running shorter simulations of less than 42 days and using ending values from the previous run as starting values for the next run until the whole simulation is done.

Another limitation of STELLA® is that the simulation is based on instantaneous data, which makes it very sensitive to the order in which equations are calculated. For example, when simulating Equation (2.3) to calculate PCE dechlorination rate, STELLA® will use the most recent value of hydrogen concentration. If hydrogen production from butyrate fermentation is simulated before dechlorination, the hydrogen concentration used by STELLA® to simulate PCE dechlorination will be a comparatively high value instead of the equilibrium one, and hence, a higher-than-desired dechlorination rate is calculated. Conversely, if a hydrogen-using reaction (e.g., methanogenesis or dechlorination) is simulated before fermentation, it is possible for the small hydrogen concentration to go negative (or, with use of proper logic functions, to zero). Additionally, STELLA® handles pulse events (additions or removals) in an unrealistic way — it treats them as continuous events happening uniformly throughout a particular dt, rather than as truly instantaneous events. Neither of these idiosyncrasies is necessarily insurmountable, but they do dictate the use of very small dt values to prevent them from adversely impacting model results — and as described above, small dt values are problematic in Stella as desired duration of simulation increases. One can imagine wanting to simulate a bioremediation application or natural attenuation process lasting months or years.

Finally, the graphic user interface of STELLA® — its strength in making dynamic modeling available to the masses — becomes a liability as model complexity grows. It's difficult to grasp the complex mass of connective lines and arrows in a model as comprehensive as those that are the subject of this thesis.

CHAPTER THREE — METHOD AND MODEL DEVELOPMENT

3.A Modeling with MATLAB

One objective of this study is to convert the Fennell/Heavner model to run in MATLAB®. MATLAB® is a high-level programming language and interactive environment for numerical computation and visualization (MathWorks, 2014). Without a limitation on the total number of time steps for one simulation, MATLAB® can use an extremely small time step (dt) to achieve accurate calculation (i.e., avoiding numerical artifacts). Additionally, the coding language, tools and built-in math functions of MATLAB® enable the model developer to completely control and optimize the model and reduce the errors brought by different calculation orders. In addition, MABTLAB® has advantages in use of memory and implementation speed.

In this study, the STELLA® model constructed by Heavner et al. (2013) was converted to run in MATLAB® Version 2013b. This MATLAB® model mimicked the continuous-feed (pseudo-steady state) experiments in Heavner et al.'s study (2013). Continuous and pulse inputs of chlorinated ethenes, pulse feedings of electron donors and FYE were simulated, as were waste and purge events. MATLAB® was run on a MacBook Pro. Data collected during the model simulation were transferred to a spreadsheet in Microsoft® Excel and compared to the model simulation results of the original STELLA® model.

3.A.1 Runge-Kutta 4th-Order Integration Method

The model was run using the Runge-Kutta 4th-order integration method (RK4) on both platforms. In the new MATLAB® model, all of the continuous processes modeled, including the continuous feeding of chlorinated ethenes and hydrogen donors, dechlorination, donor fermentation, methanogenesis, biomass growth and mass transfer between the aqueous and

gaseous phases, were expressed as the changing rate in ordinary differential equations (ODEs) and then integrated using RK4.

The reaction rates were expressed in ODEs taking the form,

$$y'(t) = f(t, y(t)), \tag{3.1}$$

on an interval $0 \leq t \leq T$ (total simulation time), with given initial value $y(0)$. Calculation in MATLAB® with RK4 starts with $y_0 = y(0)$ and on reaching $y_n \approx y(t_n)$, takes a step of size dt in the direction of T to form an approximate solution at $t_{n+1} = t_n +$ dt. Runge-Kutta integration provides approximate solution at t_{n+1}, but it can be supplemented with a continuous extension and an inexpensive approximation to $y(t)$ for $t_n \leq t \leq t_{n+1}$ (Shampine, 2005).

3.A.2 Modeling of Discontinuous Events

In addition to continuous processes, there were some discontinuous events in the operations of serum bottle experiments. These events included culture wasting to maintain a constant liquid volume, purging of the volatile compounds from gaseous and aqueous phases to avoid high concentration accumulation, and pulse feeding of chloroethenes, hydrogen donors and FYE. STELLA® treats these discontinuous events as continuous events happening uniformly throughout dt. However, this is not realistic, especially when dt is not small enough. Furthermore, this simulation method is likely to introduce errors. For example, the aqueous and gaseous concentrations of volatile compounds after purge are not always nil in STELLA® simulation, which contradicts intention. Due to these reasons, a different simulation method was used in the MATLAB® model for discontinuous events in this study.

A function named PULSE is defined in MATLAB® taking the form:

x = PULSE(<time>, <first pulse time>, <interval>)

where <time> is the current simulated time; <first pulse time> is the time at which the first pulse occurs; <interval> is the time interval between subsequent pulses; and *x* is the returned value from the PULSE function. *x* is 1 when a pulse event occurs (either purging, wasting or pulse feeding). Otherwise *x* is zero. The MATLAB® codes of the PULSE function are included in the APPENDIX.

3.A.2.1 Pulse Feedings

The pulse feedings of electron acceptors (EA) at appropriate times were simulated by defining the following control-term:

Pulse_Control_Feed_EA =

PULSE (t_n, Feed_Pulse_Time_EA, Feed_Increment_Time_EA);

Pulse_Control_Feed_EA is 1 when there is a pulse feeding event of electron acceptor at t_n, and it is 0 when no electron acceptor is fed instantaneously. The amounts of electron acceptors were then calculated:

$$Mw_{CE}(t_n)^* = Mw_{CE}(t_n) + \text{Pulse\_Control\_Feed\_EA} \times feeding\_volume \quad (3.2a)$$

$$Mw_{CE}(t_{n+1}) = Mw_{CE}(t_n)^* + \text{Runge-Kutta Integration} \quad (3.2b)$$

where $Mw_{CE}(t_n)$ is the total amount of chloroethene (PCE, TCE, *cis*-1,2-DCE or VC) in the aqueous phase at t_n (μmol); $Mw_{CE}(t_n)^*$ is the total amount of chloroethene in the aqueous phase after pulse feeding (μmol); Pulse_Control_Feed_EA is the pulse feeding control term of electron acceptor to switch the pulse feedings on and off; and *feeding_volume* is the size of input (μmol).

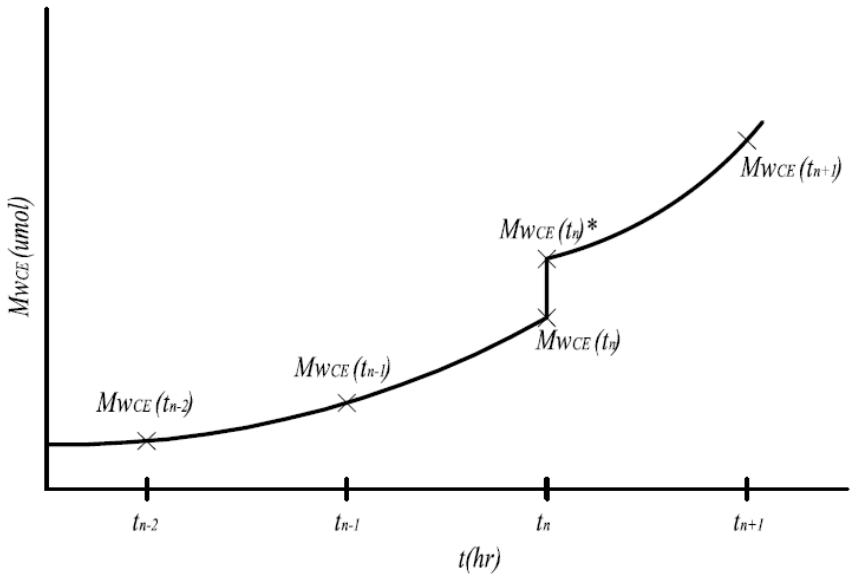

Figure 3.1. Simulation of pulse feeding of electron acceptor at t_n

$Mw_{CE}(t_n)$ is initial value or calculated from previous step using RK4 based on $Mw_{CE}(t_{n-1})$. As shown in Figure 3.1, we assume pulse feedings occur at the end of dt. If pulse feeding is happening at t_n, the feeding amount is added instantaneously at the end of t_n, resulting a new value of the amount of the targeted chloroethene at t_n (i.e. $Mw_{CE}(t_n)$*). But if there is no pulse feeding, the control term in the equation is nil and $Mw_{CE}(t_n)$* equals to $Mw_{CE}(t_n)$. $Mw_{CE}(t_n)$* is used instead of $Mw_{CE}(t_n)$ to calculate the total amount of the electron donor at the next dt (e.g. $Mw_{CE}(t_{n+1})$).

The pulse feedings of butyrate and FYE were simulated similarly.

3.A.2.1 Waste Events

Liquid and headspace samples were collected for sample analysis and to maintain the culture volume. Waste events resulted in the removal of aqueous-phase components such as chloroethenes, donors and biomass. Waste events were simulated by using a PULSE function:

Pulse_Control_Waste = PULSE (t_n, Waste_Pulse_Time, Waste_Increment_Time);

Pulse_Control_Waste is one when a waste event occurs at t_n, and is zero when there is no wasting. The aqueous masses of the components were simulated with the following equations:

$$Mw\ (t_n)^* = Mw\ (t_n) - \text{Pulse\_Control\_Waste} \times liquid\_waste\_rate \times Cw(t_n) \times Vw \quad (3.3a)$$

$$Mw\ (t_{n+1}) = Mw\ (t_n)^* + \text{Runge-Kutta Integration} \quad (3.3b)$$

where $Mw\ (t_n)$ is the amount of a specific component in aqueous phase at t_n before wasting (μmol or cells); $Mw\ (t_n)^*$ is the amount of a specific component in aqueous phase at t_n after wasting (μmol or cells); Pulse_Control_Waste is the control term for waste events at t_n; *liquid_waste_rate* is the percentage of liquid volume wasted during one waste event, which is normally 10%; *Cw* is the aqueous concentration (μmol/L or cells/L); *Vw* is the volume of the liquid in the bottle (L); and $Mw\ (t_{n+1})$ is the simulated amount of specific component in aqueous phase at t_{n+1} (μmol or cells).

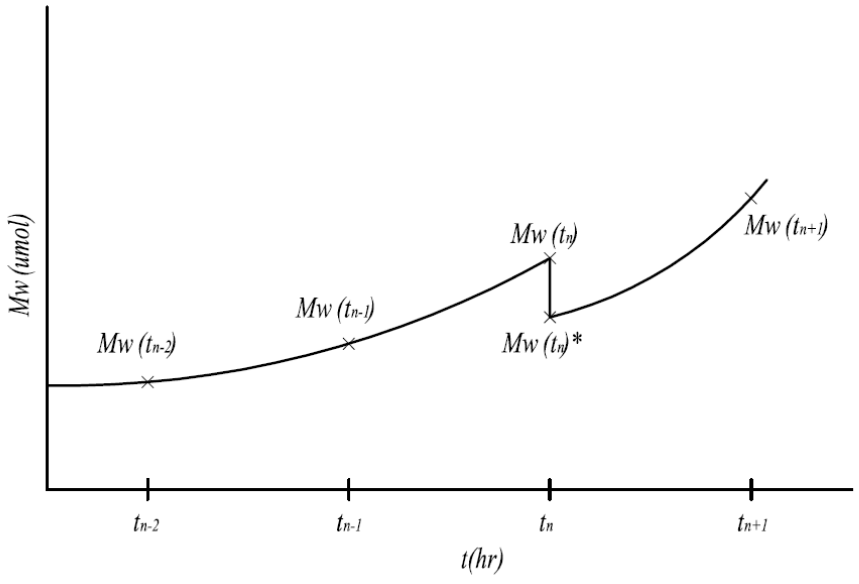

Figure 3.2. Simulation of waste event at t_n

As was the case with simulation of pulse feedings, pulse waste events are also considered

to happen at the end of dt. $Mw\ (t_n)$ is the initial value or Runge-Kutta integrated value at t_n before wasting. If there is a waste event at t_n, 10% of the liquid volume is removed, and the corresponding amount of the component is subtracted from $Mw\ (t_n)$. Otherwise, Pulse_Control_Waste is zero and $Mw\ (t_n)$* equals to $Mw\ (t_n)$. $Mw\ (t_n)$* is consequently used to integrate $Mw\ (t_{n+1})$ using RK4.

3.A.2.2 Purge Events

Purging of volatile compounds (the chloroethenes, H_2 and CH_4) was simulated by using a PULSE function to empty appropriate gaseous and aqueous stocks at appropriate time.

Purge_Control = PULSE (t_n, Purge_Pulse_Time, Purge_Increment_Time).

The control term for purging is calculated at the beginning of every loop to zero all volatile compound flows by an IF… THEN… function. If Purge_Control equals to 1, then there is a purge event at the end of t_n and all gaseous and aqueous stocks of volatile compounds are set to zero.

$$Mw_{CE}\ (t_n)^* = 0;\ Mw_{H2}\ (t_n)^* = 0;\ Mw_{CH4}\ (t_n)^* = 0; \tag{3.4a}$$

$$Mg_{CE}\ (t_n)^* = 0;\ Mg_{H2}\ (t_n)^* = 0;\ Mg_{CH4}\ (t_n)^* = 0. \tag{3.4b}$$

where $Mw_{CE}\ (t_n)^*$ is the amount of chloroethene (PCE, TCE, *cis*-1,2-DCE or VC) in the liquid at t_n (μmol); $Mw_{H2}\ (t_n)^*$ is the amount of aqueous-phase hydrogen at t_n (μmol); $Mw_{CH4}\ (t_n)^*$ is amount of aqueous-phase methane at t_n (μmol); $Mg_{CE}\ (t_n)^*$ is the amount of chloroethene in the headspace at t_n (μmol); $Mg_{H2}\ (t_n)^*$ is the amount of gasous-phase hydrogen at t_n (μmol); $Mw_{CH4}\ (t_n)^*$ is amount of methane in headspace at t_n (μmol).

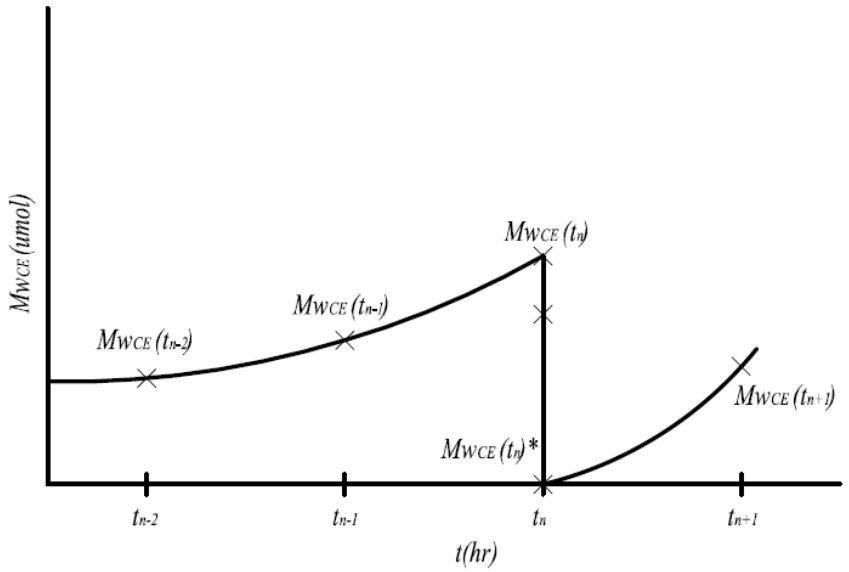

Figure 3.3. Simulation of purge event at t_n

If Purge_Control is zero, which means no purging happens at t_n., Mw (t_n)* equals Mw (t_n) and Mg (t_n)* equals Mg (t_n). Mw (t_n)* and Mg (t_n)* are used to simulate Mw (t_{n+1})* and Mg (t_{n+1})* at next dt.

3.B Haldane Inhibition Model

Heavner et al. (2013) included empirical correlation of activities with mRNA biomarkers to improve model fits at high chloroethene concentrations. However, this empirical "mRNA-tuning" adjustment makes the model descriptive instead of predictive. In this study, we wanted to eliminate the empirical mRNA-tuning and seek alternative mechanistic approaches to modeling data at higher PCE concentration.

3.B.1 Kinetics Models for Dechlorination

In Heavner et al.'s model (2013) (as with Fennell's previously), the kinetics for reductive dechlorination were of Michaelis-Menten form with the inclusion of competitive inhibition among chlorinated ethenes and of a H_2 threshold. To modify the model to fit experimental data at high

chloroethene concentrations, a Haldane-type expression was used to model the inhibition caused by PCE at high concentrations, which incorporated a second-order inhibition term into the equations for dechlorination.

$$\frac{dMw_{PCE}}{dt} = \frac{-k_{PCE} X_{DMC195} Cw_{PCE}}{Ks_{PCE}\left(1+\frac{Cw_{TCE}}{K_{CI,TCE}}\right)+\frac{Cw_{PCE}^2}{K_{HI,PCEon(PCEtoTCE)}}+Cw_{PCE}}$$

$$\times \frac{(Cw_{H2} - H_2 threshold_{DMC195})}{Ks_{H2,DMC195} + (Cw_{H2} - H_2 threshold_{DMC195})} \quad (3.5)$$

$$\frac{dMw_{TCE}}{dt} = \frac{-k_{YCE} X_{DMC195} Cw_{TCE}}{Ks_{TCE}\left(1+\frac{Cw_{DCE}}{K_{CI,DCE}}\right)+\frac{Cw_{PCE}^2}{K_{HI,PCEon(TCEtoDCE)}}+Cw_{TCE}}$$

$$\times \frac{(Cw_{H2} - H_2 threshold_{DMC195})}{Ks_{H2,DMC195} + (Cw_{H2} - H_2 threshold_{DMC195})} \quad (3.6)$$

$$\frac{dMw_{DCE}}{dt} = \frac{-k_{DCE} X_{DMC195} Cw_{DCE}}{Ks_{DCE}\left(1+\frac{Cw_{PCE}}{K_{CI,PCE}}+\frac{Cw_{TCE}}{K_{CI,TCE}}\right)+\frac{Cw_{PCE}^2}{K_{HI,PCEonDCEtoVC)}}+Cw_{DCE}}$$

$$\times \frac{(Cw_{H2} - H_2 threshold_{DMC195})}{Ks_{H2,DMC195} + (Cw_{H2} - H_2 threshold_{DMC195})} \quad (3.7)$$

$$\frac{dMw_{VC}}{dt} = \frac{-k_{VC} X_{DMC195} Cw_{VC}}{Ks_{VC}\left(1+\frac{Cw_{TCE}}{K_{CI,TCE}}+\frac{Cw_{DCE}}{K_{CI,DCE}}\right)+\frac{Cw_{PCE}^2}{K_{HI,PCEon(VCtoETH)}}+Cw_{VC}}$$

$$\times \frac{(Cw_{H2} - H_2 threshold_{DMC195})}{Ks_{H2,DMC195} + (Cw_{H2} - H_2 threshold_{DMC195})} \quad (3.8)$$

where *Mw* is the total amount of chloroethene (PCE, TCE, *cis*-1,2-DCE or VC) in the aqueous phase (μmol); *k* is the maximum specific dechlorination rate of the chloroethene (μmol/cell/h); X_{DMC195} is the dechlorinator biomass contained in the serum bottle (cells); *Cw* is the aqueous concentration of the specific chloroethene (μmol/L); *Ks* is the half velocity constant for chloroethene use (μmol/L); Cw_{H2} is the aqueous H_2 concentration (μmol/L); $Ks_{H2,DMC195}$ is the half-velocity constant for H_2 use by DMC195 (μmol/L); $H_2threshold_{DMC195}$ is the thermodynamic threshold for H_2 use by dechlorinators (μmol/L); K_{CI} is the competitive inhibition constant of each chlorinated ethene and is set equal to its respective half-velocity coefficient *Ks* (μmol/L) ; and K_{HI} is the Haldane inhibition constant pertinent to PCE's inhibition of an indicated dechlorination step (μmol/L).

Unlike other Haldane inhibition models (Yu & Semprini, 2004; Huang & Becker, 2011) that have been used to model the self-inhibition caused by high PCE concentration, experimental results presented by Heavner's study indicated that at high PCE concentration, degradation rates of PCE, TCE cDCE and VC all declined. Therefore, Haldane inhibition terms are included for each of the dechlorination steps.

Haldane inhibition constants were fit to experimental results and determined through trial and error analysis in MATLAB®. At low PCE concentrations, the equations reduce to competitive inhibition only. However, at high PCE concentration, the second-order Haldane inhibition terms become significant and efficiently reduce the degradation rates of the chlorinated ethenes simulated by the kinetic models. The second-order nature of the Haldane term produces the desired transition to accelerated inhibition at high PCE concentrations.

3.B.2 Kinetics Model for Methanogenesis

Methanogenesis was also modeled using Michaelis-Menten-type kinetics equations. Heavner's experimental data suggested that methane production at high PCE concentration virtually stalled (Heavner et al., 2013). This indicated that both methanogenesis from H_2 and from acetate were inhibited by high PCE concentration, so Haldane inhibition terms were included in both kinetic equations for methanogenesis.

Equation (3.9) is the kinetics model for acetoclastic methanogenesis. In addition to high concentrations of PCE, acetate at high concentration is also inhibitory to the methanogens. Haldane inhibition terms were used in the model to describe not only the toxicity of high concentration PCE but also the self-inhibition caused by the substrate.

$$\frac{dMt_{CH4\,fromAcetate}}{dt} = \frac{k_{Ace,meth} X_{MS} Cw_{Ace}}{Ks_{Ace,meth} + Cw_{Ace} + \frac{Cw_{Ace}^2}{K_{HI,Ace}} + \frac{Cw_{PCE}^2}{K_{HI,PCEtoAceMeth}}} \tag{3.9}$$

where $Mt_{CH4fromAcetate}$ is the total methane produced from acetate (μmol); $k_{Ace,meth}$ is the maximum rate of acetate utilization (μmol/cell/h); X_{MS} is the acetoclastic methanogens biomass contained in the bottle (cells); Cw_{Ace} is the aqueous concentration of acetate (μmol/L); $K_{S_{Ace,meth}}$ is the half-velocity coefficient for acetate use by acetoclastic methanogens (μmol/L); $K_{HI,PCEtoAceMeth}$ is the Haldane inhibition constant for PCE inhibiting acetoclastic methanogenesis (µmol/L); and $K_{HI,Ace}$ is the Haldane inhibition constant for self-inhibition caused by acetate (µmol/L).

Haldane inhibition constant by PCE ($K_{HI,PCEtoAceMeth}$) was fit to experimental results and determined through trial-and-error analysis in MATLAB®. The Haldane constant for self-inhibition by acetate ($K_{HI,Ace}$) was estimated from batch experiments conducted in Heavner's study

(2013).

Equation (3.10) is the kinetics equation for hydrogenotrophic methanogenesis incorporating the threshold for H_2 utilization by methanogens as described in a previous study (Fennell & Gossett, 1998).

$$\frac{dMt_{CH4\,fromH2}}{dt} = \frac{1}{4} \times \frac{k_{H2,meth} X_{hydrogenotoph} \times (Cw_{H2} - H_2 threshold_{meth})}{Ks_{H2,meth} + \frac{Cw_{PCE}^2}{K_{HI,PCEtoHydroMeth}} + (Cw_{H2} - H_2 threshold_{meth})} \quad (3.10)$$

where $Mt_{CH4\ from\ H2}$ is the total CH_4 produced via hydrogenotrophs (μmol); $k_{H2,meth}$ is the maximum rate of H_2 utilization (μmol/cell/h); $X_{hydrogenotroph}$ is the hydrogenotrophic methanogenic biomass contained in the bottle (cells); Cw_{H2} is the aqueous hydrogen concentration (μmol/L); $K_{S\ H2,meth}$ is the half-velocity coefficient for H_2 use by hydrogenotrophic methanogens (μmol/L); $H_2threshold_{meth}$ is the threshold for H_2 use by hydrogenotrophic methanogens (μmol/L); $K_{HI,PCEtoHydroMeth}$ is the Haldane inhibition constant for PCE inhibiting methanogenesis from hydrogen (µmol/L);.

3.C Correction of $\Delta G_{critical}$ and the Manner by Which $\{H^+\}$ is Calculated from pH

The models of Fennell and Heavner contain the same error: Namely, the manner by which activity of hydrogen ion, $\{H^+\}$, is calculated from pH value. They include an activity coefficient, $\{H^+\} = \gamma_{\pm} \times 10^{-pH}$, when in fact pH is fundamentally defined in terms of hydrogen-ion activity, and thus no activity coefficient should be used. The correct relationship is $\{H^+\} = 10^{-pH}$. This error appears in the Fennell/Heavner models for all free-energy calculations in which hydrogen ion appears, and it also affected the value of $\Delta G_{critical}$ that Fennell estimated from her experimental

data (and which Heavner subsequently also used). The issue is described below.

$$\Phi = 1 - \exp\left(\frac{\Delta G_{rxn} - \Delta G_{critical}}{RT}\right). \tag{3.11}$$

where Φ is the thermodynamic factor affecting fermentation, and ΔG_{rxn} and $\Delta G_{critical}$ are calculated by the following equations:

$$\Delta G_{rxn} = \Delta G^{O}{}_{35^{\circ}C} + RT \ln\left(\frac{[\text{products}]}{S[\text{other reactants}]}\right) \tag{3.12a}$$

$$\Delta G_{critical} = \Delta G^{O}{}_{35^{\circ}C} + RT \ln\left(\frac{[\text{products}]}{S^{*}[\text{other reactants}]}\right). \tag{3.12b}$$

Each of the donor fermentation reactions to acetate and H_2 has a single H^+ appearing as product, which means each of them has a single $\{H^+\}$ appearing in the numerators of the ln terms of <u>both</u> ΔG_{rxn} and $\Delta G_{critical}$ reactions. Fennell/Heavner mistakenly substituted $\{H^+\} = \gamma_{\pm} \times 10^{-pH}$ instead of $\{H^+\} = 10^{-pH}$. Therefore, an error of $RT\ln \gamma_{\pm}$ was introduced to both the calculation of ΔG_{rxn} and the estimation of $\Delta G_{critical}$. If both corrections are made, there is no effect on the value of Φ, since both ΔG_{rxn} and $\Delta G_{critical}$ are changed by the same constant, and only their difference is used in Eq (3.11).

The corrected $\Delta G_{critical}$ is calculated as follows: $\Delta G_{critical} = \Delta G_{critical}$ (old) $- RT\ln \gamma_{\pm} = -19$ kJ/mol $-$ (-0.6676 kJ/mol) $= -$ 18.3324 kJ/mol.

In this case, ΔG_{rxn} (new) $- \Delta G_{critical}$ (new) $= \Delta G_{rxn}$ (old) $- \Delta G_{critical}$ (old). Therefore the value of Φ is unchanged.

In the model of this thesis, these corrections to both $\{H^+\}$ and $\Delta G_{critical}$ were made throughout.

3.D Inclusion of Butyrate's Fermentation to BHB^- - like products

Experimental data from Heavner (2013) showed unaccounted-for products of butyrate degradation at high PCE loadings — i.e., disappearance of butyrate exceeded the appearance of tracked products expected from its degradation (i.e. acetate, methane, H_2). This suggests the formation of some untracked butyrate product(s) at high PCE levels. Furthermore, the detection of transcripts involved in hydroxybutyrate- and PHB-formation pathways suggests the possibility that butyrate was fermented (via dehydrogenation) to hydroxybutyrate and stored as a polymer at high PCE loading (Heavner, 2013). This condition was included in building the MATLAB model to improve the model fits of hydrogen and volatile fatty acids (VFAs) in the mixed culture.

The text below, in which butyrate conversion to alternative products is explored and modeled, was provided, with permission, by my thesis advisor, Professor J. M. Gossett. Explicity, these sections are: Section 3.D.1 (Energetics of Possible Pathways of Butyrate Converstion), and its subsections; and Section 3.D.2 (A Method for Inclusion of a BHB-like Product in Heavner's Model).

3.D.1 Energetics of Possible Pathways of Butyrate Conversion

3.D.1.1 Thermodynamic Data

Fennell (1998) acquired standard free-energy of formation (ΔG_f^0) data for species of interest. As acquired, the data were for 25˚C. To correct to ΔG_f^0 (35˚C), Fennell used ΔH_f^0 (25˚C) and the application of the van't Hoff Equation (Fennell, 1998). Table 3.1 shows her resulting ΔG_f^0 (35˚C) estimates, as well as those for species not listed by Fennell. These others are based on ΔG_f^0 (25˚C) values from Thauer et al. (1977), and 35˚C values were approximated using estimates of enthalpies of formation. See Appendix II for a complete listing of values used.

Table 3.1. Estimated Free Energies of Formation, ΔG_f^0 (35˚C) (kJ/mol)

Species	ΔG_f^0 (35˚C) (kJ/mol)	Source
H_2 (aq)	+18.3	Fennell
H^+ (aq)	0	"
HCO_3^-(aq)	–583.32	"
H_2O (liq)	–235.55	"
Acetate$^-$ (aq)	–365.50†	"
Butyrate$^-$ (aq)	–346.49	"
β-hydroxybutyrate$^-$ (aq)	–506.51	Thauer*
Crotonate$^-$ (aq)	–269.93	"
Butyraldehyde (aq)	–115.97	" **
n-Butanol (aq)	–167.54	"
Pyruvate$^-$ (aq)	–473.78	"

*Thauer reported values at 25˚C. Approximate correction to 35˚C was made by the method outlined in Fennell, but using estimates of enthalpies.

**Thauer reported value at 25˚C for *liquid* butyraldehyde. Value was first converted to aqueous butyraldehyde by using solubility, Ksp = 71 g/L (Lange's Handbook): Butyraldehyde$_{(l)}$ ---> Butyraldehyde$_{(aq)}$,. However, since MW =72.11 and salting out coefficient would be, perhaps 1.02, it means the activity of butyraldehyde at solubility limit is, conveniently, approx. 1 M. Thus, Ksp = 1 on a molar basis, and $\Delta G^0_{rxn} = -RT \text{ Ln Ksp} = 0$. Thus, coincidentally, the ΔG_f^0 (25˚C) for liquid butyraldehyde is approximately the same as for aqueous butyraldehyde = –119.67 kJ/mol. An estimated enthalpy value was then used to convert to ΔG_f^0 (35˚C).

† Corrected value – listed incorrectly in Fennell.

3.D.1.2 Possible Dehydrogenations

A. Butyrate's fermentation to acetate

From Donna Fennell's PhD dissertation (1998),

$$\text{Butyrate}^- + 2\ H_2O \rightarrow 2\ \text{Acetate}^- + H^+ + 2\ H_{2\,(aq)} \qquad \Delta G^0_{35} = 123.16 \text{ KJ/mol} \qquad (3.13)$$

B. Butyrate's fermentation to BHB$^-$ -like products

BHB$^-$ is the acronym used here for β-hydroxybutyrate, CH_3-CHOH-CH_2-COO^-. What is meant, here, by a "BHB$^-$-like product?" A product of fermentation that generates 1 mol H_2 per mol of butyrate oxidized, versus the 2 mol H_2 that are produced when acetate is the product.

$$Butyrate^- + H_2O \rightarrow BHB^- + H_{2\,(aq)} \quad (3.14)$$

The generation of a fewer number of moles of H_2 than are produced in fermentation to acetate is a key feature, for it results in a lesser slope to the line of ΔG vs. Log H_2, allowing it to cross the similar line representing butyrate's fermentation to acetate. Whether the product is truly BHB^- or not, is unknown; however, Heavner's molecular data showing levels of transcripts expected in the formation of poly-β-hydroxybutyrate (PHB) certainly suggest it. Alternative oxidation products that would fit the scenario (1 mol H_2 per mol butyrate) would include: other isomers of hydroxybutyrate; crotonate (*trans*-2-butenoate); and pyruvate + acetate:

$$Butyrate^- \rightarrow Crotonate^- + H_{2\,(aq)} \quad (3.14a)$$

$$Butyrate^- + HCO_3^- \rightarrow Pyruvate^- + Acetate^- + H_{2\,(aq)} \quad (3.14b)$$

Free energy for fermentation to BHB^-. Using data from Table 3.1,

$$Butyrate^- + H_2O \rightarrow BHB^- + H_{2\,(aq)} \qquad \Delta G^0_{35} = +93.83 \text{ KJ/mol} \quad (3.15)$$

Free energy for fermentation to crotonate. Using data from Table 3.1,

$$Butyrate^- \rightarrow Crotonate^- + H_{2\,(aq)} \qquad \Delta G^0_{35} = +94.86 \text{ KJ/mol} \quad (3.16)$$

Free energy for fermentation to pyruvate and acetate. Using data from Table 3.1,

$$Butyrate^- + HCO_3^- \rightarrow Pyruvate^- + Acetate^- + H_{2\,(aq)} \quad \Delta G^0_{35} = +108.83 \text{ KJ/mole} \quad (3.17)$$

C. Effect of Dissolved H_2 on Energetics of Butyrate Fermentation via Dehydrogenations

Using Equations (3.13), (3.15), (3.16), and (3.17) for four dehydrogenation pathways of butyrate fermentation, we can explore the effect of H_2 (aq) on their reaction free energies.

Assumptions:

- Ionic strength = 0.0856 (Fennell, 1998).
- $\gamma_{\pm}$ = 0.77059 (Guntelburg approx., Fennell, 1998).
- γ_{H2} = 1.020 (Fennell, 1998)
- $\gamma_{\text{uncharged other}}$ = 1.020 (a guess – it's really not important)

Butyrate to Acetate

Assumptions:

- [Butyrate$^-$] = 0.005 M
- pH = 7.3
- [Acetate$^-$] = 0.005 M

Note that these assumptions of concentrations are merely so that we can draw an illustrative plot to demonstrate the concepts involved here. In the model, the measured concentrations will be used to calculate free energy at every time-point.

$$\Delta G_{35^{\circ}C} = \Delta G^{0}_{35^{\circ}C} + RT \ln \frac{\gamma_{\pm}^{2}[\text{Acetate}^-]^2 10^{-pH} \gamma_{H2}^{2}[H_{2(aq)}]^2}{\gamma_{\pm}[\text{Butyrate}^-]} \qquad (3.18)$$

where RT = 2.56085 kJ at 35˚C (308˚K).

Butyrate to BHB$^-$

Assumptions:

- Same as above, with [BHB$^-$] = 1x10^{-15} M [An extraordinarily small concentration of BHB$^-$ is required for sufficiently negative free energy. Is it possible that the precursor to PHB formation is vanishingly small? Or do we simply have the wrong product, and it's something other than BHB$^-$?]

$$\Delta G_{35^\circ C} = \Delta G^0_{35^\circ C} + RT \ln \frac{\gamma_{\pm}[\mathrm{BHB}^-]\gamma_{H2}[H_{2(aq)}]}{\gamma_{\pm}[\mathrm{Butyrate}^-]} \tag{3.19}$$

Butyrate to Crotonate

Assumptions:

- Same as above, with [Crotonate$^-$] = 1x10^{-15} M [Again, an extraordinarily small concentration of crotonate is required for sufficiently negative free energy. Any of these 1 H_2-producing fermentations can be moved up and down by changing product concentration.]

$$\Delta G_{35^\circ C} = \Delta G^0_{35^\circ C} + RT \ln \frac{\gamma_{\pm}[\mathrm{Crotonate}^-]\gamma_{H2}[H_{2(aq)}]}{\gamma_{\pm}[\mathrm{Butyrate}^-]} \tag{3.20}$$

Butyrate to Propionate and Acetate

Assumptions:

- Same as above, with [Pyruvate$^-$] = 1x10^{-15} M
- [HCO_3^-] = 0.0714 M (as per basal medium used)

$$\Delta G_{35^\circ C} = \Delta G^0_{35^\circ C} + RT \ln \frac{\gamma_{\pm}[\mathrm{Pyruvate}^-]\gamma_{\pm}[\mathrm{Acetate}^-]\gamma_{H2}[H_{2(aq)}]}{\gamma_{\pm}[\mathrm{Butyrate}^-]\gamma_{\pm}[\mathrm{HCO_3}^-]} \tag{3.21}$$

Figure 3.4 shows the effect of aqueous H_2 on reaction free energies for the four dehydrogenation fermentations of butyrate considered here. As repeatedly pointed out, all of these free energies can be markedly affected (i.e., their lines can be moved up or down) by the choice one makes for reactant and product concentrations. All require exceptionally low concentrations of products for free energy to be favorable. Fermentation to pyruvate and acetate seems particularly unlikely — both because of energetics, and because the pathway produces acetate,

which doesn't fit with the observation that the "lost" butyrate is unaccounted for by formation of acetate.

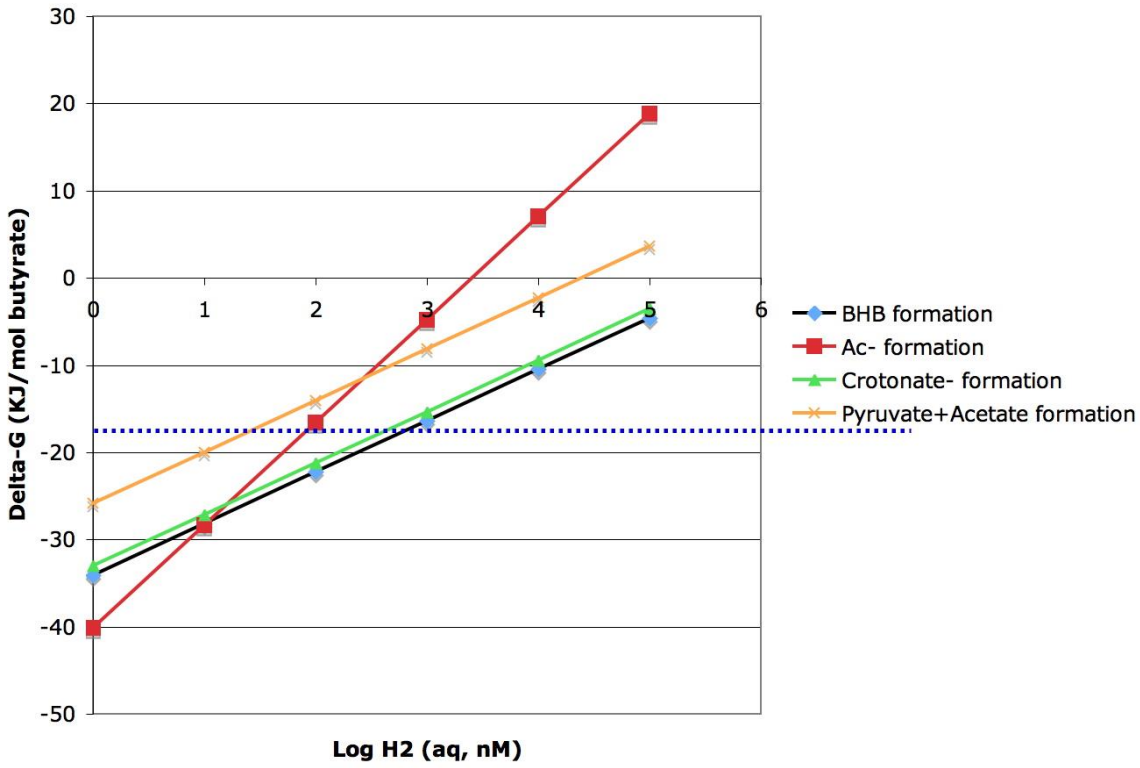

Figure 3.4. Reaction free energy (kJ) vs. Log_{10} H_2 aqueous concentration (nM) for butyrate dehydrogenation fermentations to either acetate, BHB, crotonate, or pyruvate+acetate. The dotted blue line represents approximately $\Delta G_{critical}$, above which the reaction cannot functionally proceed. [Butyrate$^-$] = [Acetate$^-$] = 0.005 M; [BHB$^-$] = [Crotonate$^-$] = [Pyruvate$^-$] = 10^{-15} M; pH = 7.3; I = 0.0856 M.

Figure 3.5 shows the same free energy data (except fermentation to pyruvate+acetate has been omitted), but plotted against aqueous [H_2] on an arithmetic scale, focusing in on the range near the critical value of reaction free energy (–18.33 kJ/mol). Figure 3.6 shows the values of the respective thermodynamic factors (Φ-values) affecting fermentation kinetics, vs. aqueous [H_2].

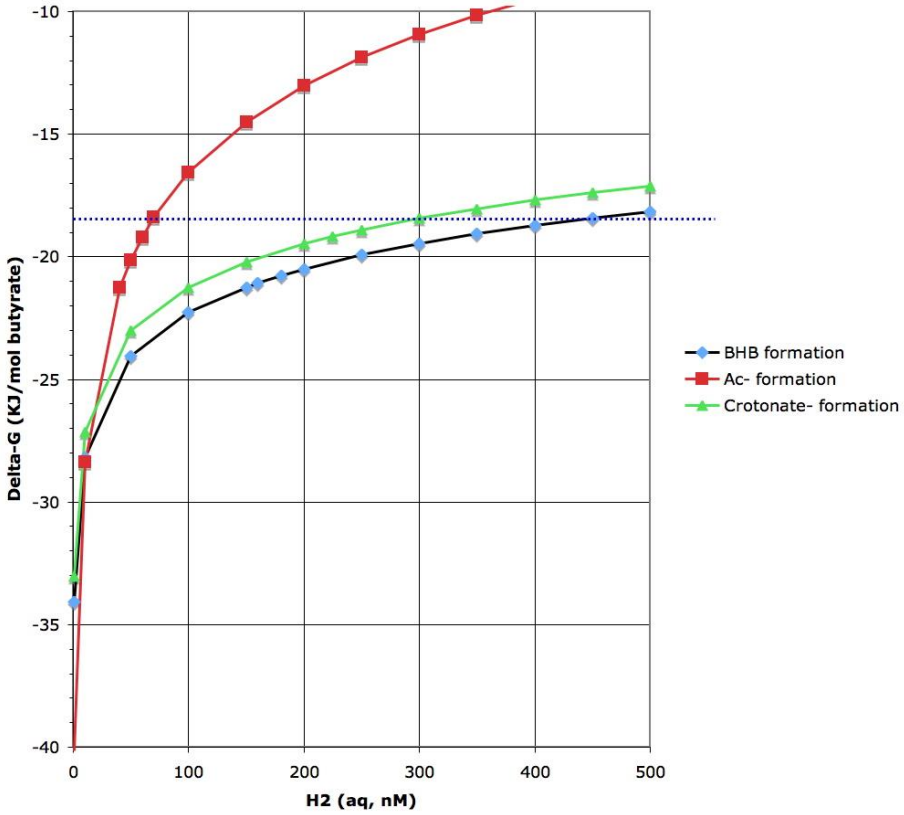

Figure 3.5. Arithmetic plot of reaction free energies vs. aqueous H_2 concentration for three dehydrogenation fermentation reactions of butyrate (productions of acetate, BHB, or crotonate). Dotted blue horizontal line is approximate value of critical free energy. [Buyrate$^-$] = [Acetate$^-$] = 0.005 M; [BHB$^-$] = [Crotonate$^-$] = 10^{-15} M; pH = 7.3; I = 0.0856 M.

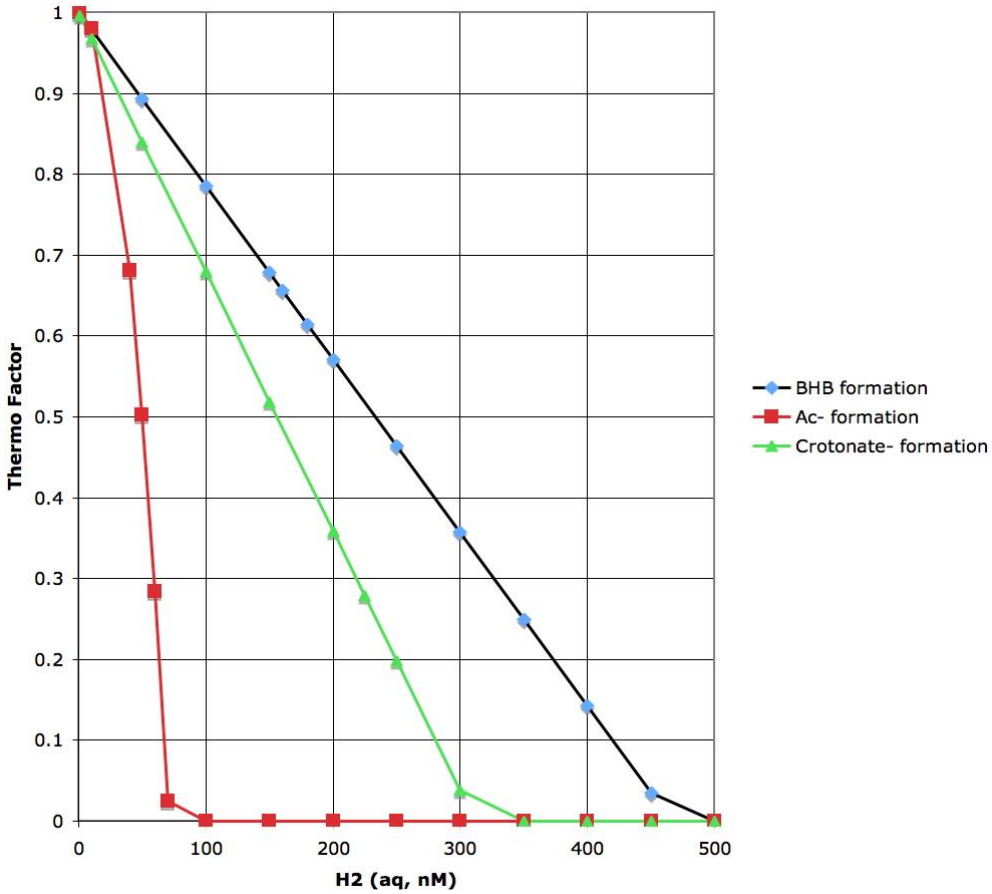

Figure 3.6. Thermodynamic factors (Φ-values) vs. aqueous H_2 concentration for three dehydrogenation fermentation reactions of butyrate (productions of acetate, BHB, or crotonate). [Buyrate$^-$] = [Acetate$^-$] = 0.005 M; [BHB$^-$] = [Crotonate$^-$] = 10^{-15} M; pH = 7.3; I = 0.0856 M.

In this example, fermentation to acetate would have a ceiling of about 75 nM dissolved H_2; fermentation to crotonate$^-$ would have a ceiling of about 300 nM of dissolved H_2; and fermentation to BHB$^-$ would have a ceiling of about 450 nM dissolved H_2. All could proceed below 75 nM H_2, but as dissolved H_2 decreases, fermentation to acetate becomes much more favorable, energetically. Therefore, below 75 nM H_2, we'd expect little, if any, BHB-like products.

The assumption of extremely low BHB$^-$ or Crotonate$^-$ concentrations is a bit troubling, but it might be that we have erred in assuming them as possible products. Regardless, changes in

assumed product or concentrations merely raise and lower their ΔG lines — they don't change the slopes. What we are clearly doing, here, is inventing a product or products to fit the observed circumstances: namely, loss of butyrate without concomitant appearance of acetate or methane in systems experiencing high PCE loadings with relatively high aqueous hydrogen concentrations (300 nM or so). In that sense, what we are doing is clearly empirical, with some underlying mechanistic structural "shape." With a bit more effort, we might be able to hypothesize a different product scheme that doesn't require the assumption of such a low product concentration to make the free energy calculations fit Heavner's observations.

The hypothesized scenario, in which dehydrogenations poise aqueous [H_2] in the 200-300 nM range, is that in the absence of effective hydrogen removal by dechlorination or methanogenesis (because of inhibition by PCE), butyrate dehydrogenation to acetate proceeds until aqueous [H_2] rises to its ceiling of about 75 nM. Above that concentration, butyrate dehydrogenation shifts to production of some BHB-like product. This product is kept very low because it is rapidly converted to a storage material (e.g., PHB). Absent sufficient hydrogen-removal reactions, the system is poised at 200-300 nM concentration of H_2 because that is the ceiling for the dehydrogenation reaction forming BHB-like-product. Unless one is attempting an equivalence balance of products, this might go unnoticed, since butyrate degradation continues. It's only the lack of agreement between butyrate degraded and the appearance of normally expected products (acetate, methane, dechlorination products, and H_2) that provides a clue to this shift in butyrate fermentation pathway.

3.D.1.3 Possible Hydrogenations

Two anaerobic hydrogenation reactions will be considered here: production of butyraldehyde (butanal); and production of n-butanol.

A. Butyrate's Hydrogenation to Butyraldehyde

Using data from Table 3.1,

$Butyrate^- + H^+ + H_{2\,(aq)} \text{---> } Butyraldehyde_{\,(aq)} + H_2O \quad \Delta G^0_{35} = -23.33$ KJ/mol (3.22)

B. Butyrate's Hydrogenation to n-Butanol

Using data from Table 3.1,

$Butyrate^- + H^+ + 2H_{2\,(aq)} \text{---> } n\text{-}Butanol_{\,(aq)} + H_2O \quad \Delta G^0_{35} = -93.20$ KJ/mol (3.23)

C.Effect of Dissolved H_2 on Energetics of Butyrate via Hydrogenations

Using Equations (3.22) and (3.23) for the two hydrogenation pathways of butyrate fermentation, we can explore the effect of H_2 (aq) on their reaction free energies.

Assumptions:

- Ionic strength = 0.0856 (Fennell, 1998).
- $\gamma_{\pm} = 0.77059$ (Guntelburg approx., Fennell, 1998).
- $\gamma_{H2} = 1.020$ (Fennell, 1998)
- $\gamma_{\text{uncharged other}} = 1.020$ (a guess – it's really not important)
- pH = 7.3
- $[Butyrate^-] = 0.005$ M
- [Butyraldehyde] = 5×10^{-16} M
- [n-Butanol] = 10^{-10} M

Butyrate to Butyraldehyde

$$\Delta G_{35^{\circ}C} = \Delta G^{0}_{35^{\circ}C} + RT \ln \frac{\gamma_{\text{uncharged}}[\text{Butyraldehyde}]}{\gamma_{\pm}[\text{Butyrate}^{-}] \cdot 10^{-pH} \cdot \gamma_{H2}[\text{H}_{2(\text{aq})}]} \quad (3.24)$$

Butyrate to n-Butanol

$$\Delta G_{35^{\circ}C} = \Delta G^{0}_{35^{\circ}C} + RT \ln \frac{\gamma_{\text{uncharged}}[n-\text{Butanol}]}{\gamma_{\pm}[\text{Butyrate}^{-}] \cdot 10^{-pH} \cdot \gamma^{2}_{H2}[\text{H}_{2(\text{aq})}]^{2}} \quad (3.25)$$

Figure 3.7 shows the effect of aqueous H_2 on reaction free energies for the two hydrogenation reactions of butyrate considered here. As with the dehydrogenation fermentations considered earlier, very low product concentrations are required for these reactions to have sufficiently negative free energies at aqueous [H_2] concentrations in the vicinity of the values observed at high-PCE loadings (ca. 200-400 nM). So, unless the concentrations of products (butyraldehyde or n-butanol) are very low, these fermentations would be incapable of bringing aqueous [H_2] down to observed levels. And what fermentations would be producing H_2 at levels above 200-400 nM? More complex organics (alcohols, carbohydrates) might. Therefore, one scenario is that under conditions of inhibition by PCE, hydrogen levels potentially get high from such "other" dehydrogenation reactions because the usual reactions that keep hydrogen low (dechlorination and methanogenesis) are not operating effectively. Under such conditions, buyrate reduction to n-butanol would occur, but the only way this could be sustained would be if the n-butanol formed were rapidly converted to some other storage product, thus poising aqueous [H_2] down into the range observed.

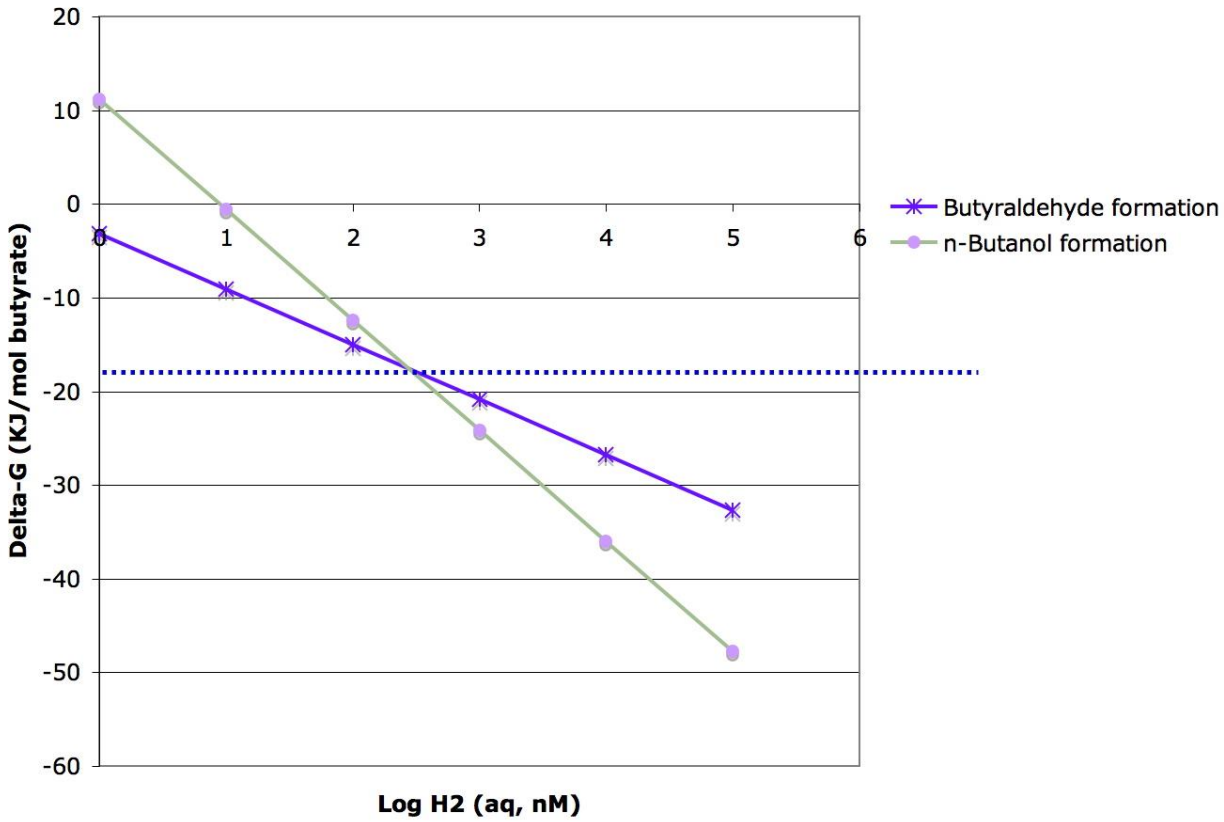

Figure 3.7. Reaction free energy (kJ) vs. Log_{10} H_2 aqueous concentration (nM) for butyrate hydrogenation to either Butyraldehyde or n-Butanol. The dotted blue line represents approximately $\Delta G_{critical}$, above which the reactions cannot functionally proceed. [$Butyrate^-$] = 0.005 M; [Butyraldehyde] = 5 x 10^{-16} M; [n-Butanol] = 10^{-10} M; pH = 7.3; I = 0.0856 M.

3.D.2 A Method for Inclusion of a BHB-like Product in Heavner's Model

In a manner analogous to what is used for other fermentations, we define a thermodynamic factor applicable to BHB formation from butyrate's fermentation,

$$\Phi_{BHBf} = 1 - \exp\left(\frac{\Delta G_{BHBf} - \Delta G_{critical}}{RT}\right) \tag{3.26}$$

for $\Delta G_{BHBf} < \Delta G_{critical}$; otherwise, $\Phi_{BHBf} = 0$.

where

$$\Delta G_{35^\circ C} = \Delta G^0_{35^\circ C} + RT \ln \frac{\gamma_{\pm}[\mathrm{BHB}^-]\gamma_{H2}[H_{2(aq)}]}{\gamma_{\pm}[\mathrm{Butyrate}^-]} \tag{3.27}$$

Absent any real data, a very small, constant value is used for [BHB^-], such as the 10^{-15} M value used to draw Figure 3.4.

A logic function is then applied to kinetics of butyrate to BHB^-:

If $\Phi_{BHBf} \geq \Phi_{butyr}$

Then mass rate of butyrate conversion to a BHB-like product

$$= \frac{k_{BHBf} \times M_{t(butyrferment)} \times Cw_{(butyr)} \times (\Phi_{BHBf} - \Phi_{butyr})}{Ks_{(BHBf)} + Cw_{(butyr)}} \qquad (3.29)$$

Else mass rate of butyrate conversion to a BHB-like product = 0.

What we are attempting to do here, is to shut off butyrate fermentation to BHB-like product whenever it's not energetically preferred. [We could eliminate the subtraction of Φ_{butyr} in the equation, but at really low hydrogen concentrations, both thermo factors will be near 1.0, and their difference might not always calculate such that the factor for BHB^- formation is less than the factor for acetate production. Putting the difference into the equation should eliminate that problem because when the two factors are near unity, the difference will make the BHB-production pathway nil.] Thus, at very low hydrogen levels, BHB^- production will effectively be turned off. As hydrogen rises to levels that cause Φ_{butyr} to become less than 1.0, a mixture of the two pathways will occur. Then at still higher hydrogen levels, acetate production will shut down and only BHB-like product will be formed until its thermo factor goes to zero.

As far as butyrate-fermenter biomass growth is concerned, we'll assume butyrate to acetate supports growth, but butyrate to BHB-like product does not.

3. E Inclusion of Acetate's Hydrogenation to BHB^- -Products

The presence of storage compounds such as PHB in activated sludge cultures has been

repeatedly reported. Acetate, which is the most commonly used substrate to study aerobic dynamic feeding (ADF), is preferentially stored as a homopolymer of PHB (Dionisi et al., 2001). Beun et al.'s study (2000) indicated that if acetate was presented in excess, 66% to almost 100% of the acetate was taken up for PHB synthesis processes. Serafim et al. (2004) showed that in a mixed culture, the cellular PHB content may reach 78.5% (gHB/gVSS) by using acetate as substrate. Therefore, there is the possibility that the missing acetate eeqs in Heavner et al.'s (2013) study was because of acetate's hydrogenation to BHB^- -like products subsequently stored as PHB. This pathway is included in the MATLAB model to improve the poor model fits of acetate at high electron donor feedings. Using data from Table 3.1, the reaction of acetate's hydrogenation to BHB^- -like products is:

$$2\ Acetate^- + H^+ + H_2 \rightarrow BHB^- + H_2O \qquad \Delta G^0_{35} = -29.36\ kJ/mol \tag{3.30}$$

Equation (3.30) was used to explore the effect of H_2 (aq) and [$Acetate^-$] individually on its reaction free energy.

$$\Delta G_{rxn} = \Delta G^{O}_{35^{\circ}C} + RT \ln\left(\frac{\gamma_{\pm}[BHB^-]}{\gamma_{\pm}^2[Acetate^-]^2 10^{-pH}\gamma_{H2}[H_{2(aq)}]}\right) \tag{3.31}$$

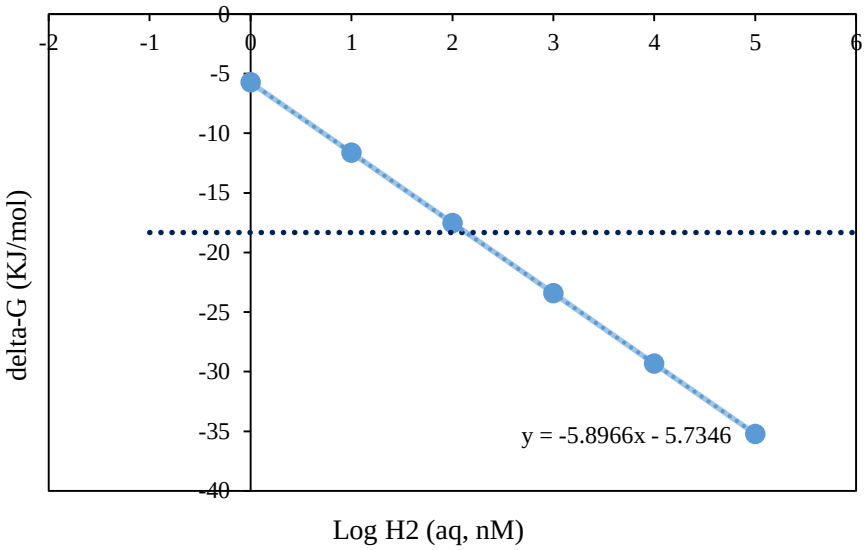

Figure 3.8. Reaction free energy (KJ) vs. Log_{10} H_2 aqueous concentration (nM) for acetate hydrogenation to BHB^- -like products. The dotted blue line represents approximately $\Delta G_{critical}$, above which the reaction cannot functionally proceed. The assumptions for this Figure are: [$Acetate^-$] = 0.005M; [BHB^-] =1×10^{-17} M; pH = 7.3; I = 0.0856M; $\gamma_{\pm}$ = 0.77059; γ_{H2} = 1.020.

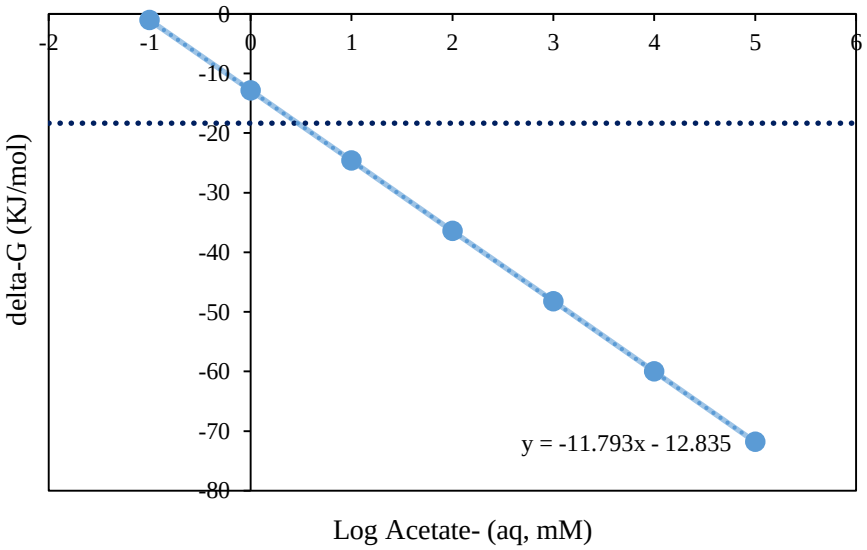

Figure 3.9. Reaction free energy (KJ) vs. Log_{10} [$Acetate^-$] aqueous concentration (mM) for acetate hydrogenation to BHB^- -like products. The dotted blue line represents approximately $\Delta G_{critical}$, above which the reaction cannot functionally proceed. The assumptions for this figure are: [H_2] = 400 nM; [BHB^-] =1×10^{-17} M; pH = 7.3; I = 0.0856M; $\gamma_{\pm}$ = 0.77059; γ_{H2} = 1.020.

Figure 3.8 and Figure 3.9 depict the effect of aqueous H_2 and [$Acetate^-$] on the reaction free energies for the acetate's hydrogenation to BHB^- -like products, respectively. If aqueous

[Acetate$^-$] is in the experimentally observed range and aqueous [H_2] is higher than 230 nM, or [Acetate-] ≥ 3.8 mM and [H_2] concentration is in the vicinity of the values observed, the reaction free energy can be sufficiently negative. Since BHB^- can easily polymerize to PHB, the aqueous concentration of BHB^- might be extremely low. The [BHB^-] concentration used in the calculation is 1×10^{-17} M, which was obtained through trial-and-error analysis in including butyrate's fermentation to BHB^- -like products. If the real aqueous concentration of [BHB^-] is lower than 1×10^{-17} M, the aqueous concentration of [Acetate$^-$] and [H_2] required for the reaction to proceed thermodynamically could be even lower than the ones estimated in Figure 3.8 and Figure 3.9. Therefore, one scenario is that at high PCE loadings, the hydrogen removal by dechlorination and hydrogenotrophic methanogenesis and acetate removal by acetoclastic methanogenesis are highly inhibited, so the levels of hydrogen or acetate are potentially high. Meanwhile, the polymerization from BHB^- to PHB happens rapidly, keeping [BHB-] low. Thus, the reaction free energy is lower than $\Delta G_{critical}$ and the conversion from acetate to BHB^- -like products can potentially occur. Therefore, [Acetate$^-$] is reduced to the observed level.

To include acetate's hydrogenation to BHB^- -like products, a thermodynamic factor is applied, and the mass rate of acetate conversion to a BHB^- -like product is:

$$\frac{dMt_{Acetate}}{dt} = \frac{-k_{AcetoBHB} X_{donor} Cw_{Acetate} \Phi_{AcetoBHB}}{Ks_{AcetoBHB} + Cw_{Acetate}} \tag{3.32}$$

where $Mt_{Acetate}$ is the total mass of acetate converted to BHB^- -like products (μmol); $k_{AcetoBHB}$ is the maximum rate of acetate conversion to BHB^- -like products (μmol/cell/h); X_{donor} is the donor-fermenting biomass in the serum bottle (cells); $Cw_{Acetate}$ is the aqueous concentration of acetate (μmol/L); $Ks_{AcetoBHB}$ is half-velocity coefficient for acetate conversion to a BHB^- -like product; and $\Phi_{AcetoBHB}$ is the thermodynamic factor of the reaction, define by the following equation:

$$\Phi_{AcetoBHB} = 1 - \exp\left(\frac{\Delta G_{rxn,AcetoBHB} - \Delta G_{critical,AcetoBHB}}{RT}\right) \quad (3.33)$$

ΔG_{rxn} is calculated by Equation (3.31). $\Delta G_{critical}$ is -18.3324 KJ/mol. $\Phi_{AcetoBHB}$ =1 when $\Delta G_{rxn} << \Delta G_{critical}$, and the reaction can thermodynamically happen. And $\Phi_{AcetoBHB}$ =0 when $\Delta G_{rxn} \geq \Delta G_{critical.}$

When aqueous concentration of hydrogen or acetate is really low, ΔG_{rxn} is not sufficiently negative and the reaction will be turned off. But when hydrogen or acetate removal reactions are inhibited by high PCE concentrations and hydrogen or acetate increase to significant levels, $\Phi_{AcetoBHB}$ will become 1 and acetate is converted to BHB^- -like products and stored as PHB.

CHAPTER FOUR — RESULTS AND DISCUSSION

4. A Comparison of MATLAB® and STELLA® Simulations

The objectives of this study are 1) to convert the Fennell/Heavner model to run in MATLAB®; and 2) to eliminate the empirical mRNA-tuning adjustment in Heavner's model (2013) and seek alternative mechanistic approaches to model data at high PCE concentrations. Therefore, Heavner's STELLA® model without mRNA tuning adjustment was converted into MATLAB® to be a basic model derived from previous studies and to be improved in this study. This model, which is called "barebones model" in this study, is Fennell's model (Fennell & Gossett, 1998) converted by Heavner (2013) to include molecular biological data for population densities and kinetics, and updated to describe continuously fed reactors, and with the inclusion of competitive inhibitions.

To compare the simulations of the same model using two different modeling software platforms, the same integration method and time step (dt) are desirable to avoid artifactual errors. The Runge-Kutta 4th-order integration method (RK4) was selected as the integration method to be used with both platforms. However, it's difficult to select a convenient dt that works for both STELLA® and MATLAB® because STELLA® cannot use very small dt values in extended durations of simiulation due to the limited total number of time steps it can process in one session, and MATLAB® produces jagged, sawtooth graphs if dt is not small enough. Thus, a whole 7-day experiment conducted by Heavner cannot be simulated by the two software platforms using the same dt.

Therefore, a 24-hour simulation was designed and run in both platforms using a dt of 0.001 h. The same parameters as in Heavner's HLH1_INHIB7 experiment were used, except that the length of simulation was 24 h and purge and wasting occurred every 6 hours. The detailed run specs and experimental parameters used for calibration are listed in Appendix I. Comparison of

the STELLA® and MATLAB® simulations is shown in Figure 4.1.

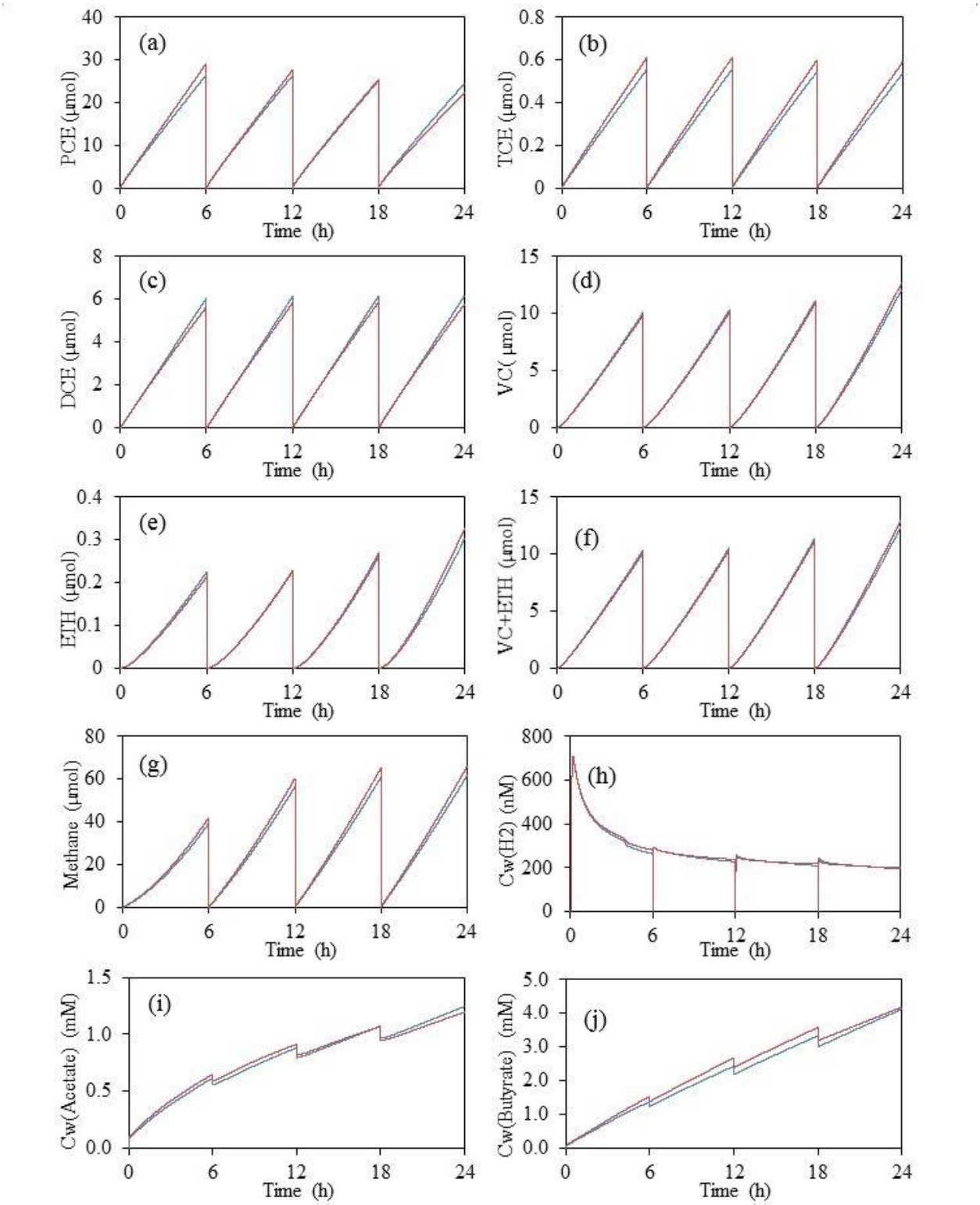

Figure 4.1. Comparison of STELLA® simulations (blue lines) with MATLAB® simulations (red lines) at high PCE feeding rate (7.5 µmol/h): (a) PCE; (b) TCE; (c) DCE; (d) VC; (e) ETH; (f) VC+ETH; (g) methane; (h) H2; (i) Acetate; and (j) Butyrate.

As shown in Figure 4.1, while some differences exist between the simulations, the simulated results of the barebones model in MATLAB® are very similar to those in STELLA®. This suggests that no major human errors were introduced in converting Heavner's barebones model from the STELLA® platform to the MATLAB® platform. Absolute values of change percentages from STELLA® simulations to MATLAB® simulations at every dt were calculated using Equation 4.1, and the average change percentages of the variables of interest are listed in Table 4.1.

$$\text{Change percentage at dt (absolute value)} = |100\% \times [(\text{MATLAB® result at dt}) - (\text{STELLA® result at dt})] / (\text{STELLA® result at dt})| \quad (4.1)$$

Table 4.1 Average Change Percentage from STELLA® to MATLAB®

Variable	%	Variable	%
PCE	5	CH_4	7
TCE	8	Cw(H_2)	2
DCE	3	Cw(Acetate)	4
VC	2	Cw(Butyrate)	8
ETH	7		

The average change percentages are all ≤ 8%, suggesting that STELLA® and MATLAB® achieved very similar results in general. However, for some dt values right after purges, change percentages could be as high as 100%. The reason for such high change percentage is that STELLA® does not always achieve 0 for the amounts of the volatile compounds after purges as the MATLAB® model does. The difference between the simulated values and 0 could be even bigger as the dt increases. Figure 4.2 depicts simulated results of PCE and DCE around a purge event in STELLA® using different dt values.

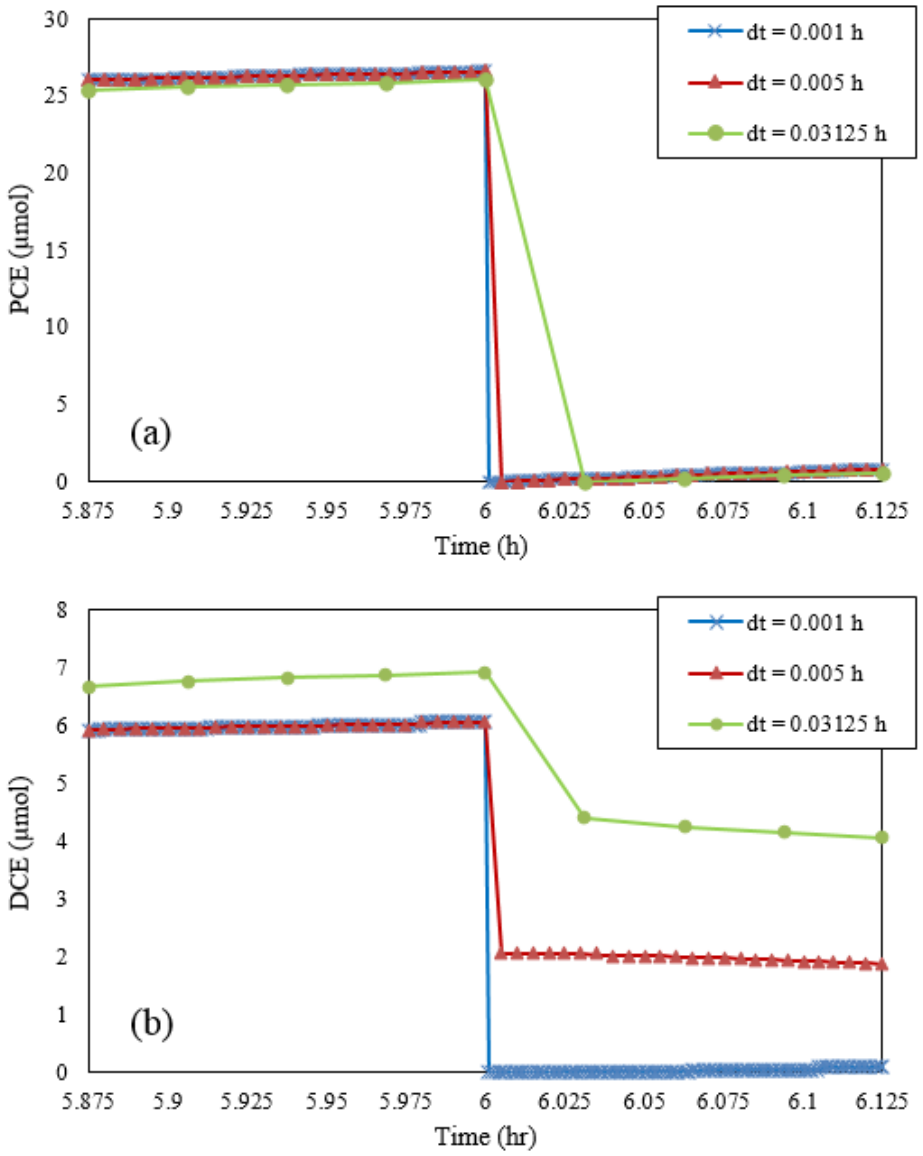

Figure 4.2 Simulation results of PCE (a) and DCE (b) around a purge event in STELLA® using different dt values.

Figure 4.2 shows the effects of dt on simulated results around a purge event in STELLA®. None of these simulations produced 0 for *Mw*(6h+dt) values. The amounts of some volatile compounds, such as Mw_{PCE}(6h+dt), are very small and increase slightly as dt increases. However, for some volatile compounds, such as DCE and VC, STELLA® can only achieve accurate simulations using very small dt. As dt increases, the difference between 0 and Mw_{DCE}(6h+dt) can

increase to very significant values. Hence, it is crucial to choose a rather small dt in STELLA® to capture the discontinuous events accurately. Limited by the total number of time steps allowed in one simulation session, the smallest dt that can be used in STELLA® to simulate a 7-day experiment is 0.008 hour. Neither 0.008 hour nor 0.03125 hour, which was used by both Fennell (1998) and Heavner (2013) is small enough to get all the purged amount of volatile compounds close to 0. So the compromise between the simulation length and size of dt in STELLA® will always lead to some inaccuracy in the simulated results.

To sum up, the MATLAB® platform can be used as a substitute for the STELLA® platform when dt is small. And when the simulation length is long, a MATLAB®-based platform for modeling can function more accurately and efficiently than can a STELLA®-based one.

4. B Model Fits

4. B.1 Barebones Model

The barebones model is the Fennell model (Fennell & Gossett, 1998) converted to include molecular biological data for population densities and kinetics, and updated to describe continuously fed reactors, and with the inclusion of competitive inhibitions. As reported by Heavner et al. (2013), the barebones model predicted dechlorination, methanogenesis, H_2 fermentation and biomass growth fairly well over a wide range of feeding rates and for various chlorinated ethenes fed (PCE, TCE and *cis*-DCE). However, when fed with PCE, as the feeding rate increased, the model fits became poorer.

Figure 4.3 presents the model fits of the barebones model at a high PCE feeding rate (7.25 μmol/h) in MATLAB® using a dt of 0.001 hour. The transformation of PCE was simulated much more rapidly after 48 hours in the model than experimental observation. The failure in simulating

PCE dechlorination rate subsequently led to the overprediction of the levels of the daughter products. In the D2 culture, butyrate is fermented to hydrogen and acetate, and methane is produced from both hydrogen and acetate. Hydrogen is also used for anaerobic reductive dechlorination. Due to the overprediction of the PCE dechlorination rate (and hydrogen consumption by this process), more butyrate was consumed in the model to provide hydrogen for dechlorination processes, and thus more acetate was produced by butyrate fermentation. Previous study showed that in the mixed culture, 80-90% of the methane produced was from acetate (Henry, 2010). Therefore, as acetate was highly overpredicted in the barebones model, the total mass of methane was also overpredicted.

The poor model fits indicated that an inhibition term is required to be added into the barebones model to slow down the PCE dechlorination rate at high PCE feedings without adversely impacting the good model fits under other, lower chlorinated-ethene feeding conditions.

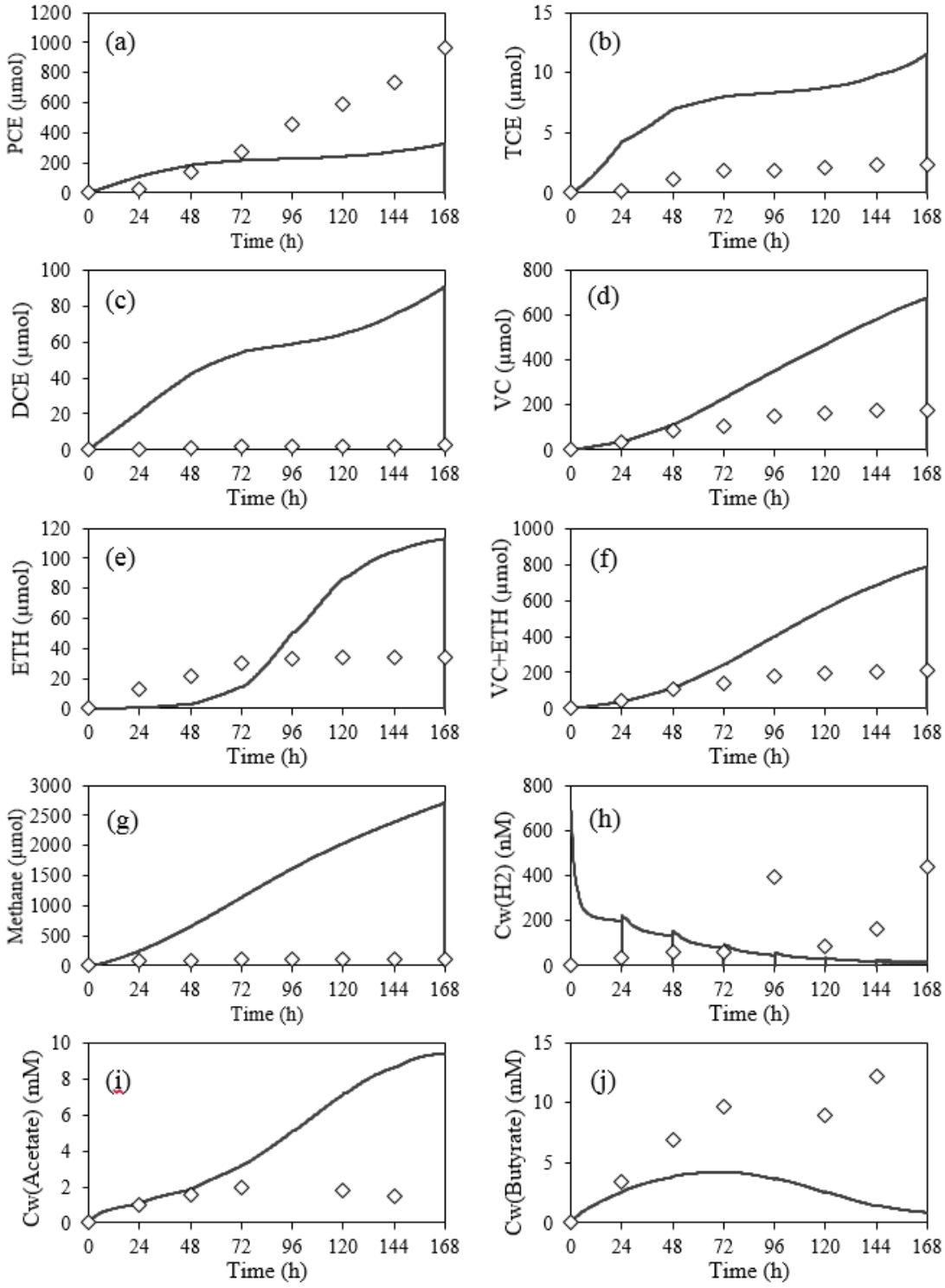

Figure 4.3. Model fits of barebones model (lines) at high PCE feeding rate (7.25 µmol/h) as compared to experimental data (diamonds): (a) PCE; (b) TCE; (c) DCE; (d) VC; (e) ETH; (f) VC+ETH; (g) methane; (h) H2; (i) Acetate; and (j) Butyrate. The chlorinated ethenes and methane are cumulative values while acetate, butyrate and H_2 are instantaneous values.

4. B.2 Haldane-BHB Model at High PCE Loadings

The Haldane-BHB model is derived from the barebones model and with the inclusion of Haldane inhibition by PCE and butyrate and acetate's fermentation to BHB-like products. The model was tested against data collected from Heavner et al.'s (2013) study, over a wide concentration range of feeding rates and for various chlorinated ethenes (PCE, TCE and *cis*-DCE). The K_{HI} values obtained from the fitting of the experiments were used (Table 4.1).

Table 4.2. Haldane Inhibition Constants Used for Model Simulations

Parameter	Value (μM)
$K_{HI,PCEon(PCEtoTCE)}$	17
$K_{HI,PCEon(TCEtoDCE)}$	10000
$K_{HI,PCEon(DCEtoVC)}$	60000
$K_{HI,PCEon(VCtoETH)}$	20
$K_{HI,PCEonAceMeth}$	0.01
$K_{HI,PCEonHydroMeth}$	0.01

Figure 4.4 depicts the comparison of experimental data at a high PCE feeding rate (7.25 μmol/h) with simulations of both Haldane-BHB model in this thesis research (solid lines) and Heavner's (2013) mRNA-tuning model (dashed lines). Since purging occurred every 24 hours, the data points and model simulation of the volatile compounds (PCE, TCE, *cis*-DCE, VC, ETH and CH_4) are presented as cumulative values. H_2, acetate and butyrate are presented as instantaneous values of aqueous concentrations. The sawtooth appearance in Figure 4.4 (i) and (g) is a result of the waste events at every 24 hours.

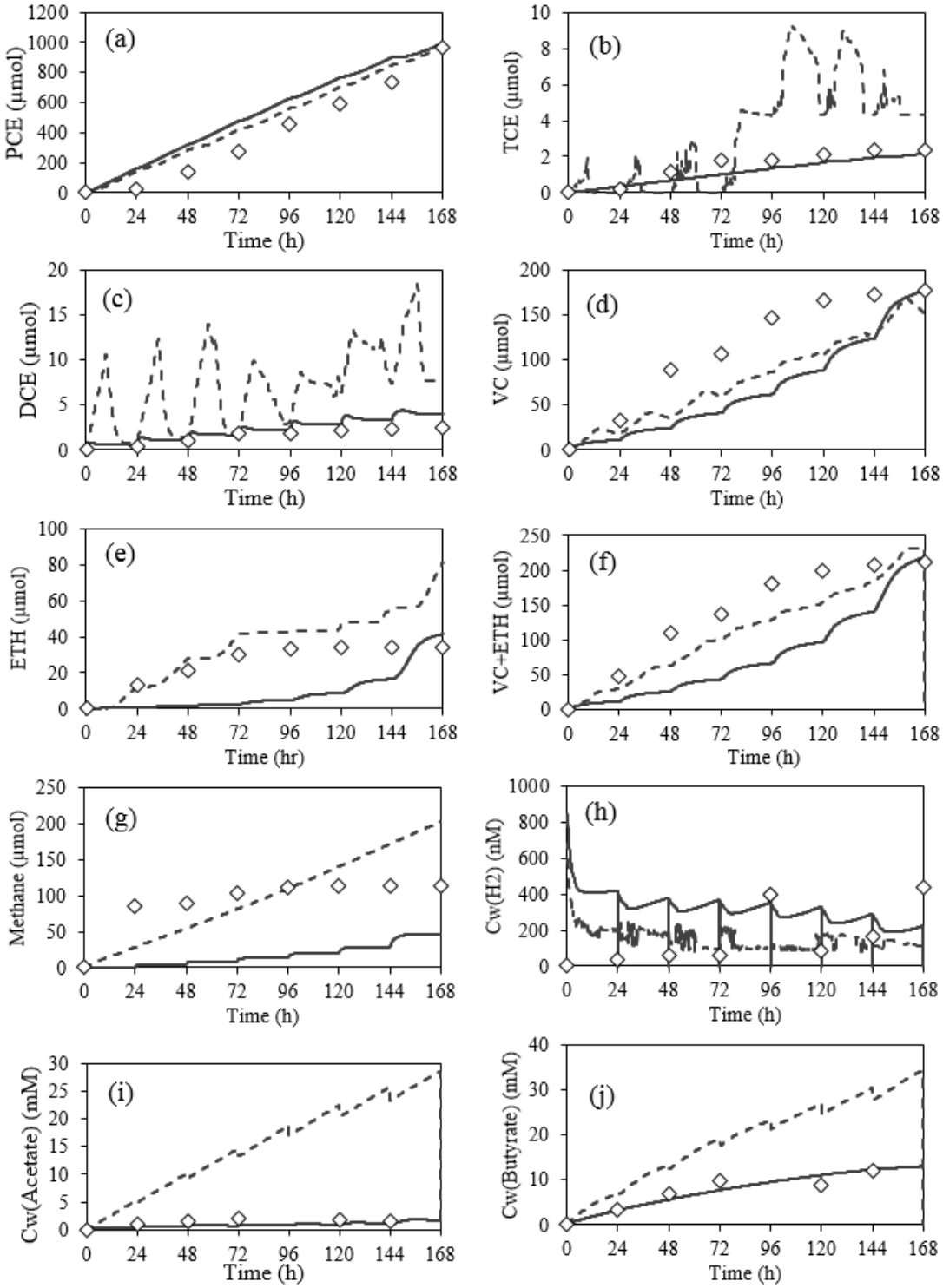

Figure 4.4. Comparison of experimental data at high PCE feeding rate (7.25 µmol/h) with model simulations. The diamonds indicate experimental data. The solid lines present model simulations with both Haldane inhibition and fermentation to BHB-like products. The dash lines are model simulations of Heavner's full model with both competitive inhibition and mRNA tuning: (a) PCE; (b) TCE; (c) DCE; (d) VC; (e) ETH; (f) VC+ETH; (g) methane; (h)

H_2; (i) Acetate; and (j) Butyrate.

4. B.2.1 Model Fits of Dechlorination

The Haldane-BHB model simulations capture the overall shapes and trends of the data of chlorinated ethenes very well, except that experimentally VC and ETH accumulated and stabilized more rapidly than predicted by the model. The cumulative data of VC and ETH plateaued after 120 hours and 72 hours, respectively, suggesting that dechlorination stalled at the end of the experiment. The sampling frequency (every 24 hours) may not have been tight enough to capture the drop in dechlorination rate and the corresponding time point, so we are unable to model the rate of the decline. However, by optimizing the K_{HI} s, the model can efficiently lower the dechlorination rates at high PCE concentrations by including large enough Haldane inhibition terms in the denominators of the kinetic equations and therefore model the eventual results of VC and ETH. As shown in Figure 4.4 (d) (e) and (f), although there are differences between model-predicted and experimental results, the model captures the final results of both VC+ETH and VC and ETH individually fairly well. The dashed lines in Figure 4.4 present the model simulations of Heavner's (2013) model. Heavner et al. (2013) applied mRNA biomarkers to modify model fits at high PCE loadings. This empirical model predicts PCE dechlorination very well. However, neither the overall shape of the data of TCE and DCE, nor the stall of VC and ETH production after some days of experimental operation, is successfully captured.

As listed in Table 4.2, the K_{HI} values for PCE inhibiting the degradation of PCE, TCE, *cis*-DCE and VC of 17, 10000, 60000 and 20 μM were obtained by heuristic fits of the experimental data in the Haldane-BHB model. The Haldane inhibition constants for PCE and VC dechlorination indicate significant Haldane effects. The high Haldane inhibition constants for TCE and *cis*-DCE dechlorination, however, show comparatively weak Haldane inhibition. Therefore, at relatively

high PCE concentrations, significant decreases in PCE and VC dechlorination rates are expected, while less reduction in TCE and *cis*-DCE dechlorination rates would occur. One possible explanation for the different Haldane inhibition effects is the differences in the dehalogenases and mechanisms of the stepwise dechlorination of PCE to ETH. DMC195 is the only *Dehalococcoides* in the D2 culture. It catalyzes PCE to TCE via PceA, and dechlorinates TCE to *cis*-DCE and *cis*-DCE to VC via TceA (Maymó-Gatell et al. 1997; Maymó-Gatell et al. 1999; Magnuson et al., 2000; Seshadri et al., 2005; Löffler et al., 2013b). The dechlorination of VC to ETH is a cometabolic step and does not produce energy (Maymó-Gatell et al., 1999). The cometabolic step of VC to ETH is also catalyzed by TceA, although at much lower degradation rates (Magnuson et al., 1998; Magnuson et al., 2000). It is likely that at high PCE concentrations, the enzyme activities of PceA as well as the cometabolic process from VC to ETH are strongly inhibited. But PCE at high loadings has comparatively weak toxicity to TceA, resulting in high Haldane constants and weak Haldane effects to the dechlorination rate of TCE and *cis*-DCE. An alternate explanation is that near-saturating levels of PCE simply inhibit the overall activity of the cell, essentially by dampening *k* for dechlorination rather than mechanistically affecting just the dehalogenases.

Among a number of models that have been developed to describe reductive dechlorination of PCE, only a few of them described the sequential transformation of PCE and TCE over a wide range of concentrations. Yu and Semprini (2004) showed that a kinetic model incorporating both competitive and Haldane inhibition better simulated experimental data than one using only competitive inhibition at high PCE concentrations. Haldane kinetics of TCE, DCE and VC were included in Yu's model as self-inhibition at high PCE concentrations. Haest et al. (2010) reported that the reductive dechlorination of TCE was self-inhibited by TCE's toxicity at high TCE concentrations. The experimental data of Heavner's (2013) study and the model simulations of this

research showed very different results from these previous studies. Firstly, no Haldane inhibition by TCE or DCE was detected (Heavner et al., 2013). Moreover, PCE at high concentration is not only self-inhibitory but also inhibitory to other dechlorination steps. These differences are likely due to stain-specific reductive dehalogenases catalyzing the stepwise reductive dechlorination of PCE to ethene.

4. B.2.2 Model Fits of Methanogenesis

The fits of the models to data of total methane production are shown in Figure 4.4 (g). The experimentally cumulative amount of methane plateaued after the first 24 hours, suggesting that both methanogenesis from H_2 and from acetate almost completely stalled within 24 hours. Figure 4.5 presents the experimental data as instantaneous concentration measurements (noncumulative data), and the model simulations prepared the same way for comparison. Except for the high methane production (85.33 μmol) during the first 24 hours, the subsequent amounts of methane were all detected below 20 μmol, and from hour 120, the detected amounts of methane were 1.06 μmol/24h, 0.11 μmol/24h and 0.05 μmol/24h, respectively. The experimental data indicate that metabolisms of acetoclastic methanogens and hydrogenotrophic methanogens were profoundly inhibited by high PCE concentration, and both processes soon ceased. Therefore, very small $K_{HI,PCEonAceMeth}$ and $K_{HI,PCEonHydroMeth}$ were chosen (Table 4.2) by trial-and-error analysis to enlarge the Haldane inhibition terms and predict the rapid drop of methanogenesis rate at high PCE concentration. As shown in Figure 4.5, except for not capturing the data point at 24 h, the Haldane-BHB model predicts the low methane production rate at high PCE loadings reasonably well. Experimentally, the bottle reactor was purged every 24 hours under high PCE-fed conditions, and the high level of methane in the first 24 hours did not accumulate in the bottle and hence was not significant in the whole experimental operation. Therefore, the Haldane inhibition terms improve

the model fits of methane production at high PCE concentrations compared to the Heavner's model (Figure 4.4 (g)).

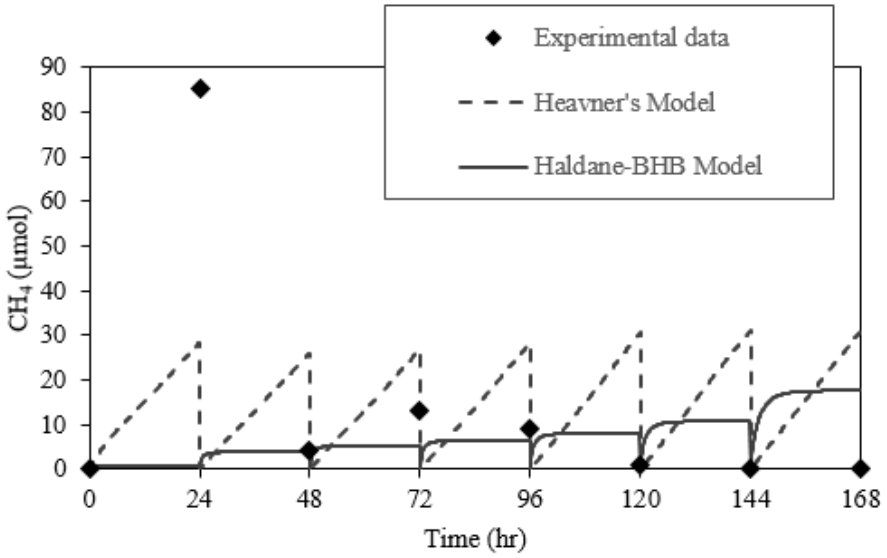

4.5. Comparison of instantaneous total methane amounts with model predictions at high PCE feeding rates (7.25 µmol/hr).

Yang and McCarty (2000) observed that high concentrations of PCE, *cis*-DCE and ethene can be inhibitory to methanogenesis, consistent with the results of this research. Among all the developed models, only three of them have been modeled mixed cultures as a whole: Fennell and Gossett (1998), Heavner et al. (2013), and Lee et al. (2004). Fennell's model got poor model fits of methane production at high PCE concentrations (Figure 4.3(g)). Heavner et al. (2013) used mRNA tuning adjustment to improve the model fits under high PCE fed conditions. However, this model did not capture the stall of methane production (dashed line in Figure 4.4 (g)). In the first 24 hours, methane production was underpredicted in the model, but when methanogens stopped producing methane experimentally, Heavner's model still predicted relatively high rates of methane production (Figure 4.5). Therefore, the model with mRNA tuning adjustment did not work

well to simulate the inconsequential, later methane production rates. Lee et al. (2004) modeled dechlorination and methanogenesis at low PCE concentrations, and simulated CH_4 productions agree generally well with experimental values.

4. B.2.3 Model Fits of Organic Acids in the Mixed Culture

Heavner et al.'s (2013) study indicated the possibility that acetate and butyrate were stored as PHB granules when there was excess butyrate available. The Haldane-BHB model included both butyrate's fermentation and acetate's hydrogenation to BHB^--like products. Without knowing the detailed reactions and the exact proportions of the butyrate or acetate converted to BHB^--like products, we are unable to calculate the real kinetic constants (i.e. *k* and *Ks*) for these processes in the model. Therefore, *k* and *Ks* were determined by trial-and-error analysis and their values are listed in Table 4.3.

Table 4.3. The Tested Parameters for Including Butyrate and Acetate's Fermentations to BHB^- -like poducts

Parameter	Value	Unit
$Ks_{\ Acetate\ to\ BHB}$	500	μmol/L
$Ks_{\ Butyrate\ to\ BHB}$	500	μmol/L
$k_{\ Acetate\ to\ BHB}$	7.5×10^{-9}	μmol/cell/h
$k_{\ Butyrate\ to\ BHB}$	1.0×10^{-8}	μmol/cell/h

Comparative simulations are shown in Figure 4.6 for the model with only Haldane inhibition included, versus the model with both Haldane inhibition and acetate and butyrate's conversion to BHB^- -like products.

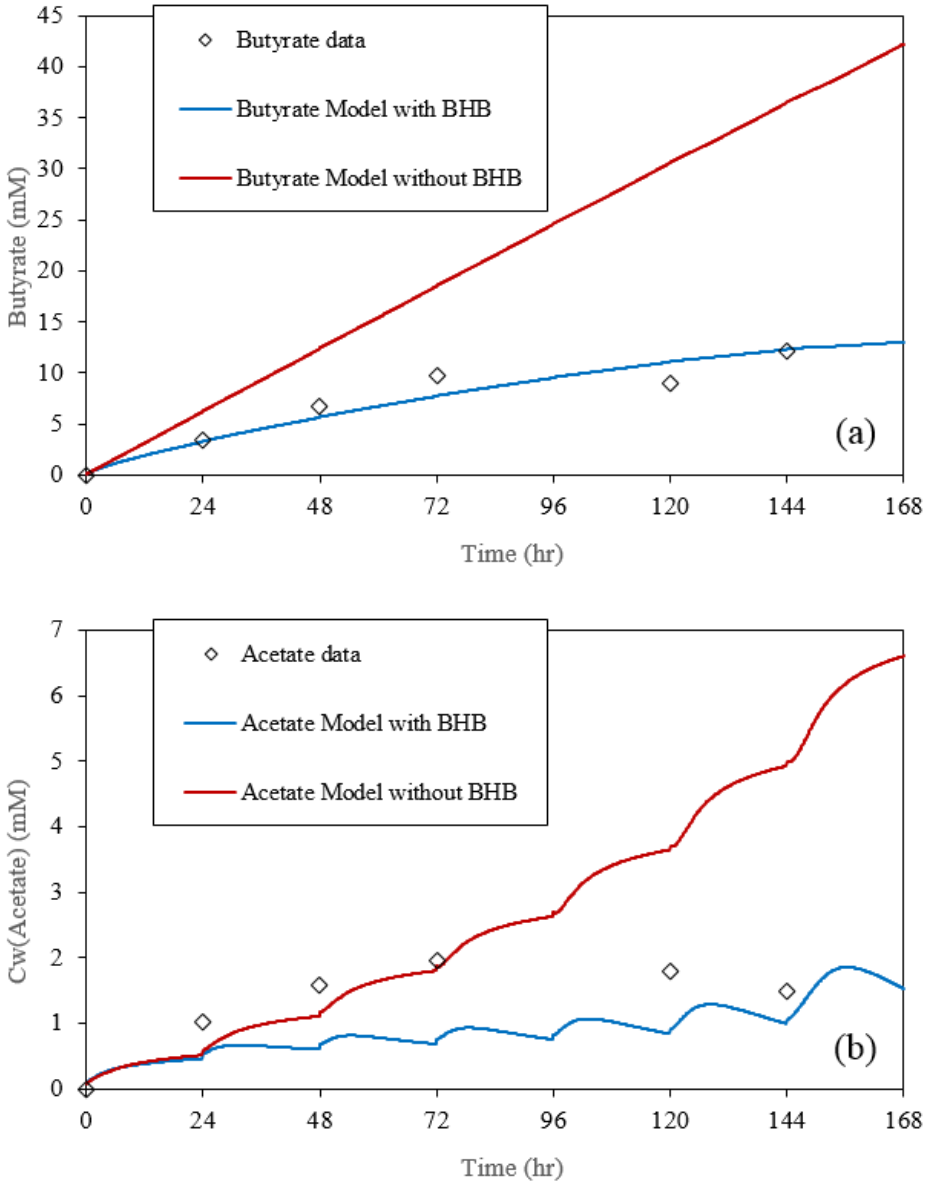

Figure 4.6. Comparison of aqueous concentration of butyrate (a) and acetate (b) with model predictions. The diamonds present the experimental data; blue line is the simulation of complete Haldane-BHB model; red line is the simulation with the inclusion of Haldane inhibition but without BHB^- -like products.

Without the inclusion of butyrate's fermentation to BHB^--like products, the accumulation of butyrate is predicted to occur more rapidly than was actually observed. Model simulations with the inclusion of butyrate's fermentation to BHB^--like products simulate the experimental data

much better.

Similarly, as shown in Figure 4.6 (b), the inclusion of acetate's hydrogenation to BHB^- -like products improves the model's agreement with experimental data. Experimentally, the total amount of acetate decreased after 72 hours. Although neither of the two models captures the decrease in acetate concentration, the Haldane-BHB model predicts the concentration of acetate generally well. It's significant to control the concentration of acetate to a reasonable level because it directly impacts the predicted production rate of methane from acetate. Therefore, the inclusion of the anaerobic hydrogenation of acetate to BHB^- -like products is useful not only to get better model fits but also to choose a $K_{HI,PCEonAceMeth}$ that works for more PCE feeding rate conditions.

Heavner et al.'s (2013) study suggested that at high PCE feeding rates, many butyrate and acetate eeqs were unaccounted for by the measured metabolic products. The gene expression levels of PHB synthase, a key enzyme in PHB production, was detected to be proportional to missing butyrate eeqs. However, Heavner et al. did not include butyrate's fermentation to products other than acetate, or acetate's conversion to products other than methane in the model, so butyrate and acetate were not predicted well. The conversion of acetate and butyrate to form storage compounds such as PHB was reported and studied by many researchers, but all of these studies were based on activated sludge systems, rather than dechlorinating cultures (Beun et al., 2002; Lemos et al., 2006). The experimental results from Heavner's study as well as the improved model fits in this study suggest that the storage of butyrate and acetate also exists in the D2 culture at high butyrate loadings. Additional research is needed to confirm this. Serafim et al. (2004) determined polyhydroxyalkanoates according to Braugegg et al. (1978) and Comeau et al. (1988) with some modifications introduced by Satoh et al. (1992). The sampled culture was centrifuged, lyophilized

and treated with chemicals before analysis by gas chromatography. This method can be used in future research for PHB determination.

4. B.3 Haldane-BHB Model at Low PCE Loadings

Figure 4.7 depicts the predictions of the Haldane-BHB model and Heavner's (2013) model overlaid with the experimental data from a low-PCE feeding experiment. The bottle reactors in this experiment were sampled and wasted every 24 hours. Butyrate was constantly fed as hydrogen donor, and there was a pulse feed of yeast extract at Hour 72.

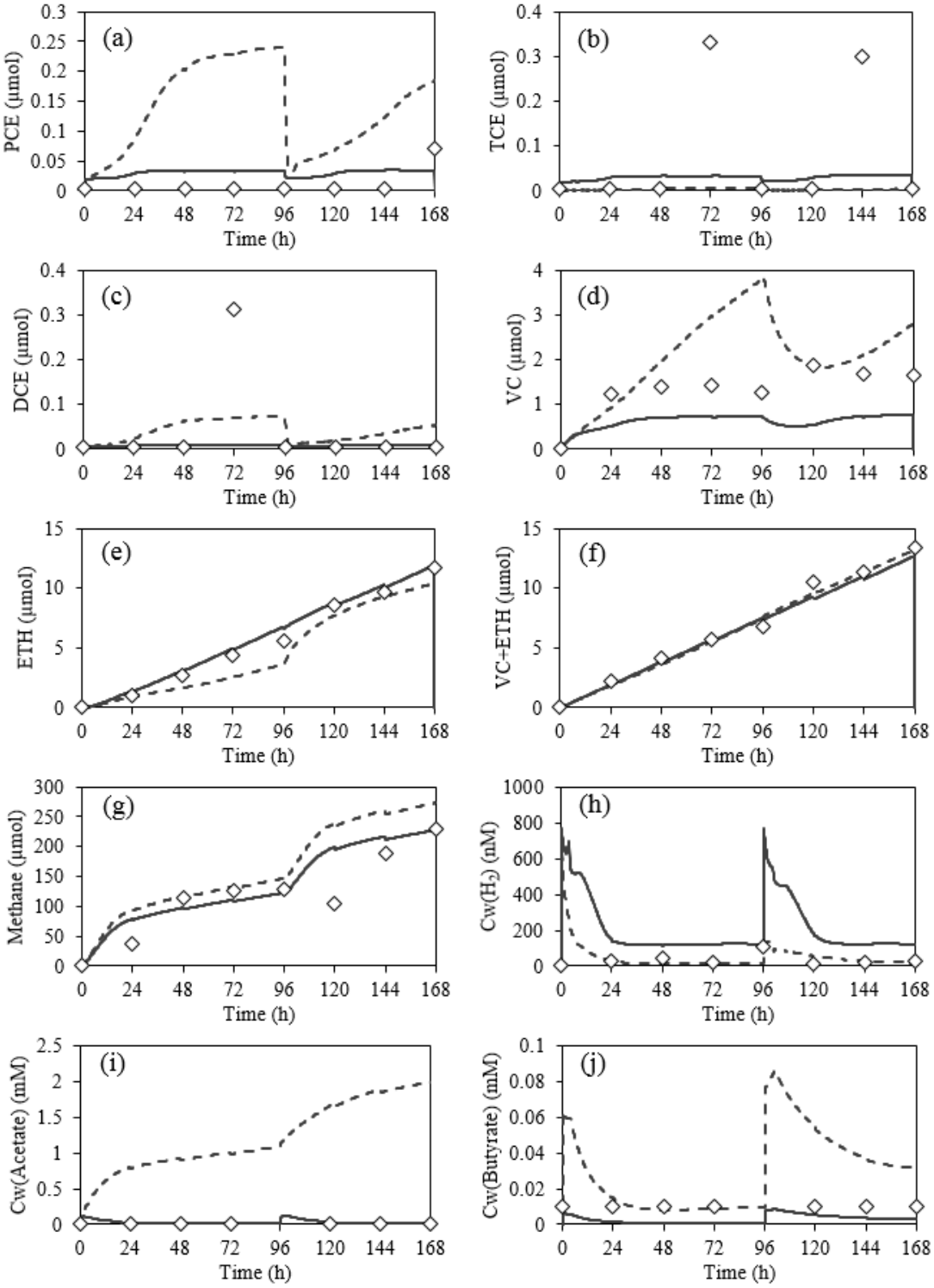

Figure 4.7. Comparison of experimental data at low PCE feeding rates (0.08 µmol/h) with model simulations. The diamonds indicate experimental data. The solid lines present model simulations with both Haldane inhibition and fermentation to BHB-like products. The dash lines are model simulations of Heavner's model: (a) PCE; (b) TCE; (c) DCE; (d) VC; (e) ETH; (f) VC+ETH; (g) methane; (h) H_2; (i) Acetate; and (j) Butyrate.

Heavner's model (dashed lines in Figure 4.7) captures the overall shapes and trends of the data set very well except that the simulated acetate (Figure 4.7 (i)) accumulation is more rapid than experimental observation. The Haldane-BHB model (solid lines in Figure 4.7) predicts the aqueous concentration of acetate quite well. Also, the Haldane-BHB model better fits the levels of PCE, TCE, DCE, and CH_4. The aqueous concentrations of hydrogen appear not to be captured in the Haldane-BHB model as well as in Heavner's model; however, the experimental data were not gathered with sufficient frequency to capture the brief spikes in H_2 predicted by the Haldane-BHB model. Butyrate concentrations were better predicted by the Haldane-BHB model than by Heavner's model. Overall, we conclude that the Haldane-BHB model simulates the experimental data at low PCE feedings very well. The changes introduced to achieve better results at high PCE loadings have apparently not compromised the model's ability to predict results at low PCE loadings.

Model fits of the Haldane-BHB model and Heavner's (2013) model for other experimental conditions in Heavner's study are represented in APPENDIX A3.B. The Haldane-BHB model can predict dechlorination, methanogenesis and donor fermentation fairly well over a wide range of PCE feeding rates and at low TCE or *cis*-DCE feeding rates.

CHAPTER FIVE — CONCLUSIONS

The following conclusions were drawn from this study:

1. The Fennell/Heavner model in STELLA® was successfully converted to run in MATLAB®. The two different modeling platforms produced similar simulated results (average absolute value difference ≤ 8%) when utilizing the Runge-Kutta 4th-order (RK4) integration method and a small dt of 0.001 h. The MATLAB® platform removes some of the limitations of STELLA® — its limited number of time-steps per simulation session (thus limiting how small a dt may be used); its unrealistic handling of discontinuous events (pulses and purges); and its sensitivity to the order of calculation of the many reaction processes in so complex a model.
2. Heavner's model was reworked to eliminate the empirical, mRNA tuning adjustment Heavner inserted to model high-PCE-loading conditions. Instead, the inhibitory effects of high PCE on dechlorination and methanogenesis were modeled as 2nd-order Haldane inhibitions (i.e., as functions of the square of PCE concentration). This approach successfully fit Heavner's data at high PCE loadings, while not adversely affecting the fit at lower PCE loadings.
3. Heavner's data for conditions of high butyrate loading evidenced a lack of mass-balance — i.e., there was greater butyrate consumed than accounted for in the ultimate products expected from it (acetate, methane, H_2, and dechlorination daughter products). This situation, unaddressed by Heavner's model, was modeled in this thesis research by postulating additional pathways of butyrate/acetate's conversion to BHB/PHB-like storage products — pathways that would become thermodynamically feasible only at higher H_2 levels. The approach, while it

remains conjectural due to lack of data on candidate storage products, was able to fit Heavner's data quite well, suggesting a fruitful area of further research.

CHAPTER SIX — SUGGESTIONS FOR FUTURE RESEARCH

The following avenues for future research are suggested by this thesis study:

1. Attempt to confirm the existence of products from butyrate fermentation (other than acetate and H_2) and acetate conversion (other than CH_4). The revised model in this study postulated BHB-like storage materials. However, neither Heavner et al.'s (2013) study nor this research provide evidence of the existence of BHB-like products. Therefore, experiments conducted with high butyrate, which will generate potentially high acetate as well, and also separate experiments with high acetate fed directly are needed to confirm the existence of the postulated products and validate the approach taken in this study.
2. The 2nd-order Haldane inhibition model appeared to simulate well the experimental data at high PCE loading. However, the various Haldane coefficients were not rigorously derived from a large data-set. We suggest that more experiments be run at high PCE loadings -- or artificially manipulating PCE concentrations by pulse-loading it. This would allow rigorous, statistical fit of the model parameters to the data, rather than reliance on the relatively crude, trial-and-error fitting by eye that was done in this thesis research.
3. Some of the model results show temporal changes, especially in H_2, acetate and butyrate. These changes are not apparent in the existing data, perhaps because the data were not gathered frequently enough to see them, if they exist. Some experiments should be conducted with greater sampling frequency, to better test the model.
4. For any model to be environmentally relevant, parameter values need to be known at environmentally relevant temperatures (e.g., 15 - 20 °C), not 30-35 °C. The effects of

temperature -- and pH, for that matter – should be evaluated.

APPENDIX I: PARAMETERS USED TO COMPARE STELLA® AND MATLAB® SIMULATIONS

Table A1.1. Parameters used to compare STELLA® and MATLAB® simulations

Parameter	Values
Length of Simulation (h)	24
dt (h)	0.001
PCE Feed Rate (µmol/h)	7.25
Electron Donor	Butyrate
Feed Increment Time (Butyrate and YE) (h)	6
µL YE Fed (µL)	100
Constant ED Feed Rate (µmol/h)	26
Average Sampling Time (h)	6
Sampling/Wasting Volume (mL)	10
Purge Increment Time (h)	6

APPENDIX II. ESTIMATED STANDARD FREE ENERGIES OF FORMATION AT 35˚C

Compound	ΔGf˚ (25˚C) kJ/mol	ΔHf˚ (25˚C) kJ/mol	K (25˚C)	K (35˚C)	ΔGf˚ (35˚C) kJ/mol
Acetate (aq)	-369.41	-486	5.2222E+64	9.0115E+61	-365.50
Butyrate (aq)	-352.63	-535.55	5.9996E+61	5.4120E+58	-346.49
Ethanol (aq)	-181.75	-288.3	6.9380E+31	1.5928E+30	-178.18
Lactate (L(+) ion (aq)	-517.81	-686.64	5.2049E+90	6.4962E+86	-512.15
Propionate (aq)	-361.08	-566.38	1.8134E+63	1.0926E+60	-354.19
H2 (aq)	17.57	-4.18	8.3535E-04	7.9087E-04	18.30
H+ (aq)	0	0	1.0000E+00	1.0000E+00	0.00
HCO3- (aq)	-586.85	-691.99	6.4819E+102	7.5428E+98	-583.32
Formate (aq)	-351.04	-425.6	3.1591E+61	1.2020E+59	-348.54
H2O (liq)	-237.18	-285.83	3.5658E+41	8.4552E+39	-235.55
		estimates:			
beta-Hydroxybutyrate (aq)	-506.3	-500	5.0113E+88	7.1995E+85	-506.51
Crotonate (aq)	-277.4	-500	3.9664E+48	5.6983E+45	-269.93
Butyraldehyde (aq)	-119.67	-230	9.2317E+20	4.5464E+19	-115.97
n-Butanol (aq)	-171.84	-300	1.2737E+30	2.5089E+28	-167.54
Pyruvate (aq)	-474.63	-500	1.4178E+83	2.0368E+80	-473.78

APPENDIX III MODEL FITS

A3.A Parameters used for model simulations

Table A3.1. Experimental Parameters for Model Calibration

Experiment	Cultue title	Length of Experiment	Calculated EA Feed Rate	eeq ratio ED/EA as H2	Respiration Rate	EA	ED	Culture Dilution	Calculated EA Feed Rate	Feed Increment Time (butyrate & YE)	YE fed volume	Constant ED Feed Rate	Average Sampling Time	Sampling/ Wasting Volume (mL)	Purge Time
		days	μeeq/L/h		μeeq/h				μmol/h		μL	μmol/h	h	mL	h
PCE half Butyrate	PHB1	7	104.30	0.74	8.46	PCE	But	1	1.74	24	100	1	24	9	24
	PHB2	7	45.66	1.68	3.93	PCE	But	1	0.76	24	100	1	24	9	24
	PHB3	7	106.26	0.72	9.72	PCE	But	1	1.77	24	100	1	24	9	24
PCE high low	HLH1_INHIB2	2	316.20		14.12	PCE	But	1	5.27	24	100	26	24	10	24
	HLH2_INHIB2	2	481.93		15.65	PCE	But	1	8.03	24	100	26	24	10	24
	HLH1_INHIB7	7	435.11	1.90	7.86	PCE	But	1	7.25	24	100	26	24	10	24
	HLH2_INHIB7	7	481.28	1.72	8.23	PCE	But	1	8.02	24	100	26	24	10	24
	HLH3	7	183.06	4.52	13.78	PCE	But	1	3.05	24	100	26	24	10	24
	HLL1	7	4.91	4.14	0.49	PCE	But	1	0.08	96	100	0.22	24	2.5	-
	HLL2	7	4.75	4.14	0.48	PCE	But	1	0.08	96	100	0.22	24	2.5	-
	HLL3	7	5.95	3.31	0.59	PCE	But	1	0.10	96	100	0.22	24	2.5	-
PCE 0 YE	P0FY01	4	6.60	0.00	0.17	PCE	-	1	0.11	-	-	-	24	2.5	-
	P0FY02	4	5.39	0.00	0.16	PCE	-	1	0.09	-	-	-	24	2.5	-
	P0FYY1	7	4.94	2.79	0.45	PCE	-	1	0.08	120	100	-	24	2.5	-
	P0FYY2	7	4.68	2.79	0.43	PCE	-	1	0.08	120	100	-	24	2.5	-
PCE high	HiP1	1	259.05	3.37	14.08	PCE	But	1	4.32	12	100	26.00	6	20	6
	HiP2	1	231.29	3.78	13.31	PCE	But	1	3.85	12	100	26.00	6	20	6
	HiP3	1	279.01	3.13	16.72	PCE	But	1	4.65	12	100	26.00	6	20	6
TCE 3 rate	T3A1	4	34.22	3.79	3.42	TCE	But	1	0.86	48	100	4.08	24	10	24
	T3B1	4	6.88	5.14	0.69	TCE	But	1	0.17	-	100	0.87	24	10	-
	T3C1	4	1.46	11.40	0.15	TCE	But	1	0.04	-	100	0.20	24	10	-
DCE 3 rate	D3A2	4	32.39	3.04	3.24	DCE	But	1	1.62	72	100	4.08	24	10	24&72
	D3B2	4	8.17	3.25	0.82	DCE	But	1	0.41	-	100	0.87	24	10	-
	D3C2	4	2.31	5.37	0.23	DCE	But	1	0.12	-	100	0.20	24	10	-

A3.B Comparison of Model Simulations and Experimental Data

Figures in this section depict the comparison of Heavner's experimental data with model simulations. The diamonds indicate experimental data. The experimental parameters used for model simulations are listed in Table A3.1. The solid lines present model simulations with both Haldane inhibition and fermentation to BHB-like products. The dash lines are model simulations of Heavner's model: (a) PCE; (b) TCE; (c) DCE; (d) VC; (e) ETH; (f) VC+ETH; (g) methane; (h) H_2; (i) Acetate; and (j) Butyrate. Note that some butyrate and acetate data are unavailable from Heavner.

A. PHB1

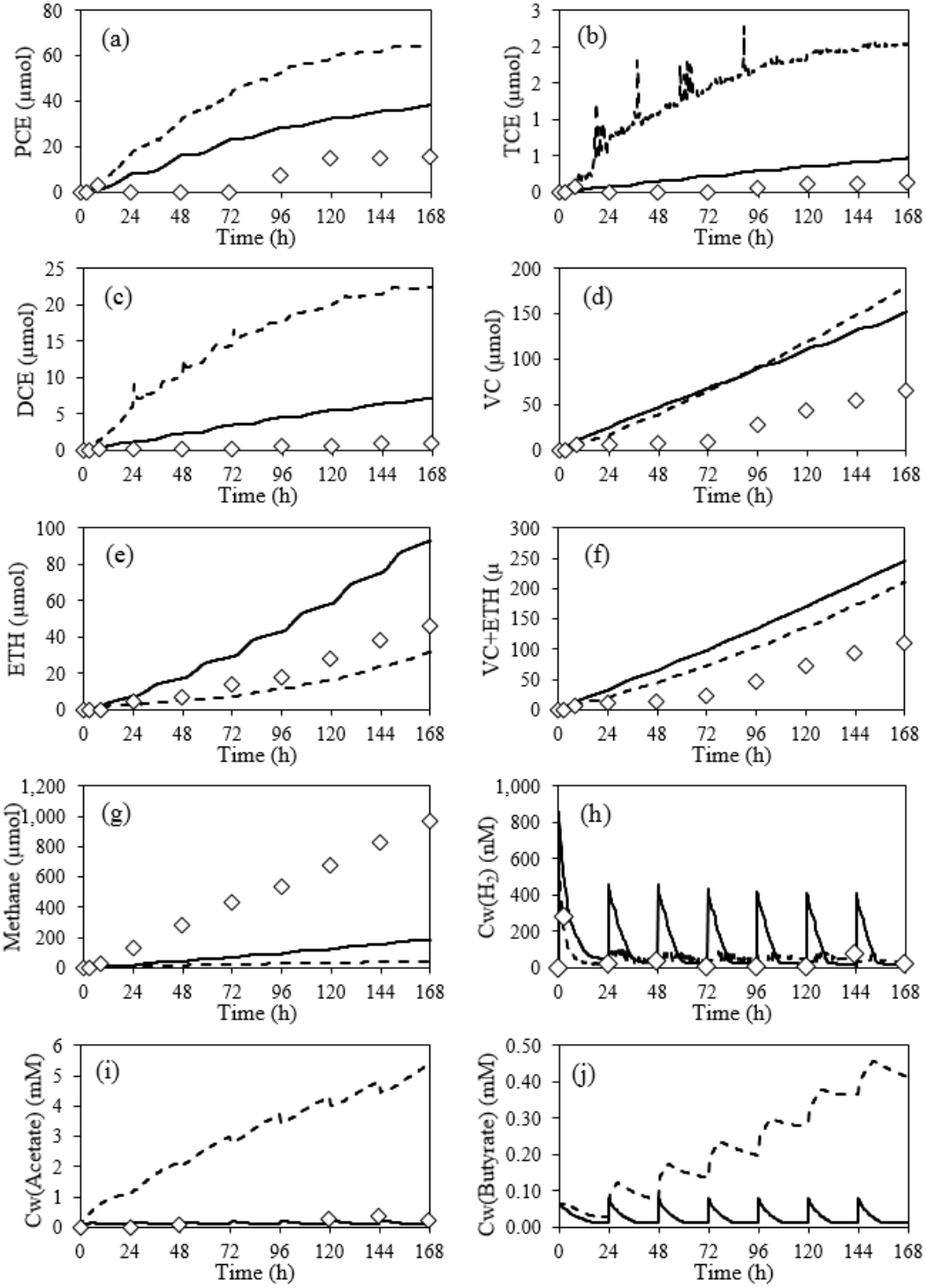
(a)
PCE (µmol)
Time (h)
(b)
TCE (µmol)
Time (h)
(c)
DCE (µmol)
Time (h)
(d)
VC (µmol)
Time (h)
(e)
ETH (µmol)
Time (h)
(f)
VC+ETH (µ
Time (h)
(g)
Methane (µmol)
Time (h)
(h)
Cw(H2) (nM)
Time (h)
(i)
Cw(Acetate) (mM)
Time (h)
(j)
Cw(Butyrate) (mM)
Time (h)

B. PHB2

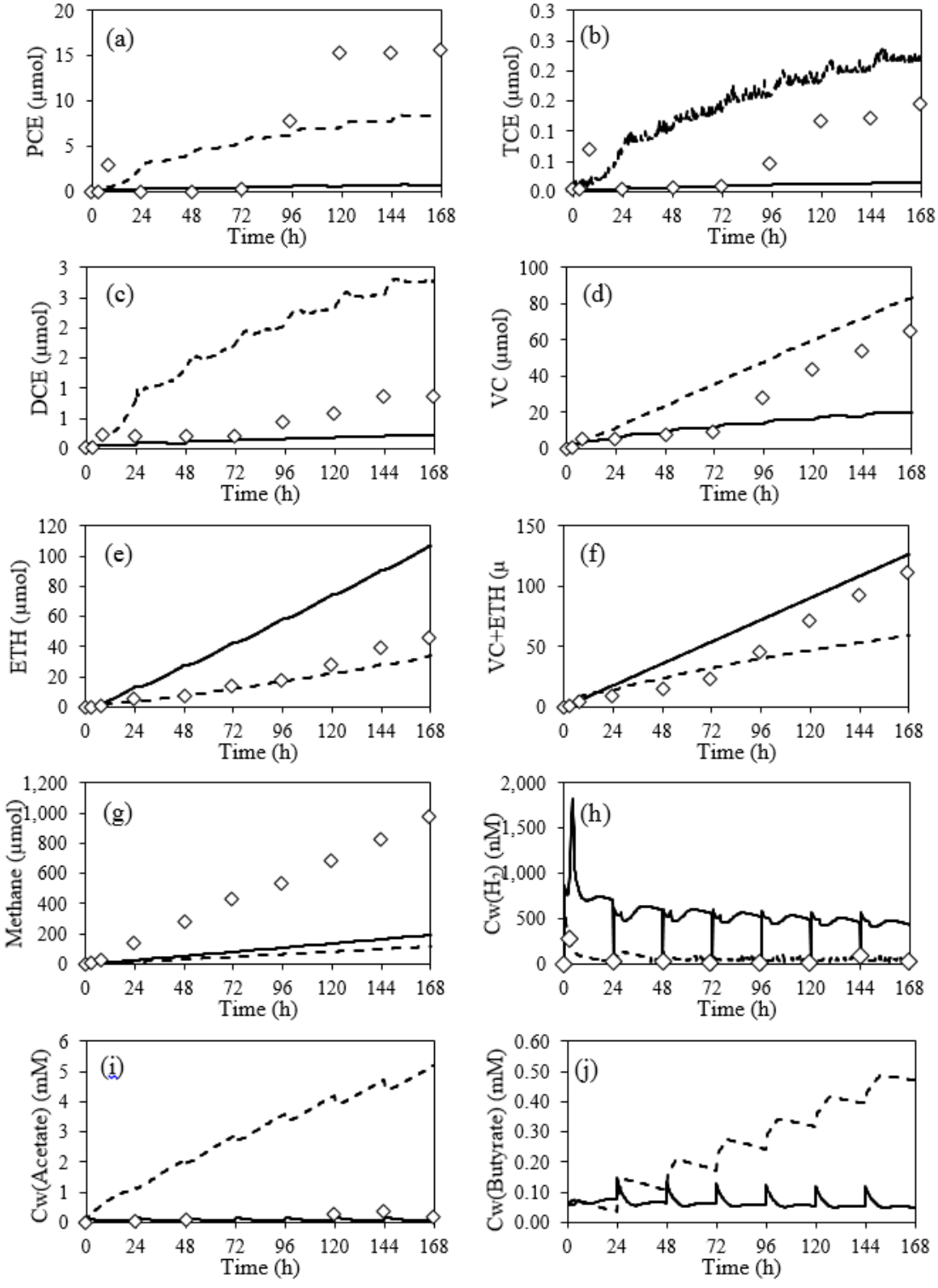
(a)
PCE (µmol)
Time (h)
(b)
TCE (µmol)
Time (h)
(c)
DCE (µmol)
Time (h)
(d)
VC (µmol)
Time (h)
(e)
ETH (µmol)
Time (h)
(f)
VC+ETH (µ
Time (h)
(g)
Methane (µmol)
Time (h)
(h)
Cw(H2) (nM)
Time (h)
(i)
Cw(Acetate) (mM)
Time (h)
(j)
Cw(Butyrate) (mM)
Time (h)

C. PHB3

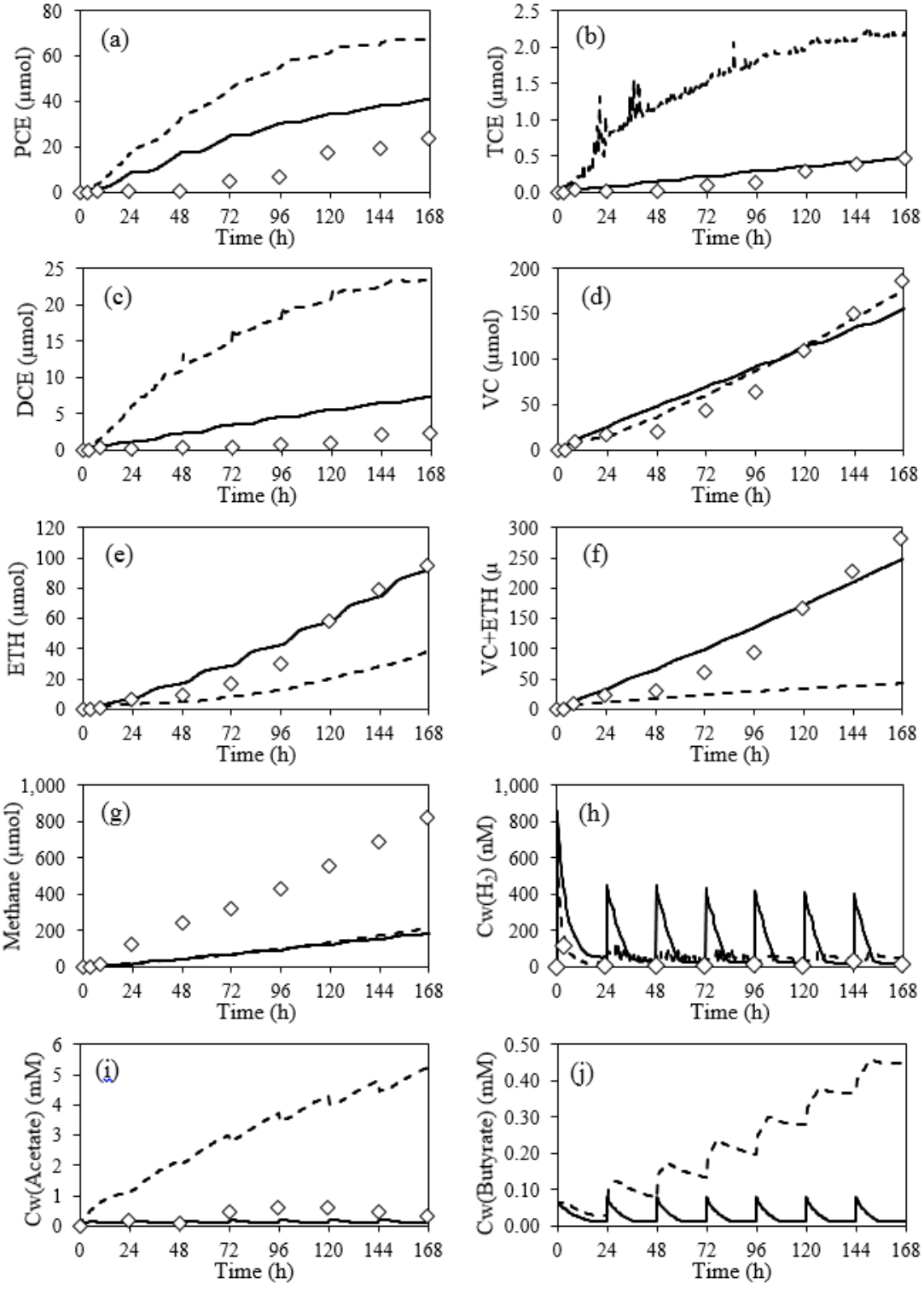
(a)
PCE (µmol)
Time (h)
(b)
TCE (µmol)
Time (h)
(c)
DCE (µmol)
Time (h)
(d)
VC (µmol)
Time (h)
(e)
ETH (µmol)
Time (h)
(f)
VC+ETH (µ
Time (h)
(g)
Methane (µmol)
Time (h)
(h)
Cw(H2) (nM)
Time (h)
(i)
Cw(Acetate) (mM)
Time (h)
(j)
Cw(Butyrate) (mM)
Time (h)

D. HLH2_INHIB7

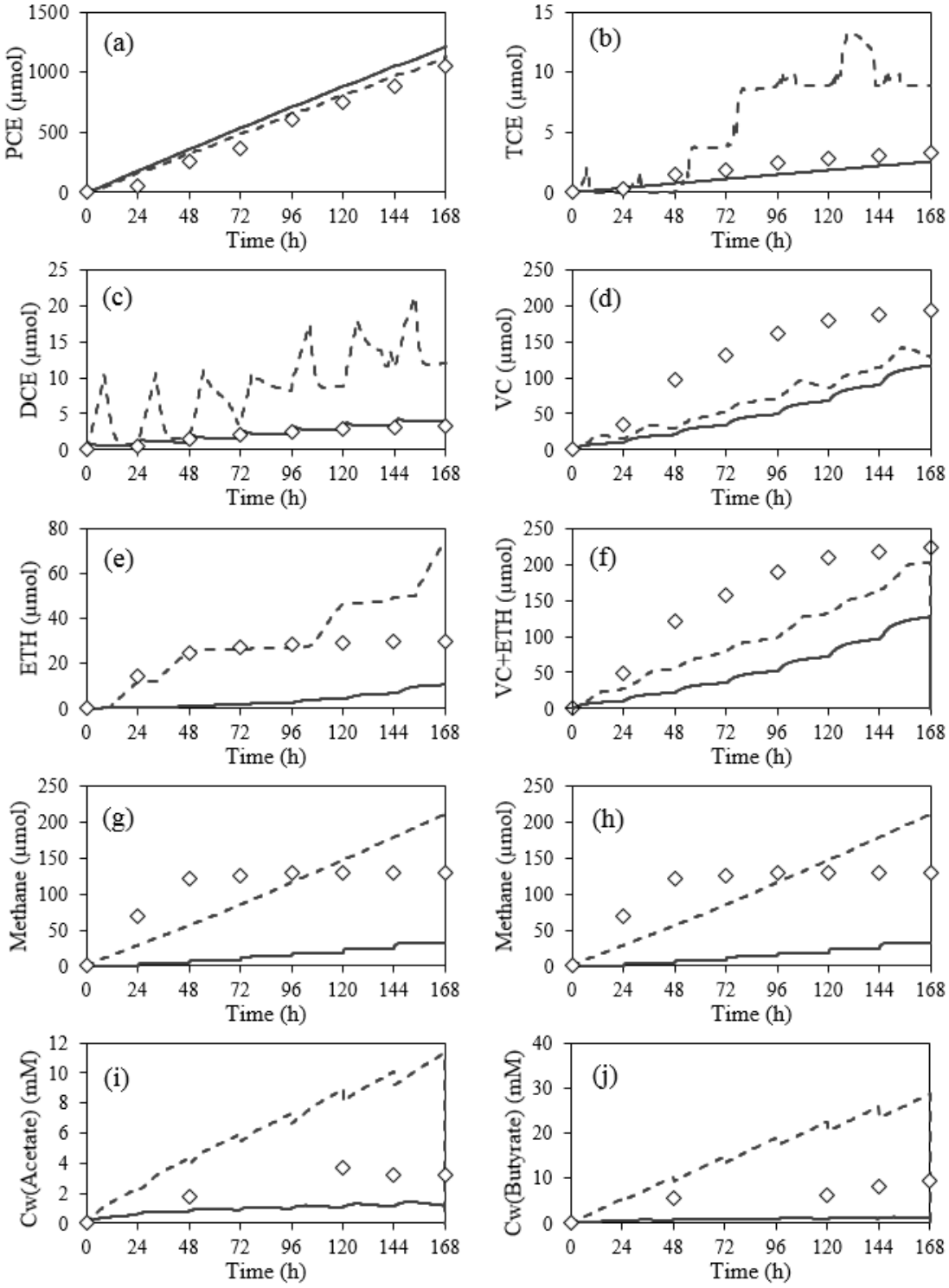

E. HLH3

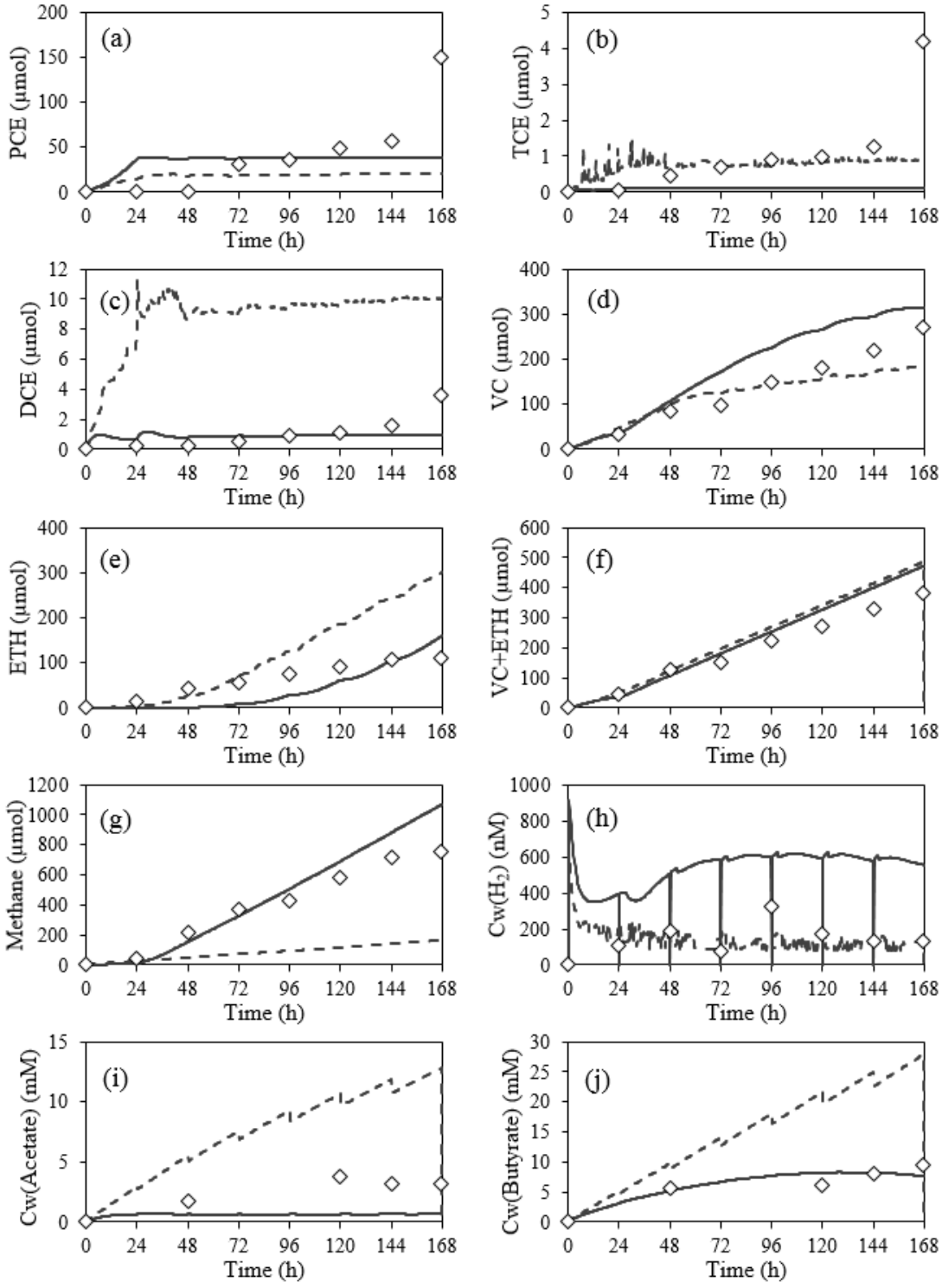
(a)
PCE (µmol)
Time (h)
(b)
TCE (µmol)
Time (h)
(c)
DCE (µmol)
Time (h)
(d)
VC (µmol)
Time (h)
(e)
ETH (µmol)
Time (h)
(f)
VC+ETH (µmol)
Time (h)
(g)
Methane (µmol)
Time (h)
(h)
Cw(H2) (nM)
Time (h)
(i)
Cw(Acetate) (mM)
Time (h)
(j)
Cw(Butyrate) (mM)
Time (h)

F. HLL2

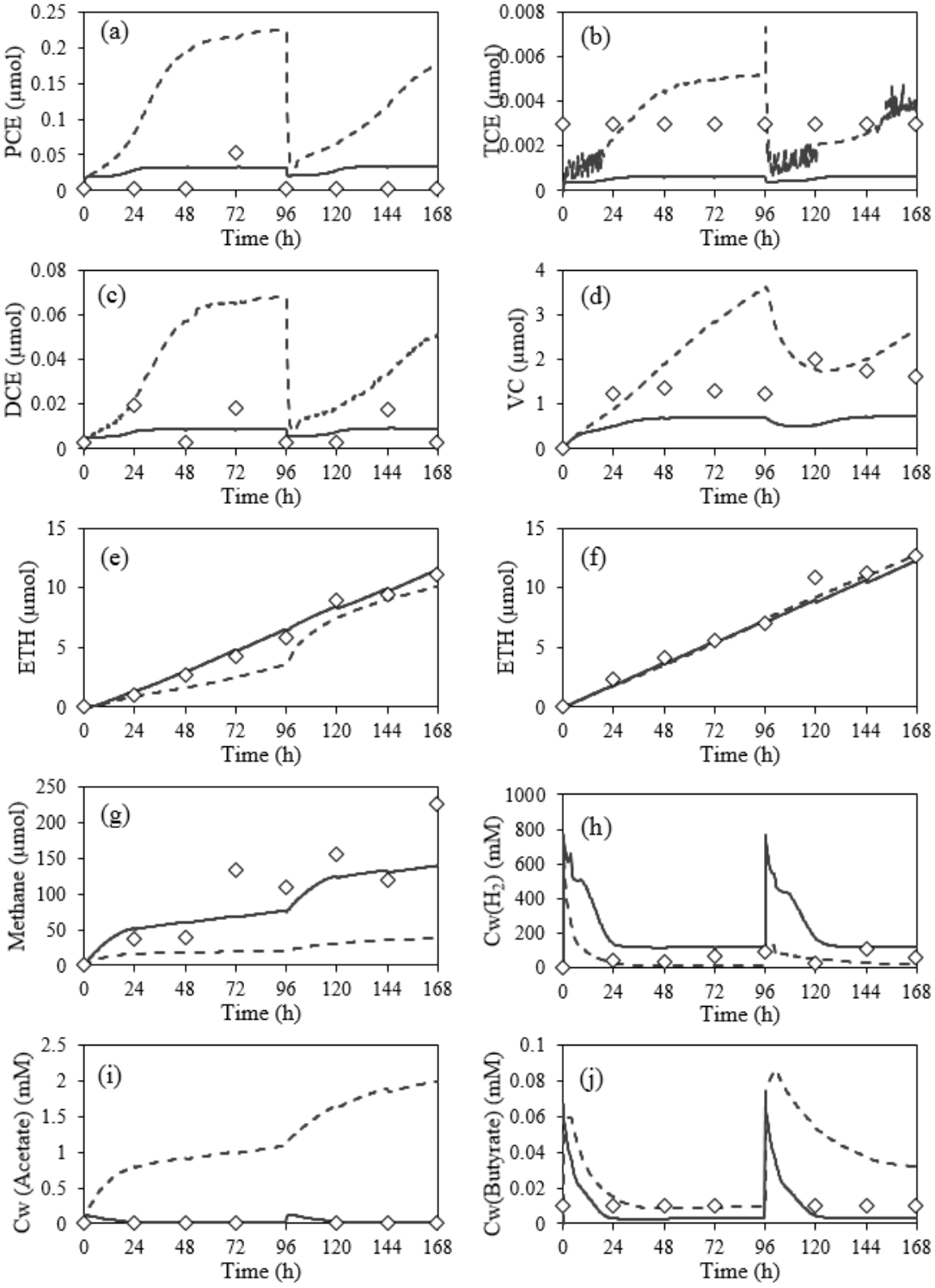
(a)
PCE (µmol)
0.25
0.2
0.15
0.1
0.05
0
0 24 48 72 96 120 144 168
Time (h)
(b)
TCE (µmol)
0.008
0.006
0.004
0.002
0
0 24 48 72 96 120 144 168
Time (h)
(c)
DCE (µmol)
0.08
0.06
0.04
0.02
0
0 24 48 72 96 120 144 168
Time (h)
(d)
VC (µmol)
4
3
2
1
0
0 24 48 72 96 120 144 168
Time (h)
(e)
ETH (µmol)
15
10
5
0
0 24 48 72 96 120 144 168
Time (h)
(f)
ETH (µmol)
15
10
5
0
0 24 48 72 96 120 144 168
Time (h)
(g)
Methane (µmol)
250
200
150
100
50
0
0 24 48 72 96 120 144 168
Time (h)
(h)
Cw(H2) (mM)
1000
800
600
400
200
0
0 24 48 72 96 120 144 168
Time (h)
(i)
Cw (Acetate) (mM)
2.5
2
1.5
1
0.5
0
0 24 48 72 96 120 144 168
Time (h)
(j)
Cw(Butyrate) (mM)
0.1
0.08
0.06
0.04
0.02
0
0 24 48 72 96 120 144 168
Time (h)

G. HLL3

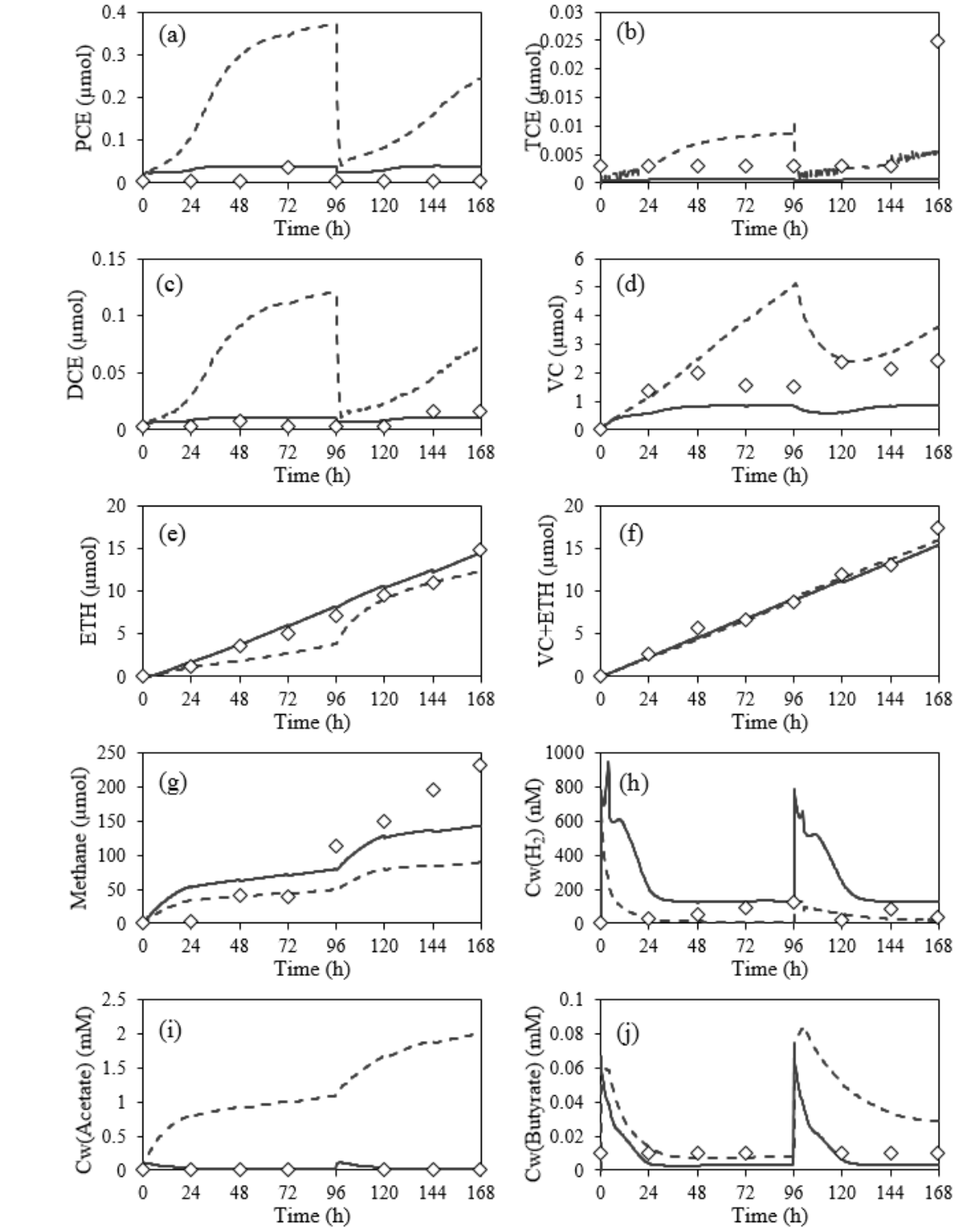
(a)
PCE (µmol)
Time (h)
(b)
TCE (µmol)
Time (h)
(c)
DCE (µmol)
Time (h)
(d)
VC (µmol)
Time (h)
(e)
ETH (µmol)
Time (h)
(f)
VC+ETH (µmol)
Time (h)
(g)
Methane (µmol)
Time (h)
(h)
Cw(H2) (nM)
Time (h)
(i)
Cw(Acetate) (mM)
Time (h)
(j)
Cw(Butyrate) (mM)
Time (h)

H. P0FY01

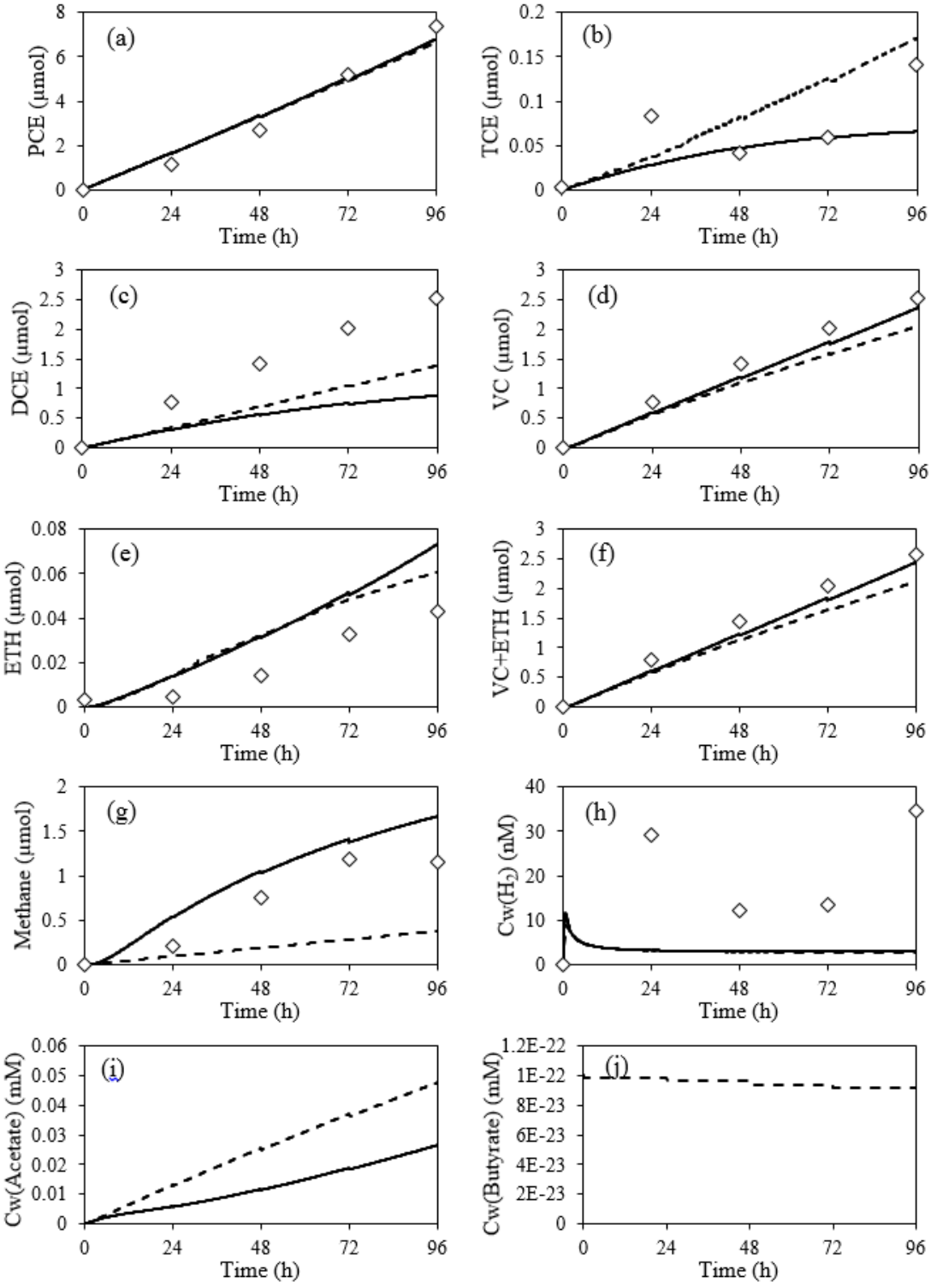
(a)
PCE (µmol)
Time (h)
(b)
TCE (µmol)
Time (h)
(c)
DCE (µmol)
Time (h)
(d)
VC (µmol)
Time (h)
(e)
ETH (µmol)
Time (h)
(f)
VC+ETH (µmol)
Time (h)
(g)
Methane (µmol)
Time (h)
(h)
Cw(H2) (nM)
Time (h)
(i)
Cw(Acetate) (mM)
Time (h)
(j)
Cw(Butyrate) (mM)
Time (h)

I. P0FY02

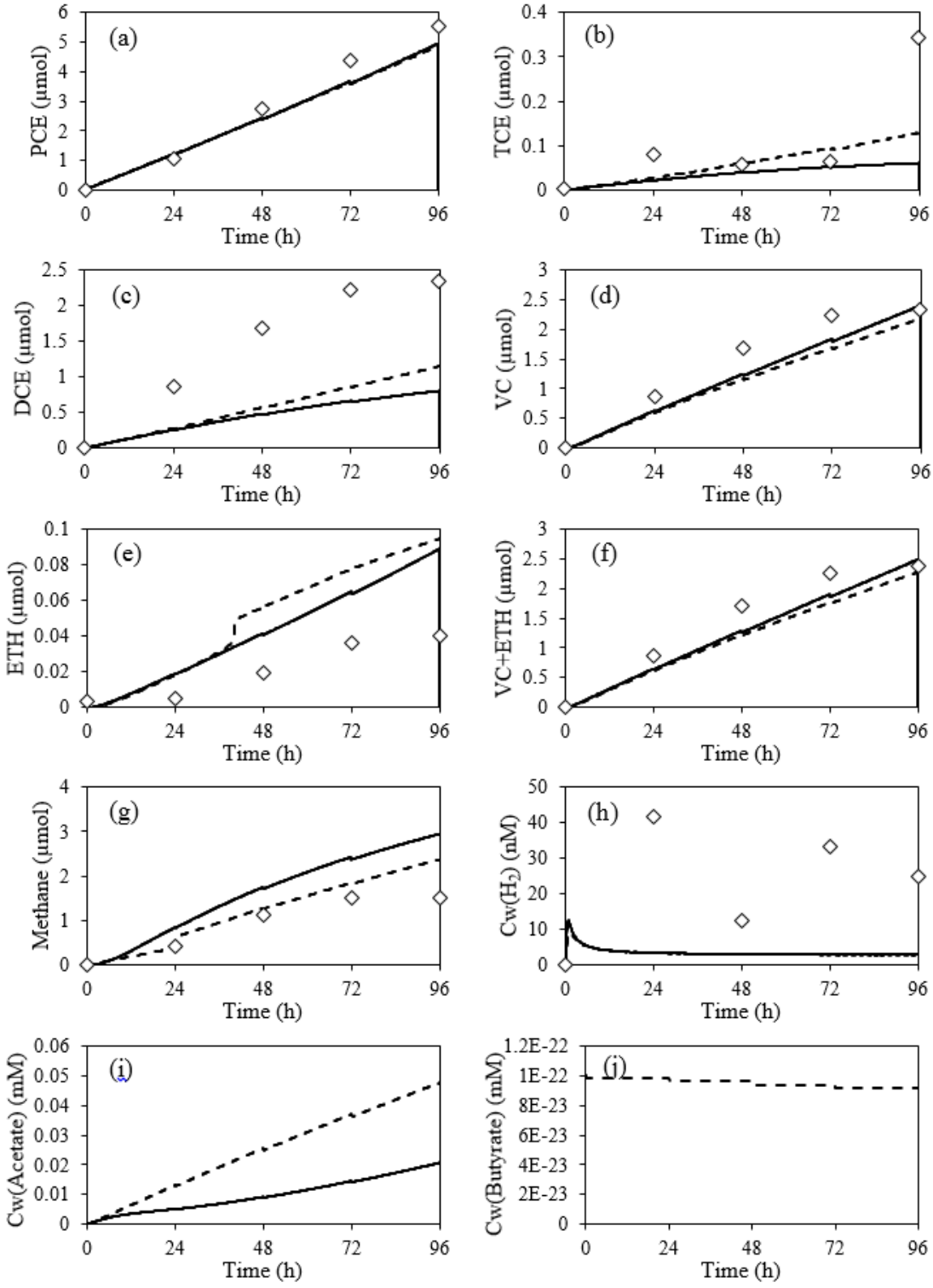
(a)
PCE (µmol)
Time (h)
(b)
TCE (µmol)
Time (h)
(c)
DCE (µmol)
Time (h)
(d)
VC (µmol)
Time (h)
(e)
ETH (µmol)
Time (h)
(f)
VC+ETH (µmol)
Time (h)
(g)
Methane (µmol)
Time (h)
(h)
Cw(H2) (nM)
Time (h)
(i)
Cw(Acetate) (mM)
Time (h)
(j)
Cw(Butyrate) (mM)
Time (h)

J. P0FYY1

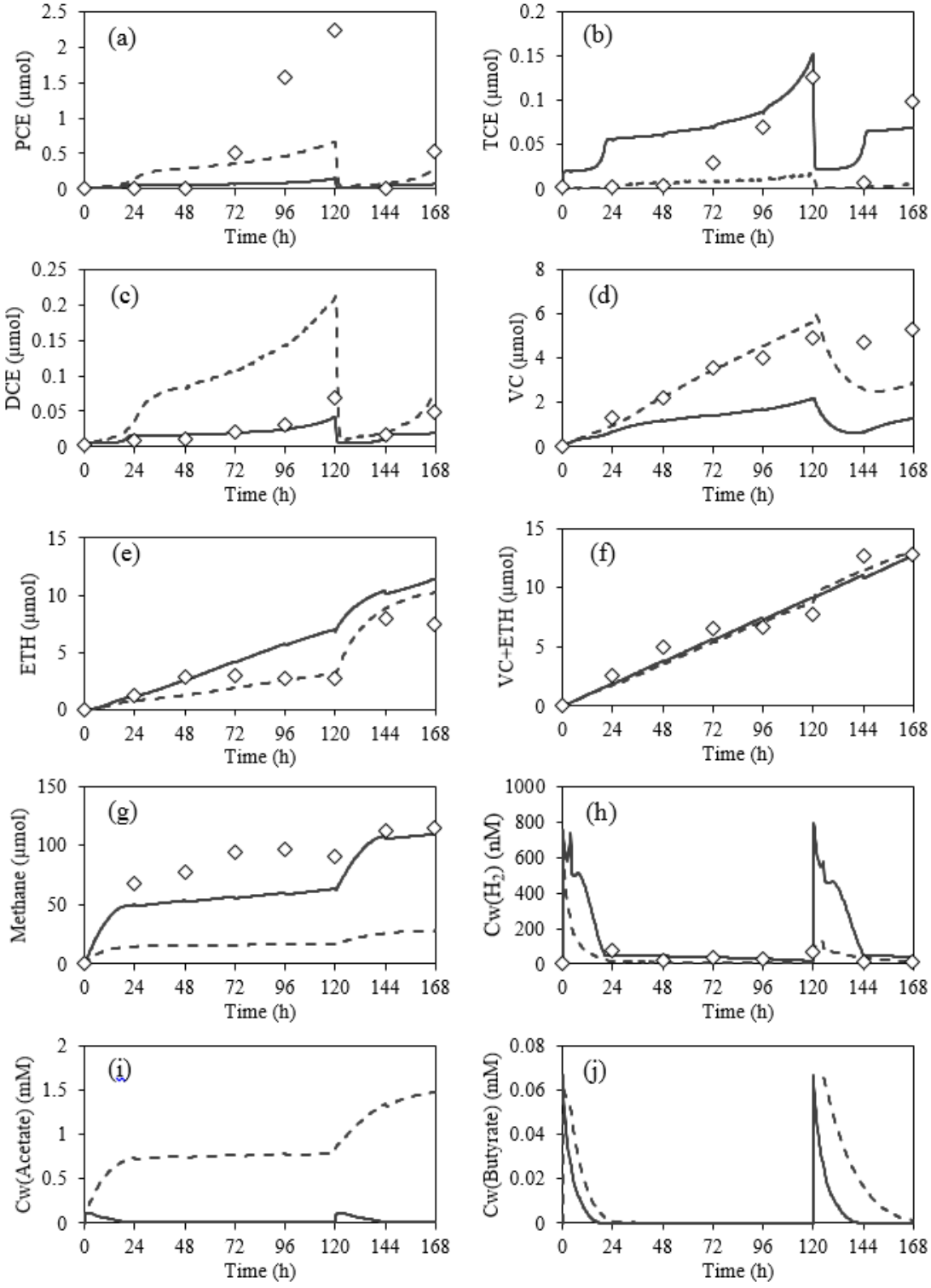
(a)
PCE (µmol)
Time (h)
(b)
TCE (µmol)
Time (h)
(c)
DCE (µmol)
Time (h)
(d)
VC (µmol)
Time (h)
(e)
ETH (µmol)
Time (h)
(f)
VC+ETH (µmol)
Time (h)
(g)
Methane (µmol)
Time (h)
(h)
Cw(H2) (nM)
Time (h)
(i)
Cw(Acetate) (mM)
Time (h)
(j)
Cw(Butyrate) (mM)
Time (h)

K. P0FYY2

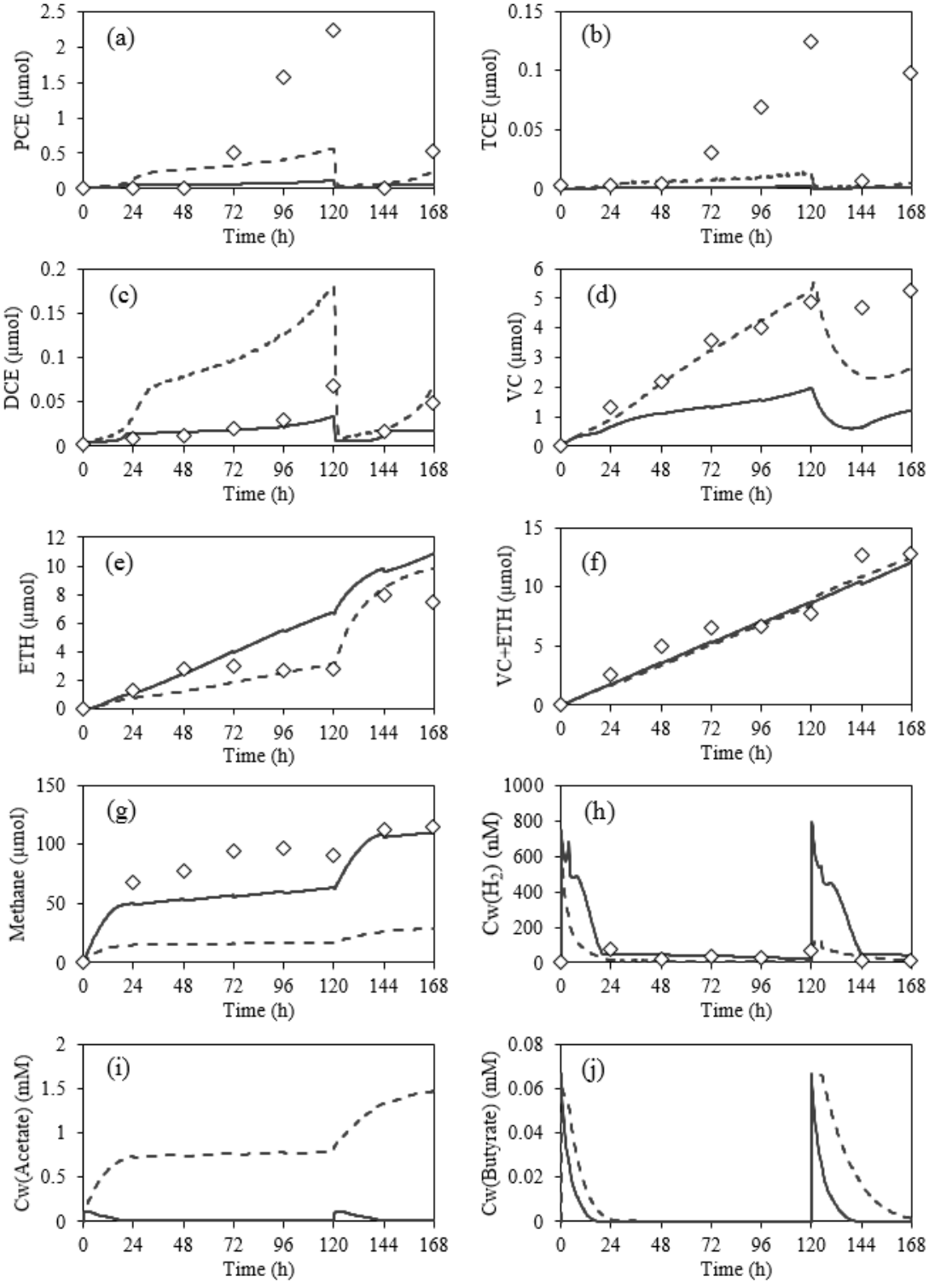
(a)
PCE (µmol)
Time (h)
(b)
TCE (µmol)
Time (h)
(c)
DCE (µmol)
Time (h)
(d)
VC (µmol)
Time (h)
(e)
ETH (µmol)
Time (h)
(f)
VC+ETH (µmol)
Time (h)
(g)
Methane (µmol)
Time (h)
(h)
Cw(H2) (nM)
Time (h)
(i)
Cw(Acetate) (mM)
Time (h)
(j)
Cw(Butyrate) (mM)
Time (h)

L. HiP1

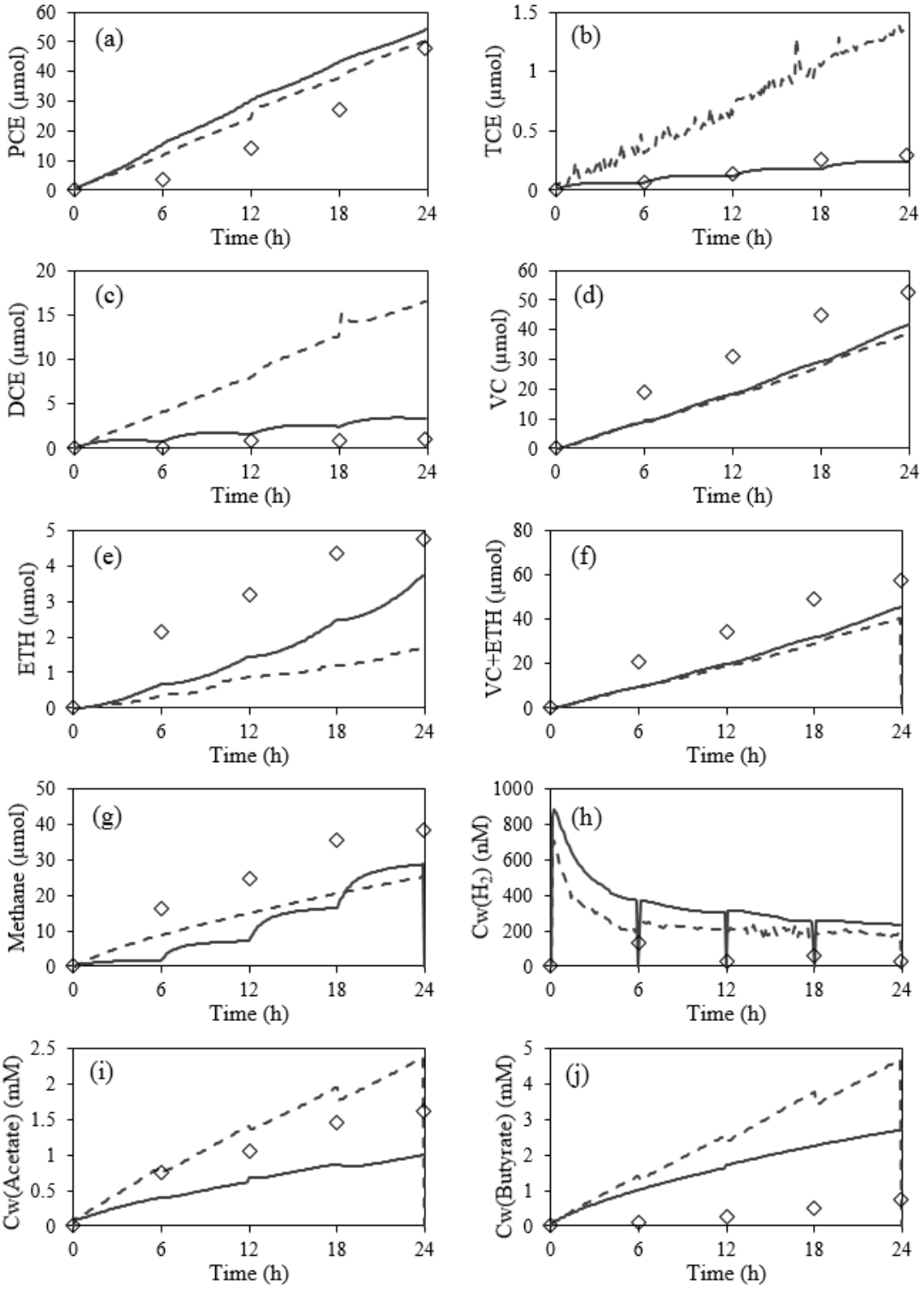
(a)
PCE (µmol)
Time (h)
(b)
TCE (µmol)
Time (h)
(c)
DCE (µmol)
Time (h)
(d)
VC (µmol)
Time (h)
(e)
ETH (µmol)
Time (h)
(f)
VC+ETH (µmol)
Time (h)
(g)
Methane (µmol)
Time (h)
(h)
Cw(H2) (nM)
Time (h)
(i)
Cw(Acetate) (mM)
Time (h)
(j)
Cw(Butyrate) (mM)
Time (h)

M. HiP2

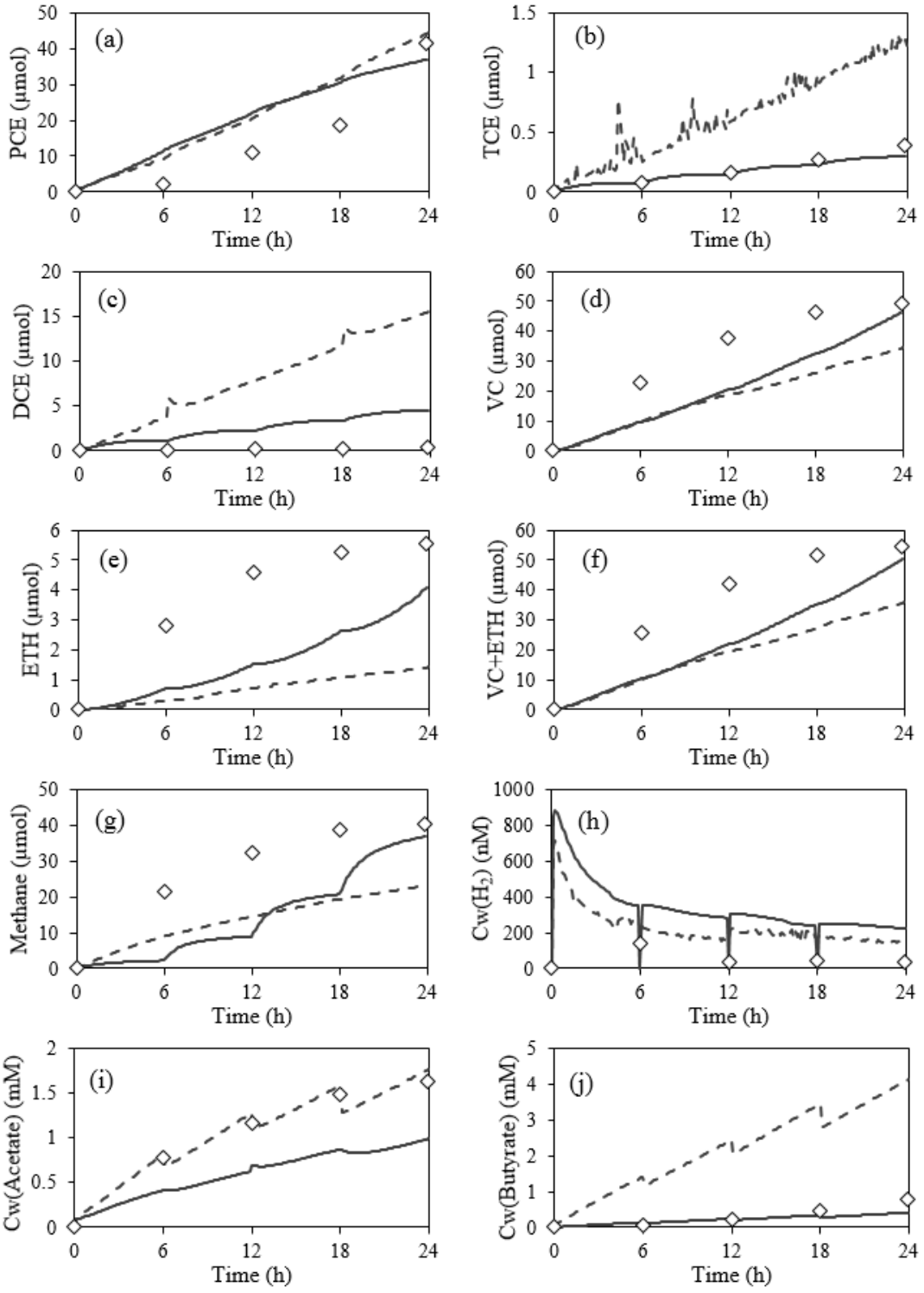
(a)
PCE (µmol)
Time (h)
(b)
TCE (µmol)
Time (h)
(c)
DCE (µmol)
Time (h)
(d)
VC (µmol)
Time (h)
(e)
ETH (µmol)
Time (h)
(f)
VC+ETH (µmol)
Time (h)
(g)
Methane (µmol)
Time (h)
(h)
Cw(H2) (nM)
Time (h)
(i)
Cw(Acetate) (mM)
Time (h)
(j)
Cw(Butyrate) (mM)
Time (h)

N. HiP3

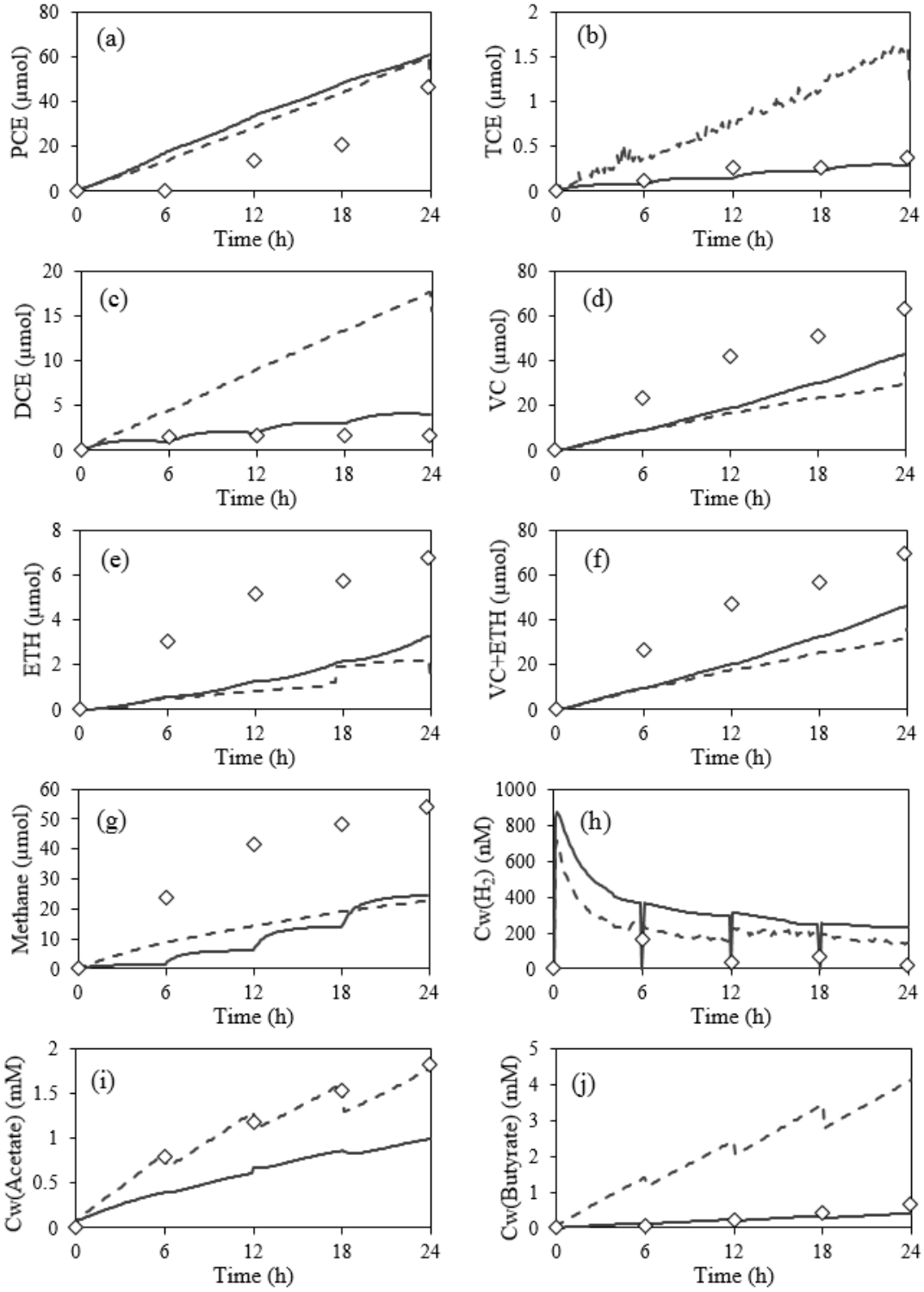
(a)
PCE (µmol)
Time (h)
(b)
TCE (µmol)
Time (h)
(c)
DCE (µmol)
Time (h)
(d)
VC (µmol)
Time (h)
(e)
ETH (µmol)
Time (h)
(f)
VC+ETH (µmol)
Time (h)
(g)
Methane (µmol)
Time (h)
(h)
Cw(H2) (nM)
Time (h)
(i)
Cw(Acetate) (mM)
Time (h)
(j)
Cw(Butyrate) (mM)
Time (h)

O. T3A1

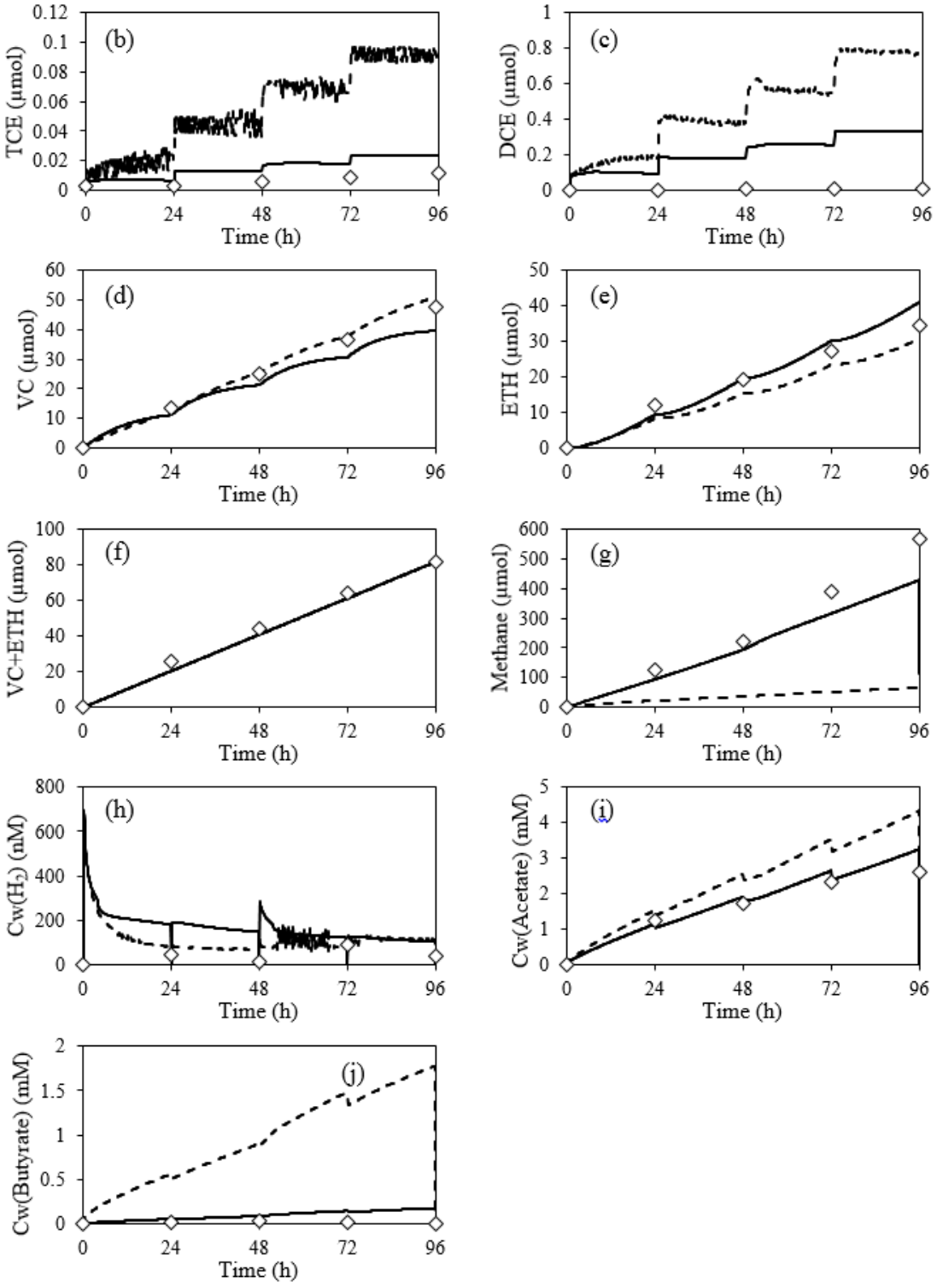
(b)
TCE (µmol)
Time (h)
(c)
DCE (µmol)
Time (h)
(d)
VC (µmol)
Time (h)
(e)
ETH (µmol)
Time (h)
(f)
VC+ETH (µmol)
Time (h)
(g)
Methane (µmol)
Time (h)
(h)
Cw(H2) (nM)
Time (h)
(i)
Cw(Acetate) (mM)
Time (h)
(j)
Cw(Butyrate) (mM)
Time (h)

P. T3B1

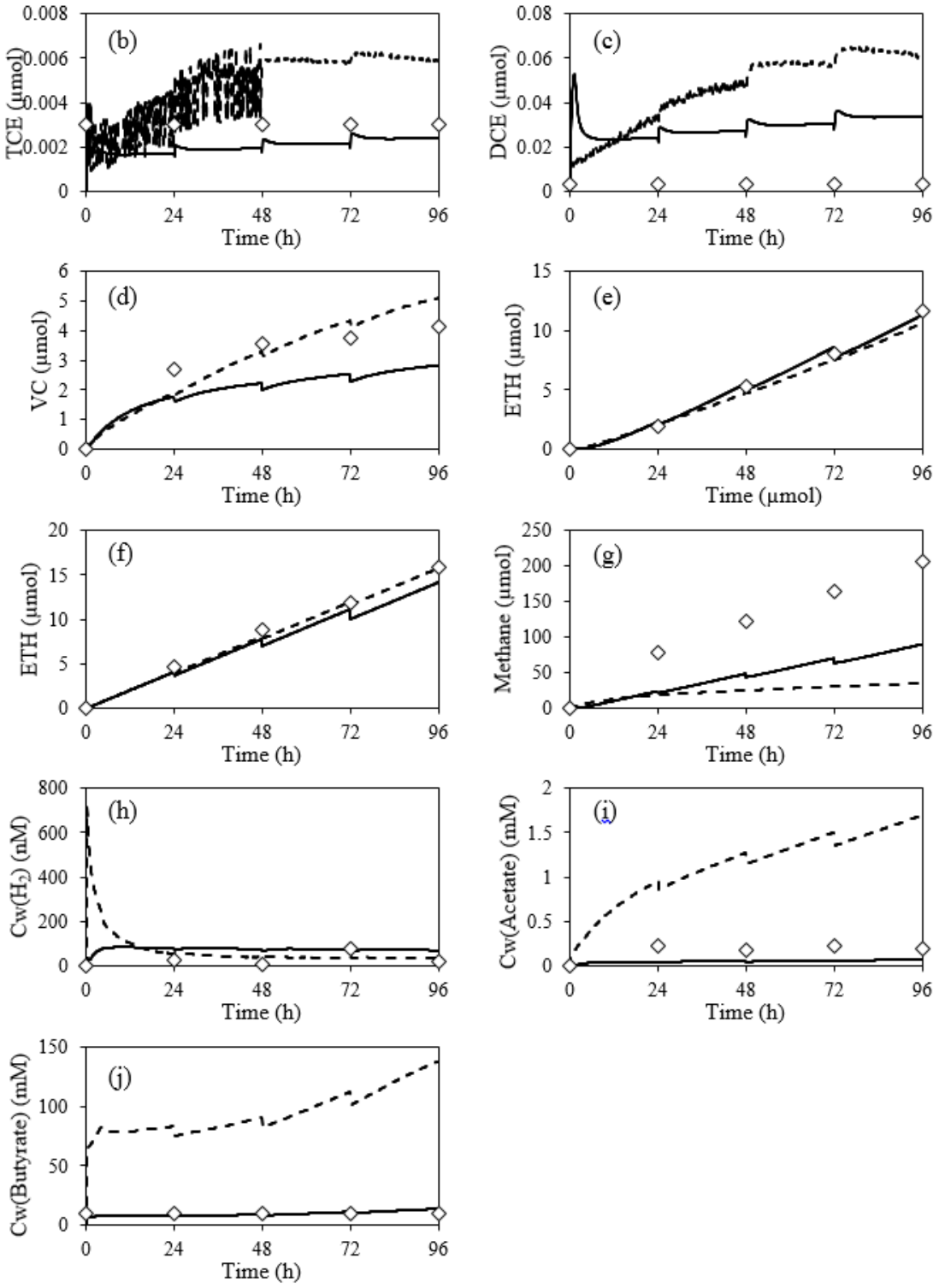
(b)
TCE (µmol)
0.008
0.006
0.004
0.002
0
0
24
48
72
96
Time (h)
(c)
DCE (µmol)
0.08
0.06
0.04
0.02
0
Time (h)
(d)
VC (µmol)
6
5
4
3
2
1
0
Time (h)
(e)
ETH (µmol)
15
10
5
0
Time (µmol)
(f)
ETH (µmol)
20
15
10
5
0
Time (h)
(g)
Methane (µmol)
250
200
150
100
50
0
Time (h)
(h)
Cw(H2) (nM)
800
600
400
200
0
Time (h)
(i)
Cw(Acetate) (mM)
2
1.5
1
0.5
0
Time (h)
(j)
Cw(Butyrate) (mM)
150
100
50
0
Time (h)

Q. T3C1

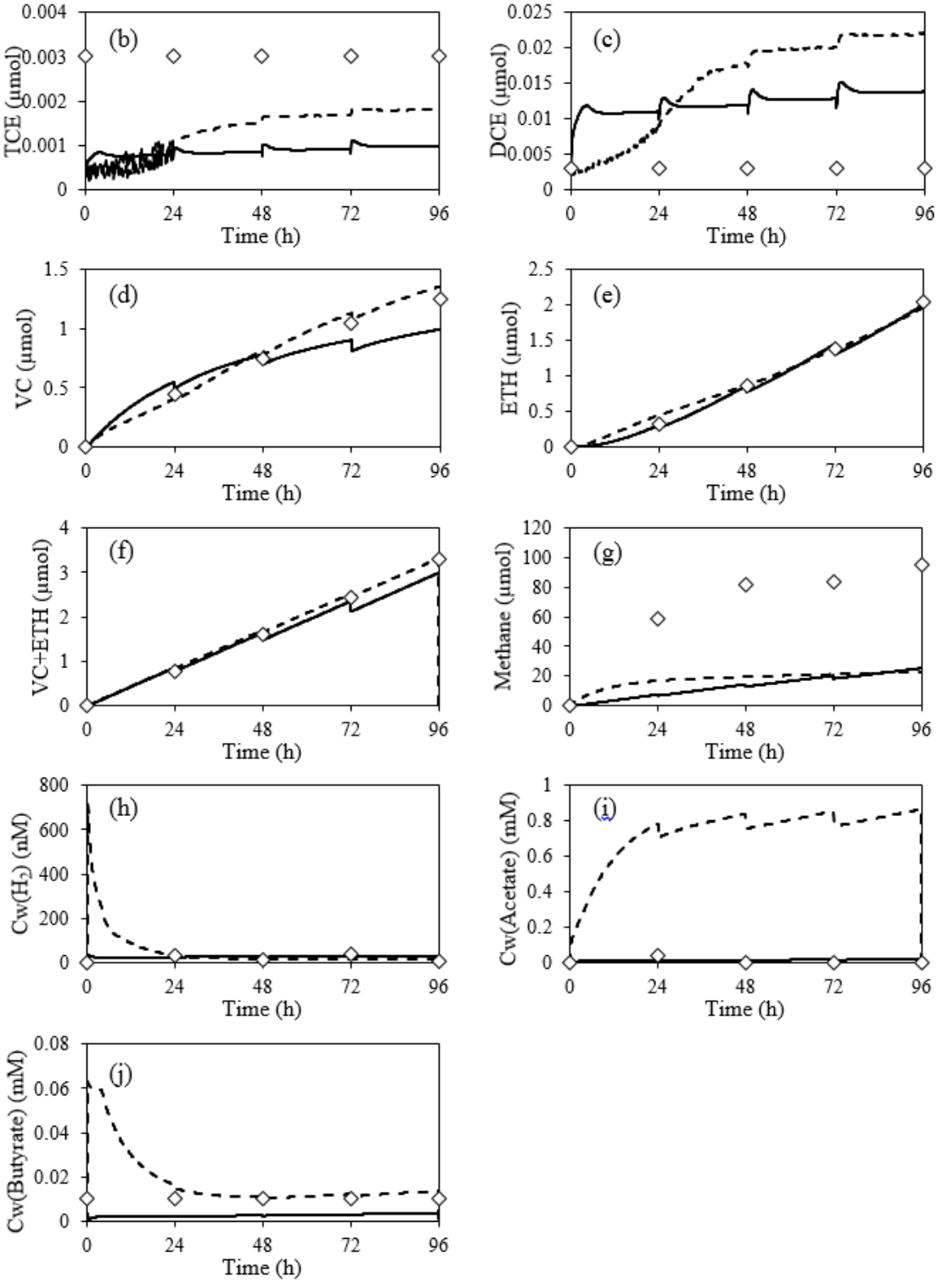
(b)
TCE (µmol)
0.004
0.003
0.002
0.001
0
0
24
48
72
96
Time (h)
(c)
DCE (µmol)
0.025
0.02
0.015
0.01
0.005
0
Time (h)
(d)
VC (µmol)
1.5
1
0.5
0
Time (h)
(e)
ETH (µmol)
2.5
2
1.5
1
0.5
0
Time (h)
(f)
VC+ETH (µmol)
4
3
2
1
0
Time (h)
(g)
Methane (µmol)
120
100
80
60
40
20
0
Time (h)
(h)
Cw(H2) (nM)
800
600
400
200
0
Time (h)
(i)
Cw(Acetate) (mM)
1
0.8
0.6
0.4
0.2
0
Time (h)
(j)
Cw(Butyrate) (mM)
0.08
0.06
0.04
0.02
0
Time (h)

R. D3A2

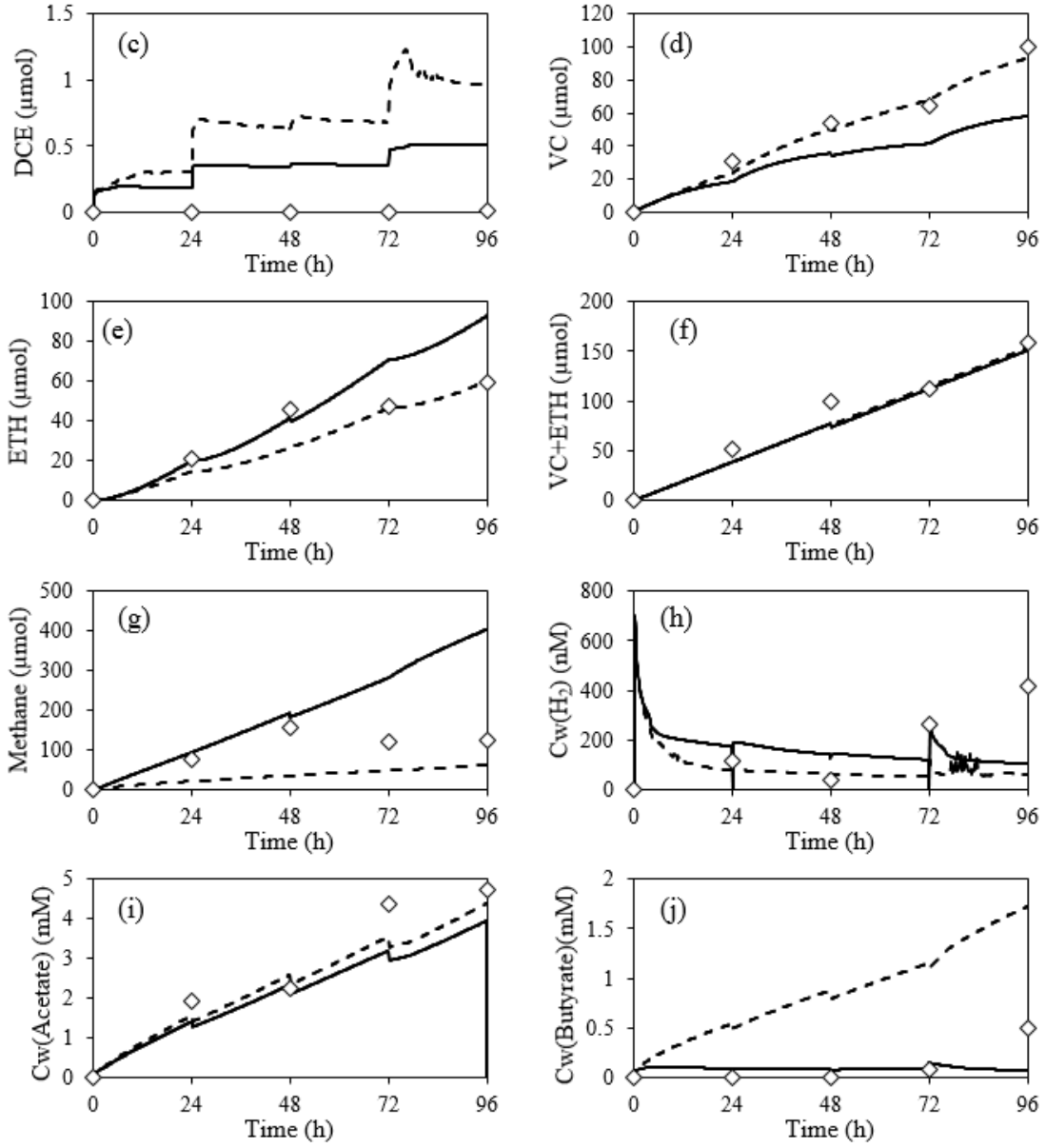
(c)
DCE (µmol)
Time (h)
(d)
VC (µmol)
Time (h)
(e)
ETH (µmol)
Time (h)
(f)
VC+ETH (µmol)
Time (h)
(g)
Methane (µmol)
Time (h)
(h)
Cw(H2) (nM)
Time (h)
(i)
Cw(Acetate) (mM)
Time (h)
(j)
Cw(Butyrate)(mM)
Time (h)

S. D3B2

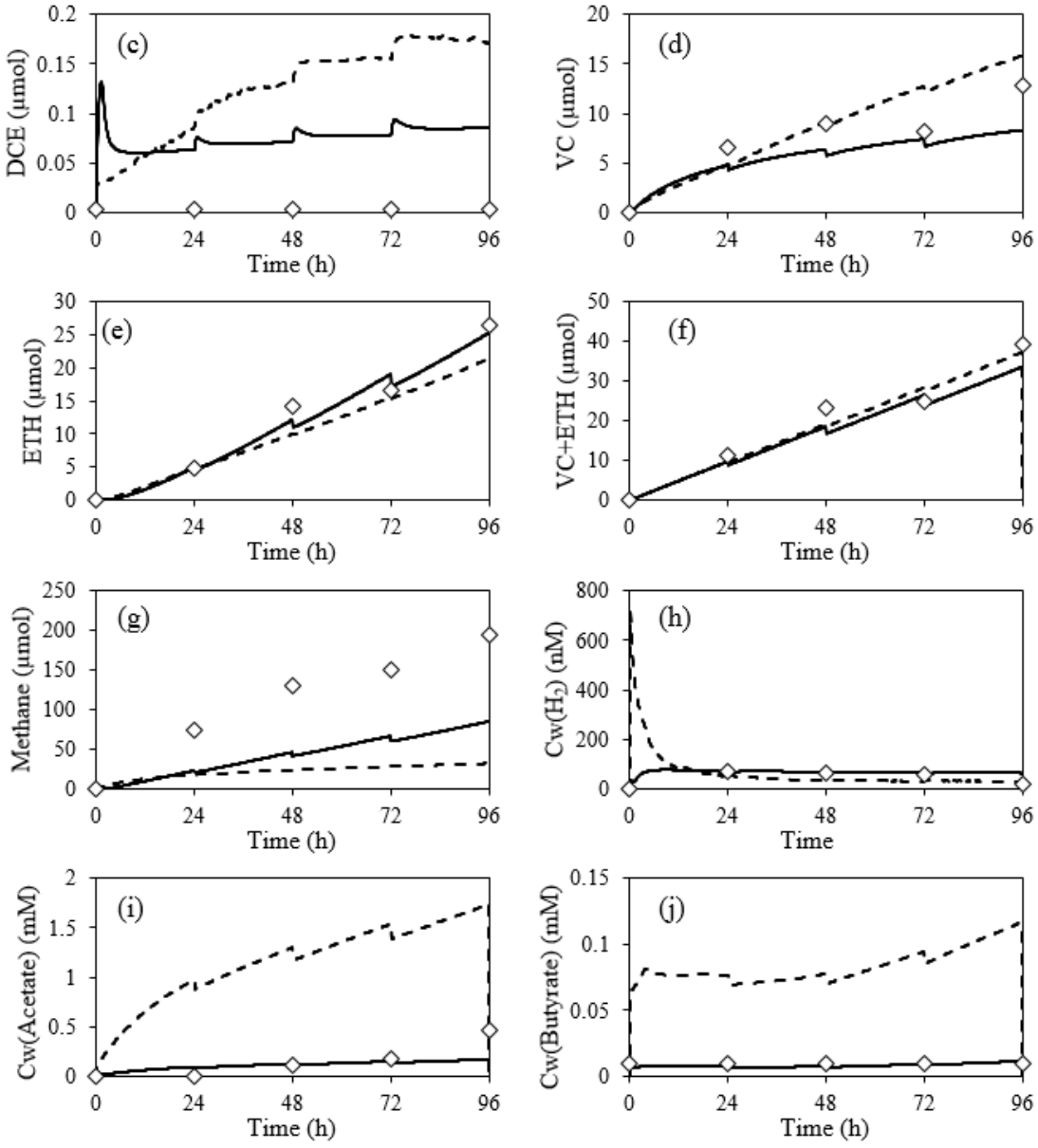
(c)
DCE (µmol)
Time (h)
(d)
VC (µmol)
Time (h)
(e)
ETH (µmol)
Time (h)
(f)
VC+ETH (µmol)
Time (h)
(g)
Methane (µmol)
Time (h)
(h)
Cw(H2) (nM)
Time
(i)
Cw(Acetate) (mM)
Time (h)
(j)
Cw(Butyrate) (mM)
Time (h)

T. D3C2

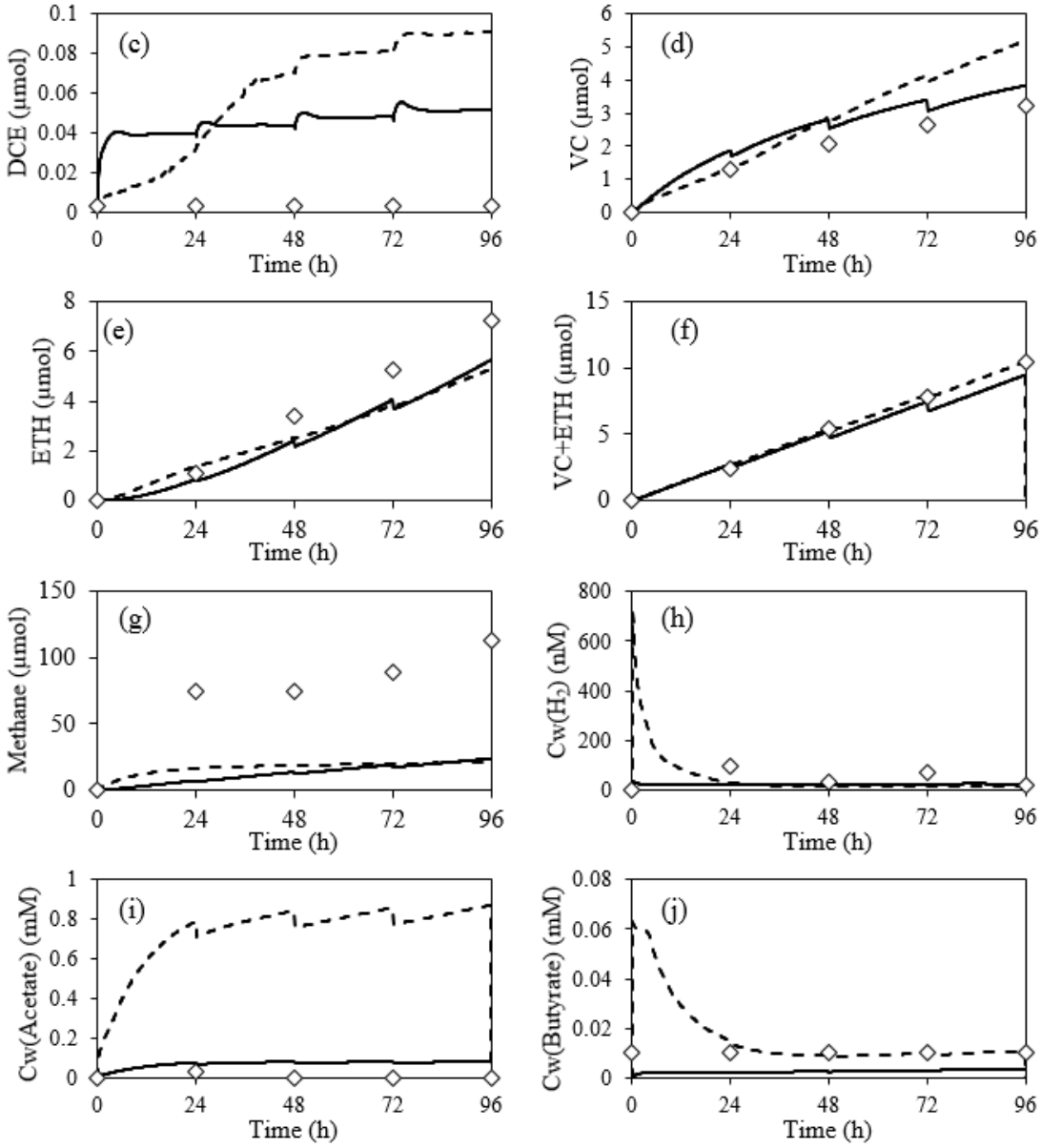
(c)
DCE (µmol)
Time (h)
(d)
VC (µmol)
Time (h)
(e)
ETH (µmol)
Time (h)
(f)
VC+ETH (µmol)
Time (h)
(g)
Methane (µmol)
Time (h)
(h)
Cw(H2) (nM)
Time (h)
(i)
Cw(Acetate) (mM)
Time (h)
(j)
Cw(Butyrate) (mM)
Time (h)

APPENDIX IV CONSTANTS USED IN MODEL SIMULATOINS

In this section, each numbered entry is a constant used in model simulations. Entries in black are the regular kinetic constants used in running the model. Entries in red are the ones can be changed by the model operators to control the model simulating conditions. The values of the entries in blue are tested and determined in this research study by trial-and-error analysis. Text in green is supplementary information.

1. Ac_Inhibition = 1.
   Control factor for substrate inhibition (Haldane inhibition) by acetate, Ac_Inhibition = 1 for models with Haldane inhibition by acetate; Ac_Inhibition = 0 for models without Haldane inhibition by acetate.
2. Ac_Methanogens_mgVSS_per_cell = 4.37×10^{-10} mgVSS/cell.
3. Acetate_Formed_per_Butyrate = 2 µmol acetate formed/µmol butyrate fermented to acetate.
4. Acetate_Formed_per_Lactate = 1 µmol acetate formed/µmol lactate fermented to acetate.
5. Acetate_Formed_per_Lactate_to_Propionate = 1/3 µmol acetate formed/µmol lactate fermented to propionate.
6. Acetate_Formed_per_Propionate = 1 µmol acetate formed/µmol propionate.
7. Acetotrophs_DNA_Copies_per_Cell = 2.
   Number of copies of the 16S gene per cell.
8. Acetotrophs_Initial_Copies = 1.13×10^{10} copies in 100 mL.
   Initial copies of 16S gene in 100 mL of culture.
9. Butyrate_ueq_per_umol = 4 µeq/µmol HBu.
10. Const_End_Decay = 0.02 /h.
    Endogenous decay coefficient.
11. Constant_Butyrate_Feed = 1.
    Control factor for constant butyrate feed. When there is constant butyrate feed, Constant_Butyrate_Feed = 1; else, Constant_Butyrate_Feed = 0.
12. Constant_EA_Feed = 1.
    Control factor for constant EA feeding. When there is constant EA feeding, Constant_EA_Feed = 1; else, Constant_EA_Feed = 0.
13. Constant_Endogenous_Decay = 0.
    Control factor for endogenous decay. If endogenous decay is considered in the model, Constant_Endogenous_Decay = 1; else, Constant_Endogenous Decay = 0.
14. Constant_Hydrogen_Feed = 0.
    Control factor for constant hydrogen feed. When there is constant hydrogen feed, Constant_Hydrogen_Feed = 1; else, Constant_Hydrogen_Feed = 0.
15. Cw_BHB = 1.0×10^{-17} mol/L.
    Aqueous concentration of BHB^--like products.
16. Cw_Bicarbonate = 0.714 mol/L.
    Bicarbonate concentration in the basal salts medium.
17. DCE_to_VC_Competitive_Inhibition = 1.
    Control factor for competitive inhibition: DCE dechlorination.
18. DHC_DNA_Copies_per_Cell = 1.
    DHC has one copy of the 16S gene per cell.
19. DHC_Initial_Copies = 2.73×10^{10} copies in 100mL.
    Initial copies of 16S gene in 100mL of culture.
20. Decay_Acetotrophs = 1.0×10^{-3} /h.

21. Decay_Butyrate_Fermenters = 1.0×10^{-3} /h
22. Decay_Dechlorinators = 1.0×10^{-3} /h
23. Decay_Hydrogenotrophic_Methanogens = 1.0×10^{-3} /h.
24. Dechlorinators_mgVSS_per_cell = 2.688×10^{-11} mgVSS/cell.
25. Ethanol_ueq_per_umol = 4 µeq/µmol ethanol.
26. Feed_Increment_Time = 1000 h.
    This is the increment time (h) between feedings.
27. Feed_Increment_Time_Donor = 24 h.
    This is the increment time (h) between pulse ED feedings
28. Feed_Increment_Time_EA = 24 h.
    This is the increment time (h) between pulse EA feedings
29. Feed_Pulse_Time_Donor = 0 h.
    The time (h) at which the first feed pulse of ED occurs
30. Feed_Pulse_Time_EA = 0 h.
    The time (h) at which the first feed pulse of ED occurs
31. Feed_Rate_PCE = 0 µL/min.
    The rate at which PCE is fed to the microcosm (µL/min) beginning at 0 h until the end of the experiment.
32. Feed_Rate_TCE = 0 µL/min.
    The rate at which TCE is fed to the microcosm (µL/min) beginning at 0 h until the end of the experiment.
33. Feed_Rate_cDCE = 0 µL/min.
    The rate at which cDCE is fed to the microcosm (µL/min) beginning at 0 h until the end of the experiment.
34. Feed_Time_Donor = 0 h.
    The time (h) at which the first feed pulse of ED occurs.
35. Feed_Time_Electron_Acceptor = 0 h.
    The time (h) when the first input of electron acceptor occurs.
36. Fermenters_DNA_Copies_per_Cell = 3.
    The number of copies of the 16S gene per cell.
37. Fermenters_Initial_Copies = 4.93×10^{9} copies in 100 mL.
    Initial copies of 16S gene in 100 mL of culture.
38. Fermenters_mgVSS_per_cell = 7.855×10^{-10} mgVSS/cell.
39. Fraction_of_ED_pool_treated_as_butyrate = 0.
40. Fraction_of_YE_pool_treated_as_butyrate = 0.5.
41. H2_Methanogens_mgVSS_per_cell = 5.998×10^{-10} mgVSS/cell.
42. H2_Threshold_dechlor = 0.0015 µmol/L.
    Estimated by Fennell (1997) from FYE- or non-fed culture.
43. H2_Threshold_meth = 0.008 µmol/L.
    Estimated by Fennell (1997).
44. H2_per_Butyrate_Fermented_to_Acetate = 2 µmol hydrogen/µmol butyrate fermented to acetate.
45. H2_per_DCE_Dechlorinated = 1 µmol hydrogen/µmol DCE converted to VC.
46. H2_per_Lactate_Fermented_to_Acetate = 2 µmol hydrogen/µmol lactate fermented to acetate.
47. H2_per_PCE_Dechlorinated = 1 µmol hydrogen/µmol PCE converted to TCE.
48. H2_per_Propionate_Fermented_to_Acetate = 3 µmol hydrogen/µmol propionate fermented to Acetate.
49. H2_per_TCE_Dechlorinated = 1 µmol hydrogen/µmol TCE converted to DCE.
50. H2_per_VC_Dechlorinated = 1 µmol hydrogen/µmol VC converted to ETH.
51. H2_to_CH4_Molar_Conversion_Factor = 0.25 µmol CH_4 formed per µmol H2.

52. Hc_CH4 = 33.1.
    Dimensionless, 30°C.
53. Hc_DCE = 0.19.
    Dimensionless, for cis-1,2-DCE, 30°C.
54. Hc_ETH = 9.
    Pseudo-dimensionless, DiStefano (1992).
55. Hc_H2 = 52.7.
    Dimensionless, Younge (1981).
56. Hc_PCE = 0.917.
    Dimensionless, 30°C.
57. Hc_TCE = 0.491.
    Dimensionless, 30°C.
58. Hc_VC = 1.264.
    Dimensionless, 30°C.
59. Hydrogenotrophic_Methanogens_DNA_Copies_per_Cell = 4.
    The number of copies of the 16S gene per cell.
60. Hydrogenotrophic_Methanogens_Initial_Copies = 6.78×10^{10} copies in 100 mL.
61. Initial_Acetate = 0 µmol.
    The initial amount of acetate present.
62. Initial_Butyrate = 0 µmol.
    The initial amount of butyrate present
63. Initial_Culture_Dilution = 1.
    Dilution of initial culture: undiluted = 1, half = 0.5, quarter = 0.25.
64. Initial_DCE = 0 µmol/bottle.
65. Initial_ETH = 0 µmol/bottle.
66. Initial_H2 = 0 µmol/bottle.
67. Initial_Methane = 0 µmol/bottle.
68. Initial_PCE = 0 µmol/bottle.
69. Initial_Propionate = 1×10^{-20} µmol/bottle.
70. Initial_TCE = 0 µmol/bottle.
71. Initial_VC = 0 µmol/bottle.
72. Ionic_Strength = 0.0856 eq/L.
    Estimated for the basal salts medium
73. KI_Ac = 1047 µmol/L.
    Haldane inhibition constant: acetate inhibiting acetoclastic methanogenesis.
74. K_CI_DCE_on_TCE = 2.93 µmol/L.
    Competitive inhibition constant: DCE inhibiting TCE dechlorination.
75. K_CI_DCE_on_VC = 2.93 µmol/L.
    Competitive inhibition constant: DCE inhibiting VC dechlorination.
76. K_CI_PCE_on_DCE = 22.2 µmol/L.
    Competitive inhibition constant: PCE inhibiting DCE dechlorination.
77. K_CI_PCE_on_TCE = 12.91 µmol/L
    Competitive inhibition constant: PCE inhibiting TCE dechlorination.
78. K_CI_PCE_on_VC = 12.91 µmol/L.
    Competitive inhibition constant: PCE inhibiting VC dechlorination.
79. K_CI_TCE_on_DCE = 0.182 µmol/L.
    Competitive inhibition constant: TCE inhibiting DCE dechlorination.
80. K_CI_TCE_on_PCE = 0.182 µmol/L.
    Competitive inhibition constant: TCE inhibiting PCE dechlorination.

81. K_CI_TCE_on_VC = 0.182 µmol/L.
    Competitive inhibition constant: DCE inhibiting TCE dechlorination.
82. K_HI_PCE_on_CH4_Acetate = 0.01 µmol/L.
    Haldane inhibition constant: PCE inhibiting acetoclastic methanogenesis.
83. K_HI_PCE_on_CH4_H2 = 0.01 µmol/L.
    Haldane inhibition constant: PCE inhibiting hydrogenotrophic methanogenesis.
84. K_HI_PCE_on_DCE = 60000 µmol/L.
    Haldane inhibition constant: PCE inhibiting DCE dechlorination.
85. K_HI_PCE_on_PCE = 17 µmol/L.
    Haldane inhibition constant: PCE inhibiting PCE dechlorination.
86. K_HI_PCE_on_TCE = 20 µmol/L.
    Haldane inhibition constant: PCE inhibiting TCE dechlorination.
87. K_HI_PCE_on_VC = 10000 µmol/L.
    Haldane inhibition constant: PCE inhibiting VC dechlorination.
88. Kla_CH4 = 50 /h.
    Smatlak (1995).
89. Kla_DCE = 38.2 /h.
    Estimated from the molar volume and Equation 9-26 of Schwarzenbach et al. (1993) and the relationship developed by Smatlak (1995).
90. Kla_ETH = 60 /h.
    Smatlak (1995).
91. Kla_H2 = 69.3 /h.
    Smatlak (1995).
92. Kla_PCE = 25 /h.
    Smatlak (1995).
93. Kla_TCE = 36 /h.
    Estimated from the molar volume and Equation 9-26 of Schwarzenbach et al. (1993) and the relationship developed by Smatlak (1995).
94. Kla_VC = 40 /h.
    Smatlak (1995).
95. Ks_Ace_to_BHB = 500 µmol/L.
    Half-velocity coefficient for acetate's fermentation to BHB^-- like products.
96. Ks_Acetate = 9689 µmol/L.
    Half-velocity coefficient for acetate degradation.
97. Ks_BHB = 500 µmol/L.
    Half-velocity coefficient for butyrate's fermentation to BHB^-- like products.
98. Ks_Butyrate = 260.8 µmol/L.
    Half-velocity coefficient for butyrate fermentation to acetate and hydrogen.
99. Ks_DCE = 2.93 µmol/L.
100. Ks_H2_Dechlor = 0.1 µmol/L.
    Half-velocity coefficient for H_2 for dechlorination, 0.1 µmol/L (Smatlak, 1995).
101. Ks_H2_methane = 0.5 µmol/L.
    Half-velocity coefficient for hydrogen to methane. An average value of 0.96 µmol/L was reported by Smatlak (1995); however, a slightly lower value was used for modeling.
102. Ks_Lactate_to_Acetate = 2.5 µmol/L.
    Half-velocity coefficient for lactate fermentation, 2.52 µmol/L Fennell (1996). 4x for 25°C
103. Ks_Lactate_to_Propionate = 2.5 µmol/L.
104. Ks_PCE = 12.91 µmol/L.

Half-velocity coefficient for PCE dechlorination, 0.54 µmol/L, Smatlak (1995); 0.6 µmol/L, Tandoi (1994). This value is calculated from nonlinear regression several PSS experiments by Heavner (2013).

105. Ks_Propionate = 11.3 µmol/L.
    Half-velocity coefficient for propionate fermentation, 11.3 µmol/L Fennell (1996). 4x for 25°C.
106. Ks_TCE = 0.182 µmol/L.
    This value is calculated from nonlinear regression several PSS experiments by Heavner (2013).
107. Ks_VC = 101 µmol/L.
    Half-velocity coefficient for VC, 290 µmol/L Smatlak (1995). Estimated from relative vmax/Ks in Tandoi et al. (1994), and the k/Ks for the pure culture for PCE. 3 µmol PCE to VC/16S DNA copies-h. This value is calculated from nonlinear regressions several PSS experiments by Heavner (2013).
108. Lactate_ueq_per_umol 4 µeeq/µmol Lac.
109. Liquid_Waste_Rate = 0.1.
    The liquids removed from sampling.
110. Neat_DCE_Feed_Rate = 0 µmol/h.
111. Neat_EA = 0.
    Control factor for neat EA feeding. If neat EA is fed, Neat_EA = 1; else, Neat_EA = 0.
112. Neat_PCE_Feed_Rate = 0 µmol/h.
113. Neat_TCE_Feed_Rate = 0 µmol/h.
114. PCE_Inhibition = 1.
    Control factor for PCE inhibiting dechlorinations. For models with PCE inhibiting dechlorinations, PCE_Inhibition = 1; else, PCE_Inhibition = 0.
115. PCE_Inhibition_to_CH_4 = 1.
    Control factor for PCE inhibiting dechlorinations. For models with PCE inhibiting dechlorinations, PCE_Inhibition = 1; else, PCE_Inhibition = 0.
116. PCE_to_TCE_Competitive_Inhibition = 1.
    Control factor for competitive inhibition: PCE dechlorination.
117. PCE_ueq_per_umol = 8 µeq_per_µmol.
118. Propionate_Formed_per_Lactate = 2/3 µmol propionate/µmol lactate converted to propionate.
119. Propionate_ueq_per_umol = 6 µeq/µmol Prop.
120. Pulse_Butyrate_Feed = 0.
    Control factor for pulse butyrate feedings. When there is pulse butyrate feeding, Pulse_Butyrate_Feed = 1; else, Pulse_Butyrate_Feed = 0.
121. Pulse_EA_Feed = 0.
    Control factor for pulse EA feedings. When there is pulse EA feeding, Pulse_EA_Feed = 1; else, Pulse_EA_Feed = 0.
122. Pulse_Value_Butyric_Acid = 44 µmol.
    This is the amount of butyric acid fed at each pulse beginning at 0 h (µmol).
123. Pulse_Value_DCE = 0 µmol.
    This is the amount of DCE fed at each pulse beginning at 0 h (µmol).
124. Pulse_Value_Hydrogen = 0 µmol.
    This is the amount of hydrogen fed (µmol) at each pulse beginning at 0 h and occuring every 48 h.
125. Pulse_Value_PCE = 0 µmol.
    This is the amount of PCE fed at each pulse beginning at 0 h (µmol).
126. Pulse_Value_Propionate_Acid = 0 µmol.
    This is the amount of propionic acid fed (µmol) at each pulse beginning at 0 h and occuring every 48 h.

127. Pulse_Value_TCE = 0 µmol.
    This is the amount of PCE fed at each pulse beginning at 0 h (µmol).
128. Purge_Increment_Time = 24 h.
    Time increment for purging the bottles.
129. Purge_Pulse_Time = 24 h.
    Time at which the first purge occurs.
130. R = 0.0831441 kJ/mol-K.
    For thermodynamic calculations.
131. R2 = 0.082054 L-atm/mol-K.
    To convert Cg (µmol) to partial pressure (atm).
132. Salt_Out_CH4 = 0.135 L/mol.
    Salt effect parameter for CH_4 in aqueous NaCl solution from a review of various studies. In solubility Data Series, Vol 27/28, Methane, C.L. Young, editor, (1981), Pergamon Press, Page 70.
133. Salt_Out_H2 = 0.102 L/mol.
    Salt effect parameter for H_2 in aqueous NaCl solution from a review of various studies. In solubility Data Series, Vol 5/6, Hydrogen and Deuyerium, C.L. Young, editor, (1981), Pergamon Press, Page 32.
134. Saturated_Media = 1.
135. Saturated_PCE_Concentration = 534 µmol/L.
136. Saturated_TCE_Concentration = 2169 µmol/L.
137. Step_Value_Butyric_Acid = 26 µmol/h.
    The constant butyrate feeding rate.
138. Step_Value_Hydrogen = 0.
    The constant hydrogen feeding rate.
139. TCE_to_DCE_Competitive_Inhibition = 1.
    Control factor for competitive inhibition: TCE dechlorination.
140. T_total = 168 h.
    Total simulation time.
141. Temp = 380.15 K.
    Temperature, K.
142. VC_to_ETH_Competitive_Inhibition = 1.
    Control factor for competitive inhibition: VC dechlorination.
143. Variable_Endognenous_Decay = 1.
144. Vg = 0.06 L.
    Volume (L) of the gaseous headspace of the serum bottle.
145. Vw = 0.10 L.
    Volume (L) of the aqueous content of the serum bottle.
146. Waste_Increment_Time = 24 h.
    This is the time (h) that elapses between wasting events.
147. Waste_Pulse_Time = 24 h.
    This is the initial time (h) at which all sample events occur.
148. YE_Addition_uL = 100 µL.
    Volume (µL) of YE addition.
149. YE_HAc_umol_per_uL = 0.0689 µmol acetate acid/µL YE added.
    Acetic acid produced by addition of YE.
150. YE_HBu_umol_per_uL = 0.0665 µmol butyric acid/µL YE added.
    Butyric acid produced by addition of YE. Table 5.12 of Fennell's dissertation (1998).
151. YE_Prop_umol_per_uL = 0.0160 µmol propionic acid/µL YE added.

Propionic acid formed from YE addition.

152. YE_ueq_per_uL = 2.03 µeq contributed/µL YE.
    The amount of reducing equivalents added by YE. From 1/18/10 batch experiment(and 3/4/09 no donor PSS) (1.03 µeeq/µL) by Heavner (2013). It was assumed that 10% of reduction equivalents were channelled to synthesis. (1.14^0.9=1.03).
153. Y_Acetotrophs = 419000 cells/µmol.
154. Y_Butyrate_Fermenters = 1260000 cells/µmol butyrate.
155. Yield for butyrate fermentersY_Dechlorinators = 160000000 cells/µmol.
156. Y_Hydrogenotrophic_Methanogens = 60800000 cells/µmol.
157. Z = 1.
    Charge on ionic speciesc.
158. DCE_Concentration = 4760 µmol/L.
159. dT = 0.001 h.
160. delta_G_critical_Ace_to_BHB = -18.3324 kJ/mol.
161. delta_G_critical_Butyrate = -18.3324 kJ/mol butyrate.
    The maximum value that delta G acquire that still provides organism with enough energy to make ATP. Value corrected from the –19 kJ value used by Fennell and Heavner, based on an error they each made in converting pH to hydrogen ion activity.
162. delta_G_critical_Lac_to_Acetate = -18.3324 kJ/mol lactate.
    The maximum value that delta G acquire that still provides organism with enough energy to make ATP.
163. delta_G_critical_Lac_to_Propionate = -18.3324 kJ/mol butyrate.
    The maximum value that delta G acquire that still provides organism with enough energy to make ATP.
164. delta_G_critical_Propionate_to_Acetate = -18.3324 kJ/mol.
165. delta_G_zero_Ace_to_BHB = -29.6 kJ/mol.
    delta G zero at 35°C.
166. delta_G_zero_BHB = 93.83 kJ/mol.
    delta G zero at 35°C.
167. delta_G_zero_Butyrate = 123.16 kJ/mol.
    delta G zero at 35°C.
168. delta_G_zero_Lac_to_Acetate = 71.01 kJ/mol.
    delta G zero at 35°C.
169. delta_G_zero_Lac_to_Propionate = -40.26 kJ/mol.
    delta G zero at 35°C.
170. delta_G_zero_Propionate = 166.90 kJ/mol.
    delta G zero at 35°C.
171. fe_Acetate = 0.9582
    fe-- fraction of acetate for energy.
172. fe_Butyrate = 0.9753
    fe -- the fraction of the donor butyrate that is used for energy.
173. fe_H2 = 0.8877
    fe-- fraction of hydrogen used for energy.
174. fe_H2_to_Dechlorination = 0.9023
    fe-- fraction of hydrogen used for energy.
175. fe_Lactate = 0.9482
    fe-- fraction of lactate used for energy.
176. fe_Propionate = 0.9818
    fe-- fraction of propionate used for energy.

177. fraction_decaying_biomass_to_mythical_pools = 0.5.
178. g_CH4 =1.027.
    Activity coefficient for methane under culture conditions used here.
179. g_H2 = 1.0202.
    Activity coefficient for hydrogen under culture conditions used here.
180. g_ionic_Z1 = 0.7706.
    Activity coefficient for +/- charged species.
181. k_Ace_to_BHB = 7.5×10^{-9} µmol/cell/h.
182. k_Acetate = 2.55×10^{-9} µmol/cell/h.
    Rate of acetate degration to methane.
183. k_Butyrate = 1.4×10^{-9} µmol/cell/h.
184. k_DCE = 2.18×10^{-10} µmol/cell/h.
    Estimated from relative vmax/Ks in Tandoi et al., 1994 and the k/Ks for the pure culture for PCE. 3 (umol PCE to VC/16S DNA copies-h). This value is calculated from nonlinear regression several PSS experiments by Heavner (2013).
185. k_H2_methane = 9.41×10^{-10} µmol/cell/h.
186. k_Lactate_to_Acetate = 1.7×10^{-9} µmol/cell/h.
187. k_Lactate_to_Propionate = 1.7×10^{-9} µmol/cell/h.
188. k_PCE = 3.55×10^{-10} µmol PCE to VC/16S DNA copies.
    Rate of PCE dechlorination:1.24E-10(Ramh,2008). This value is calculated from nonlinear regression several PSS experiments by Heavner (2013).
189. k_Propionate = 4.4×10^{-10} µmol/cell/h.
190. k_TCE = 2.21×10^{-10}µmol/cell/h.
191. k_VC = 1.49×10^{-10} µmol/cell/h.
192. mg_VSS_per_mmol_VSS = 113.12 % mg VSS/mmol $C_5H_7O_2N$
193. pH = 7.3.

APPENDIX V: MATLAB® CODES

A5.A PULSE Function

```
function x = PULSE(t,t0,i)
    a = t-t0;
    b = rem(a,i);
    if a<0
        x = 0;
    elseif b == 0;
    x = 1;
   else
    x = 0;
   end
end
```

A5.B Complete Codes for the Haldane-BHB Model

```
global Ac_Inhibition ... % Substrate inhibition (Haldane)
       Ac_Methanogens_mgVSS_per_cell ... % mgVSS/cell. Calculated in file
protein_to_cell_conversion.xls
       Acetate_Formed_per_Butyrate ... % umol acetate formed/umol butyrate
fermented to acetate
       Acetate_Formed_per_Lactate ...  % umol acetate formed/umol lactate
fermented to acetate
       Acetate_Formed_per_Lactate_to_Propionate ...  % umol acetate
formed/umol lactate fermented to propionate
       Acetate_Formed_per_Propionate ... % umol acetate formed/umol
propionate
       Acetotrophs_DNA_Copies_per_Cell ... % the number of copies of the 16S
gene per cell
       Acetotrophs_Initial_Copies ... % copies in 100 mL, initial copies of
16S gene in 100 mL of culture
       Butyrate_ueq_per_umol ... % ueq/umol HBu
       Const_End_Decay ...
       Constant_Butyrate_Feed ...
       Constant_EA_Feed ...
       Constant_Endogenous_Decay ...
       Constant_Hydrogen_Feed ...
       Cw_Bicarbonate ... % mol/L, bicarbonate concentration in the basal
salts medium
       DCE_to_VC_Competitive_Inhibition ...
       DHC_DNA_Copies_per_Cell ... % DHC has one copy of the 16S gene per
cell
       DHC_Initial_Copies ... % copies in 100mL, initial copies of 16S gene
in 100mL of culture
       Decay_Acetotrophs ...  % /h, .001/h, generic number
       Decay_Butyrate_Fermenters ... % /h, 0.001/h, generic number
       Decay_Dechlorinators ... % /h, 0.001/h, generic number
       Decay_Hydrogenotrophic_Methanogens ... % /h, 0.001/h, generic number
       Dechlorinators_mgVSS_per_cell ... % mgVSS/cell, calculated in file
protein_to_cell_conversion.xls
       Endog_Decay ...
       Feed_Increment_Time ... % h, this is the increment time (h) between
feedings
```

```
       Feed_Increment_Time_Donor ... % h, this is the increment time (h)
between feedings
       Feed_Increment_Time_EA ... % h
       Feed_Pulse_Time_Donor ... % h, the pulse feed time is  the time (h) at
which the first feed pulse occurs
       Feed_Pulse_Time_EA ... % h
       Feed_Rate_PCE ... % the rate at which PCE is fed to the microcosm
(uL/min) beginning at 0 h until the end of the experiment
       Feed_Rate_TCE ... % the rate at which TCE is fed to the microcosm
(uL/min) beginning at 0 h until the end of the experiment
       Feed_Rate_cDCE ... % the rate at which cDCE is fed to the microcosm
(uL/min) beginning at 0 h until the end of the experiment
       Feed_Time_Donor ... % h, the pulse feed time is the time (h) at which
the first feed pulse occurs
       Feed_Time_Electron_Acceptor ... % h, the time (h) when the first input
of electron acceptor occurs
       Fermenters_DNA_Copies_per_Cell ... % The number of copies of the 16S
gene per cell
       Fermenters_Initial_Copies ... % copies in 100 mL, initial copies of
16S gene in 100 mL of culture
       Fermenters_mgVSS_per_cell ... % mgVSS/cell, calculated in file
protein_to_cell_conversion.xls
       Fraction_of_ED_pool_treated_as_butyrate ...
       Fraction_of_YE_pool_treated_as_butyrate ...
       H2_Methanogens_mgVSS_per_cell ... % mgVSS/cell, calculated in file
protein_to_cell_conversion.xls
       H2_Threshold_dechlor ... % umol/L. Estimate, Fennell, 1997 from FYE -
or non-fed culture.
       H2_Threshold_meth ... % umol/L. Estimate, Fennell, 1997.
       H2_per_Butyrate_Fermented_to_Acetate ... % umol H2/umol Butyrate
Fermented to Acetate
       H2_per_DCE_Dechlorinated ... % umol Hydrogen/umol DCE converted to VC
       H2_per_Lactate_Fermented_to_Acetate ... %umol H2/umol Lactate
Fermented to Acetate
       H2_per_PCE_Dechlorinated ... %umol Hydrogen/umol PCE converted to TCE
       H2_per_Propionate_Fermented_to_Acetate ... % umol H2/umol Propionate
Fermented to Acetate
       H2_per_TCE_Dechlorinated ... % umol Hydrogen/umol TCE converted to DCE
       H2_per_VC_Dechlorinated ... % umol Hydrogen/umol VC converted to ETH
       H2_to_CH4_Molar_Conversion_Factor ... % umol CH4 Formed per umol H2
       Hc_CH4 ... % pseudo-dimensionless, DiStefano, 1992
       Hc_DCE ... % dimensionless, for cis-1,2-DCE, 30C
       Hc_ETH ... % pseudo-dimensionless, DiStefano, 1992
       Hc_H2 ... % Younge, 1981
       Hc_PCE ... % dimensionless, 30C
       Hc_TCE ... % dimensionless, 30C
       Hc_VC ... % dimensionless, 30C
       Hydrogenotrophic_Methanogens_DNA_Copies_per_Cell ... % the number of
copies of the 16S gene per cell
       Hydrogenotrophic_Methanogens_Initial_Copies ... % copies in 100 mL,
initial copies of 16S gene in 100 mL of culture
       Initial_Acetate ... % umol, the initial amount of acetate present
       Initial_Butyrate ... % umol, the initial amount of butyrate present
       Initial_Culture_Dilution ... % Dilution of initial culture: udiluted =
1, half = 0.5, quarter = 0.25.
       Initial_DCE ... % umol/bottle
       Initial_ETH ... % umol/bottle
```

```
        Initial_H2 ...  % umol/bottle
        Initial_Methane ... % umol/bottle
        Initial_PCE ... % umol/bottle
        Initial_Propionate ... % umol, initial amount of propioante present
        Initial_TCE ... % umol/bottle
        Initial_VC ... % umol/bottle
        Ionic_Strength ... % eq/L, estimated for the basal salts medium
        KI_Ac ...
        KI_PCE ...
        K_CI_DCE_on_TCE ...
        K_CI_DCE_on_VC ...
        K_CI_PCE_on_DCE ...
        K_CI_PCE_on_TCE ...
        K_CI_PCE_on_VC ...
        K_CI_TCE_on_DCE ...
        K_CI_TCE_on_PCE ...
        K_CI_TCE_on_VC ...
        K_HI_PCE_on_Butyrate_to_Ace ...
        K_HI_PCE_on_CH4_Acetate ...
        K_HI_PCE_on_CH4_H2 ...
        K_HI_PCE_on_DCE ...
        K_HI_PCE_on_PCE ...
        K_HI_PCE_on_TCE ...
        K_HI_PCE_on_VC ...
        Kla_CH4 ... % /h, Smatlak, 1995
        Kla_DCE ... % /h, Estimated from the molar volume and Equation 9-26 of
Schwarzenbach et al., 1993 and the relationship developed by Smatlak, 1995
        Kla_ETH ... % /h, Smatlak, 1995
        Kla_H2 ... % /h, Smatlak, 1995
        Kla_PCE ... % /h, Smatlak, 1995
        Kla_TCE ... % /h, Estimated from the molar volume and Equation 9-26 of
Schwarzenbach et al., 1993 and the relationship developed by Smatlak, 1995
        Kla_VC ... % /h, Smatlak, 1995
        Ks_Acetate ... % Half-velocity coefficient for acetate degradation.
1000 umol/L, Ohtsubo et al., 1992; Zehnder el al., 1980.
        Ks_Butyrate ... % Half-velocity coefficient for butyrate fermentation.
34.25 umol/L, Fennell est, 1996.
        Ks_DCE ... % This value is calculated from nonlinear regression
several PSS experiments in file Nonlinear_Regression.xls
        Ks_H2_Dechlor ... % Half-velocity coefficient for H2 for
dechlorination, 0.1 umol/L, Smatlak, 1995
        Ks_H2_methane ... % Half-velocity coefficient for hydrogen to methane.
An average value of 0.96 umol/L was reported by Smatlak, 1995; however, a
slightly lower value was used for modeling.
        Ks_Lactate_to_Acetate ... % Half-velocity coefficient for lactate
fermentation, 2.52 umol/L Fennell, est, 1996. 4x for 25C
        Ks_Lactate_to_Propionate ...
        Ks_PCE ... % half-velocity coefficient for PCE dechlorination, 0.54
umol/L, Smatlak, 1995; 0.6 umol/L, Tandoi, 1994. This value is calculated
from nonlinear regression several PSS experiments in file
Nonlinear_Regression.xls
        Ks_Propionate ... % Half-velocity coefficient for propionate
fermentation, 11.3 umol/L Fennell, est, 1996. 4x for 25C
        Ks_TCE ...  This value is calculated from nonlinear regression several
PSS experiments in file Nonlinear_Regression.xls
        Ks_VC ... Half-velocity coefficient for VC, 290 umol/L Smatlak, 1995.
Estimated from relative vmax/Ks in Tandoi et al., 1994, and the k/Ks for the
```

```
pure culture for PCE. 3 umol PCE to VC/16S DNA copies-h. This value is
calculated from nonlinear regressions several PSS experiments in file:
Nonlinear_Regression.xls and batch_03_18_09_VC_kinetics.xls
       Lactate_ueq_per_umol ... % ueeq/umol Lac
       Liquid_Waste_Rate ... % the liquids removed from sampling
       Neat_DCE_Feed_Rate ...
       Neat_EA ...
       Neat_PCE_Feed_Rate ... % umol/h
       Neat_TCE_Feed_Rate ... % umol/h
       PCE_Inhibition ...
       PCE_to_TCE_Competitive_Inhibition ...
       Propionate_Formed_per_Lactate ... % umol propionate/umol lactate
converted to propionate
       Propionate_ueq_per_umol ... % ueq/umol Prop
       Pulse_Butyrate_Feed ...
       Pulse_EA_Feed ...
       Pulse_Value_Butyric_Acid ... % This is the amount of butyric acid fed
at each pulse beginning at 0 h (umol)
       Pulse_Value_DCE ... % umoles
       Pulse_Value_Hydrogen ... % This is the amount of hydrogen fed (umol)
at each pulse beginning at 0 h and occuring every 48 h
       Pulse_Value_PCE ... % umoles
       Pulse_Value_Propionate_Acid ... % This is the amount of propionic acid
fed (umol) at each pulse beginning at 0 h and occuring every 48 h
       Pulse_Value_TCE ... % umoles
       Purge_Increment_Time ... % h. Time increment for purging the bottles.
       Purge_Pulse_Time ... % h. Time at which the first purge occurs.
       R ... % kJ/mol-K. For thermodynamic calculations.
       R2 ... % L-atm/mol-K. To convert Cg (umol) to partial pressure (atm)
       Salt_Out_CH4 ... % L/mol. Salt effect parameter for CH4 in aqueous
NaCl solution from a review of various studies. In solubility Data Series,
Vol 27/28, Methane, C.L. Young, editor, 1981, Pergamon Press, Page 70.
       Salt_Out_H2 ... % L/mol. Salt effect parameter for H2 in aqueous NaCl
solution from a review of various studies. In solubility Data Series, Vol
5/6, Hydrogen and Deuyerium, C.L. Young, editor, 1981, Pergamon Press, Page
32.
       Saturated_Media ...
       Saturated_PCE_Concentration ... % umol/L
       Saturated_TCE_Concentration ... % umol/L
       Step_Value_Butyric_Acid ... % umol/h
       Step_Value_Hydrogen ...
       TCE_to_DCE_Competitive_Inhibition ...
       T_total ...
       Temp ... % K. Temperature, K.
       VC_to_ETH_Competitive_Inhibition ...
       Variable_Endognenous_Decay ...
       Vg ... % L. Volume (L) of the gaseous headspace of the serum bottle.
       Vw ... % L. Volume (L) of the aqueous content of the serum bottle.
       Waste_Increment_Time ... % h. This is the time (h) that elapses
between wasting events
       Waste_Pulse_Time ... % h. This is the initial time (h) at which all
sample events occur.
       YE_Addition_uL ... % L.
       YE_HAc_umol_per_uL ... % umol Acetate acid/uL YE added. Acetic acid
produced by addition of YE.
       YE_HBu_umol_per_uL ... % umol Butyric acid/uL YE added. Butyric acid
produced by addition of YE. Table 5.12 of Donna's thesis.
```

```
       YE_Prop_umol_per_uL ... % umol Propionic acid/uL YE added. Propionic
acid formed from YE addition.
       YE_ueq_per_uL ... % ueq contributed/uL YE. The amount of reducing
equivalents added by YE. From 1/18/10 batch experiment(and 3/4/09 no donor
PSS) (1.03 ueeq/uL). It was assumed that 10% of reduction equivalents were
channelled to synthesis. (1.14^0.9=1.03)
       Y_Acetotrophs ... % cells/umol
       Y_Butyrate_Fermenters ... %cells/umol butyrate. Yield for butyrate
fermenters
       Y_Dechlorinators ... % cells/umol
       Y_Hydrogenotrophic_Methanogens ... %cells/umol
       cDCE_Concentration ...
       Z ...% Charge on ionic species
       dT ...
       delta_G_critical_Butyrate ...  %kJ/mol butyrate. The maximum value
that delta G acquire that still provides organism with enough energy to make
ATP. Analysis of butyrate data-degradation proceeds at delta G value of -20
kJ/mol butyrate. Arbitrarilly used a value of 5% higher.
       delta_G_critical_Lac_to_Acetate ... %kJ/mol lactate. The maximum value
that delta G acquire that still provides organism with enough energy to make
ATP.
       delta_G_critical_Lac_to_Propionate ... %kJ/mol butyrate. The maximum
value that delta G acquire that still provides organism with enough energy to
make ATP. Analysis of butyrate data-degradation proceeds at delta G value of
-20 kJ/mol butyrate. Arbitrarilly used a value of 5% higher.
       delta_G_critical_Propionate_to_Acetate ...
       delta_G_zero_Butyrate ... % kJ/mol. delta G zero at 35C.
       delta_G_zero_Lac_to_Acetate ... % kJ/mol. delta G zero at 35C.
       delta_G_zero_Lac_to_Propionate ... % kJ/mol. delta G zero at 35C.
       delta_G_zero_Propionate ... % kJ/mol. delta G zero at 35C.
       fe_Acetate ... % fe-- fraction of acetate for energy
       fe_Butyrate ... % fe -- the fraction of the donor butyrate that is
used for energy
       fe_H2 ... % fe-- fraction of hydrogen used for energy
       fe_H2_to_Dechlorination ... % fe-- fraction of hydrogen used for
energy
       fe_Lactate ... % fe-- fraction of lactate used for energy
       fe_Propionate ...% fe-- fraction of propionate used for energy
       fraction_decaying_biomass_to_mythical_pools ...
       k_Acetate ... %umol/cell-h. Rate of acetate degration
       k_Butyrate ... % umol butyrate/cell-h
       k_DCE ... % Estimated from relative vmax/Ks in Tandoi et al., 1994 and
the k/Ks for the pure culture for PCE. 3 (umol PCE to VC/16S DNA copies-h).
This value is calculated from nonlinear regression several PSS experiments in
file: Nonlinear_Regression.xls.
       k_H2_methane ... % umol H2/cell-h
       k_Lactate_to_Acetate ... % ...
       k_Lactate_to_Propionate ...
       k_PCE ... % umol PCE to VC/16S DNA copies. Rate of PCE
dechlorination:1.24E-10(Ramh,2008). This value is calculated from nonlinear
regression several PSS experiments in file: Nonlinear_Regression.xls.
       k_Propionate ... %umol/cell-h ...
       k_TCE ...
       k_VC ...
       mg_VSS_per_mmol_VSS ... % mg VSS/mmol C5H7O2N
       pH ...
       PCE_Inhibition_to_CH4 ...
```

```
        KI_PCE_on_CH4_Acetate ...
        KI_PCE_on_CH4_H2 ...
        KI_PCE_on_VC ...
        KI_PCE_TCE ...
        KI_PCE_DCE ...
        KI_PCE_VC ...
        KI_PCE_on_TCE ...
        Ks_BHB ...
        k_BHB ...
        delta_G_zero_BHB ...
        Cw_BHB ...
        delta_G_zero_Ace_to_BHB ...
        delta_G_critical_Ace_to_BHB ...
        k_Ace_to_BHB ...
        Ks_Ace_to_BHB

g_ionic_Z1 = 10^(-(0.5*Z^2*Ionic_Strength^0.5)/(1+Ionic_Strength^0.5));
g_H2 = 10^(Salt_Out_H2*Ionic_Strength);
g_CH4 = 10^(Salt_Out_CH4*Ionic_Strength);
Cw_Hydrogen_Ion = 10^(-pH)/g_ionic_Z1;

YE_Butyrate = YE_Addition_uL * YE_HBu_umol_per_uL;              %umol butyric
acid added by YE
YE_Acetate = YE_Addition_uL * YE_HAc_umol_per_uL;               %umol acetate
added by YE
YE_Propionate = YE_Addition_uL * YE_Prop_umol_per_uL;           %umol
propionate added by YE
YE_Unknown = YE_Addition_uL * ( YE_ueq_per_uL-
Butyrate_ueq_per_umol*YE_HBu_umol_per_uL ...
             -Propionate_ueq_per_umol*YE_Prop_umol_per_uL);     %unknown ueeq
added from YE

Initial_X_Acetotrophs =
Acetotrophs_Initial_Copies/Acetotrophs_DNA_Copies_per_Cell; %cells
Initial_X_Butyrate_Fermenters =
Fermenters_Initial_Copies/Fermenters_DNA_Copies_per_Cell;    %cells
Initial_X_Dechlorinators = DHC_Initial_Copies/DHC_DNA_Copies_per_Cell;
%cells
Initial_X_Hydrogenotrophic_Methanogens =
Hydrogenotrophic_Methanogens_Initial_Copies/ ...
                           Hydrogenotrophic_Methanogens_DNA_Copies_per_Cell;
%cells

PCE_Feed_Rate_in_umol_per_hr =
Feed_Rate_PCE*60*Saturated_PCE_Concentration*Saturated_Media/(1e6)+Neat_PCE_F
eed_Rate*Neat_EA;          %umol/h
TCE_Feed_Rate_in_umol_per_hr =
Feed_Rate_TCE*60*Saturated_TCE_Concentration*Saturated_Media/(1e6)+Neat_TCE_F
eed_Rate*Neat_EA;          %umol/h
cDCE_Feed_Rate_in_umol_per_hr =
%Feed_Rate_cDCE*60*cDCE_Concentration*Saturated_Media/(1e6)+Neat_DCE_Feed_Rat
e*Neat_EA;          %umol/h

Fraction_of_YE_pool_treated_as_lactate = 1-
Fraction_of_YE_pool_treated_as_butyrate;
```

```
Fraction_of_ED_pool_treated_as_lactate = 1-
Fraction_of_ED_pool_treated_as_butyrate;

t = 0:dT:T_total;

Purge_Control = zeros(1,length(t));

Mythical_Fermentable_Butyrate = zeros(1,length(t));
Mythical_Fermentable_Butyrate(1) = 0;
Cw_Myth_But = zeros(1,length(t));
Cw_Myth_But(1) = Mythical_Fermentable_Butyrate(1)/Vw;

Mythical_Fermentable_Lactate = zeros(1,length(t));
Mythical_Fermentable_Lactate(1) = 0;
Cw_Myth_Lac = zeros(1,length(t));
Cw_Myth_Lac(1) = Mythical_Fermentable_Lactate(1)/Vw;

Mt_Butyrate = zeros(1,length(t));
Mt_Butyrate(1) = Initial_Butyrate;
Cw_Butyrate = zeros(1,length(t));
Cw_Butyrate(1) = Mt_Butyrate(1)/Vw;
Step_Control = zeros(1,length(t));
Pulse_Control_Feed_Butyrate = zeros(1,length(t));
Pulse_Control_Feed_YE = zeros(1,length(t));

Mt_Propionate = zeros(1,length(t));
Mt_Propionate(1) = Initial_Propionate;
Cw_Propionate = zeros(1,length(t));
Cw_Propionate(1) = Mt_Propionate(1)/Vw;
Pulse_Control_Feed_Propionate = zeros(1,length(t));

X_Butyrate_Fermenters = zeros(1,length(t));
X_Butyrate_Fermenters(1) =
Initial_X_Butyrate_Fermenters*Initial_Culture_Dilution;                %cells
X_Mt_Butyrate_Fermenters = zeros(1,length(t));
X_Mt_Butyrate_Fermenters(1) = X_Butyrate_Fermenters(1);
X_Cw_Butyrate_Fermenters = zeros(1,length(t));
X_Cw_Butyrate_Fermenters(1) = X_Butyrate_Fermenters(1)/Vw;

Mt_Hydrogen = zeros(1,length(t));
Mt_Hydrogen(1) = Initial_H2;
Cw_H2 = zeros(1,length(t));
Cw_H2(1) = Mt_Hydrogen(1)/(Vw+(Hc_H2*Vg));
Cg_H2 = zeros(1,length(t));
Cg_H2(1) = Mt_Hydrogen(1)/((Vw/Hc_H2)+Vg);
H2_atm = zeros(1,length(t));
H2_atm(1) = Cg_H2(1)*R2*Temp/1E6;
Pulse_Control_Feed_H2 = zeros(1,length(t));

X_Dechlorinators = zeros(1,length(t));
X_Dechlorinators(1) = Initial_X_Dechlorinators*Initial_Culture_Dilution;
X_Mt_Dechlorinators = zeros(1,length(t));
X_Mt_Dechlorinators(1) = X_Dechlorinators(1);
X_Cw_Dechlorinators = zeros(1,length(t));
X_Cw_Dechlorinators(1) = X_Dechlorinators(1)/Vw;                    %mg VSS/L
```

```
Mw_PCE = zeros(1,length(t));
Mw_PCE(1) = 0;
Mg_PCE = zeros(1,length(t));
Mg_PCE(1) = 0;
Cw_PCE = zeros(1,length(t));
Cw_PCE(1) = Mw_PCE(1)/Vw;
Cg_PCE = zeros(1,length(t));
Cg_PCE(1) = Mg_PCE(1)/Vg;
Mt_PCE = zeros(1,length(t));
Mt_PCE(1) = Mw_PCE(1)+Mg_PCE(1);

Mw_TCE = zeros(1,length(t));
Mw_TCE(1) = 0;
Mg_TCE = zeros(1,length(t));
Mg_TCE(1) = 0;
Cw_TCE = zeros(1,length(t));
Cw_TCE(1) = Mw_TCE(1)/Vw;
Cg_TCE = zeros(1,length(t));
Cg_TCE(1) = Mg_TCE(1)/Vg;
Mt_TCE = zeros(1,length(t));
Mt_TCE(1) = Mw_TCE(1)+Mg_TCE(1);

Mw_DCE = zeros(1,length(t));
Mw_DCE(1) = 0;
Mg_DCE = zeros(1,length(t));
Mg_DCE(1) = 0;
Cw_DCE = zeros(1,length(t));
Cw_DCE(1) = Mw_DCE(1)/Vw;
Cg_DCE = zeros(1,length(t));
Cg_DCE(1) = Mg_DCE(1)/Vg;
Mt_DCE = zeros(1,length(t));
Mt_DCE(1) = Mw_DCE(1)+Mg_DCE(1);

Mw_VC = zeros(1,length(t));
Mw_VC(1) = 0;
Mg_VC = zeros(1,length(t));
Mg_VC(1) = 0;
Cw_VC = zeros(1,length(t));
Cw_VC(1) = Mw_VC(1)/Vw;
Cg_VC = zeros(1,length(t));
Cg_VC(1) = Mg_VC(1)/Vg;
Mt_VC = zeros(1,length(t));
Mt_VC(1) = Mw_VC(1)+Mg_VC(1);

Mw_ETH = zeros(1,length(t));
Mw_ETH(1) = 0;
Mg_ETH = zeros(1,length(t));
Mg_ETH(1) = 0;
Cw_ETH = zeros(1,length(t));
Cw_ETH(1) = Mw_ETH(1)/Vw;
Cg_ETH = zeros(1,length(t));
Cg_ETH(1) = Mg_ETH(1)/Vg;
Cg_ETH_Eq = zeros(1,length(t));
Mt_ETH = zeros(1,length(t));
Mt_ETH(1) = Mw_ETH(1)+Mg_ETH(1);
```

```
Mt_VC_ETH = zeros(1,length(t));
Mt_VC_ETH(1) = Mt_VC(1)+Mt_ETH(1);

Mt_Acetate = zeros(1,length(t));
Mt_Acetate(1) = Initial_Acetate;
Cw_Acetate = zeros(1,length(t));
Cw_Acetate(1) = Mt_Acetate(1)/Vw;

X_Acetotrophs = zeros(1,length(t));
X_Acetotrophs(1) = Initial_X_Acetotrophs*Initial_Culture_Dilution;
X_Mt_Acetotrophs = zeros(1,length(t));
X_Mt_Acetotrophs(1) = X_Acetotrophs(1);
X_Cw_Acetotrophs = zeros(1,length(t));
X_Cw_Acetotrophs(1) = X_Acetotrophs(1)/Vw;                              %mg VSS/L

X_Hydrogenotrophic_Methanogens = zeros(1,length(t));
X_Hydrogenotrophic_Methanogens(1) = Initial_X_Hydrogenotrophic_Methanogens
...
                                              *Initial_Culture_Dilution;
X_Mt_Hydrogenotrophic_Methanogens = zeros(1,length(t));
X_Mt_Hydrogenotrophic_Methanogens(1) = X_Hydrogenotrophic_Methanogens(1);
X_Cw_Hydrogenotrophic_Methanogens = zeros(1,length(t));
X_Cw_Hydrogenotrophic_Methanogens(1) = X_Hydrogenotrophic_Methanogens(1)/Vw;

Mt_Methane_From_Acetate = zeros(1,length(t));
Mt_Methane_From_Acetate(1) = Initial_Methane/2;
Cw_Methane_From_Acetate = zeros(1,length(t));
Cw_Methane_From_Acetate(1) = Mt_Methane_From_Acetate(1)/(Vw+(Hc_CH4*Vg));
Cg_Methane_From_Acetate = zeros(1,length(t));
Cg_Methane_From_Acetate(1) = Mt_Methane_From_Acetate(1)/((Vw/Hc_CH4)+Vg);

Mt_Methane_From_H2 = zeros(1,length(t));
Mt_Methane_From_H2(1) = Initial_Methane/2;
Cw_Methane_From_H2 = zeros(1,length(t));
Cw_Methane_From_H2(1) = Mt_Methane_From_H2(1)/(Vw+(Hc_CH4*Vg));
Cg_Methane_From_H2 = zeros(1,length(t));
Cg_Methane_From_H2(1) = Mt_Methane_From_H2(1)/((Vw/Hc_CH4)+Vg);

Mt_Total_Methane = zeros(1,length(t));
Mt_Total_Methane(1) = Initial_Methane;
Cw_Total_Methane = zeros(1,length(t));
Cw_Total_Methane(1) = Initial_Methane/(Vw+(Hc_CH4*Vg));
Cg_Total_Methane = zeros(1,length(t));
Cg_Total_Methane(1) = Initial_Methane/((Vw/Hc_CH4)+Vg);

delta_G_rxn_Butyrate = zeros(1,length(t));
one_minus_expGRT_Butyrate = zeros(1,length(t));
Thermo_Factor_Butyrate = zeros(1,length(t));
delta_G_rxn_Butyrate(1) =
delta_G_zero_Butyrate+(R*Temp*log((g_ionic_Z1*Cw_Hydrogen_Ion* ...

(g_ionic_Z1*Cw_Acetate(1)/(1E6))^2*(g_H2*Cw_H2(1)/(1E6))^2)/(g_ionic_Z1* ...
                          (Cw_Butyrate(1)+Cw_Myth_But(1))/(1E6))));
one_minus_expGRT_Butyrate(1) = 1-exp((delta_G_rxn_Butyrate(1)-
delta_G_critical_Butyrate)/(R*Temp));
```

```
   if one_minus_expGRT_Butyrate(1)>=0
      Thermo_Factor_Butyrate(1) = one_minus_expGRT_Butyrate(1);
   else
      Thermo_Factor_Butyrate(1) = 0;
   end

delta_G_rxn_BHB = zeros(1,length(t));
one_minus_expGRT_BHB = zeros(1,length(t));
Thermo_Factor_BHB = zeros(1,length(t));
delta_G_rxn_BHB(1) =
delta_G_zero_BHB+(R*Temp*log((g_ionic_Z1*Cw_BHB)*(g_H2*Cw_H2(1)/(1E6))/ ...
                        (g_ionic_Z1*(Cw_Butyrate(1)+Cw_Myth_But(1))/(1E6))));
one_minus_expGRT_BHB(1) = 1-exp((delta_G_rxn_BHB(1)-
delta_G_critical_Butyrate)/(R*Temp));
   if one_minus_expGRT_BHB(1)>=0
       Thermo_Factor_BHB(1) = one_minus_expGRT_BHB(1);
   else
       Thermo_Factor_BHB(1) = 0;
   end

delta_G_rxn_Lac_to_Acetate = zeros(1,length(t));
one_minus_expGRT_Lac = zeros(1,length(t));
Thermo_Factor_Lac_to_Acetate = zeros(1,length(t));
delta_G_rxn_Lac_to_Acetate(1) =
delta_G_zero_Lac_to_Acetate+R*Temp*log((g_ionic_Z1 ...

*Cw_Hydrogen_Ion*g_ionic_Z1*Cw_Bicarbonate*g_ionic_Z1*Cw_Acetate(1) ...

/(1E6)*(g_H2*Cw_H2(1)/(1E6))^2)/(g_ionic_Z1*Cw_Myth_Lac(1)/(1E6)));

one_minus_expGRT_Lac(1) = 1-exp((delta_G_rxn_Lac_to_Acetate(1)-
delta_G_critical_Lac_to_Acetate) ...
                              /(R*Temp));
if one_minus_expGRT_Lac(1)>=0
      Thermo_Factor_Lac_to_Acetate(1) = one_minus_expGRT_Lac(1);
else
      Thermo_Factor_Lac_to_Acetate(1) = 0;
end
delta_G_rxn_Lac_to_Propionate = zeros(1,length(t));
one_minus_expGRT_Lac_to_Propionate = zeros(1,length(t));
Thermo_Factor_Lac_to_Propionate = zeros(1,length(t));
delta_G_rxn_Lac_to_Propionate(1) =
delta_G_zero_Lac_to_Propionate+R*Temp*log(((g_ionic_Z1 ...

*Cw_Hydrogen_Ion)^(1/3)*(g_ionic_Z1*Cw_Acetate(1)/(1E6))^(1/3)*(g_ionic_Z1
...

*Cw_Bicarbonate)^(1/3)*(g_ionic_Z1*Cw_Propionate(1)/(1E6))^(2/3))/(g_ionic_Z1
* ...
                               (Cw_Myth_Lac(1))/(1E6)));
one_minus_expGRT_Lac_to_Propionate(1) = 1-
exp((delta_G_rxn_Lac_to_Propionate(1)- ...
                              delta_G_critical_Lac_to_Propionate)/(R*Temp));
if one_minus_expGRT_Lac_to_Propionate(1)>=0
      Thermo_Factor_Lac_to_Propionate(1) =
one_minus_expGRT_Lac_to_Propionate(1);
```

```
else
      Thermo_Factor_Lac_to_Propionate(1) = 0;
end

delta_G_rxn_Propionate = zeros(1,length(t));
one_minus_expGRT_Propionate = zeros(1,length(t));
Thermo_Factor_Propionate = zeros(1,length(t));
delta_G_rxn_Propionate(1) =
delta_G_zero_Propionate+R*Temp*log((g_ionic_Z1*Cw_Acetate(1)/(1E6)*(g_H2*Cw_H
2(1) ...

/(1E6))^3*g_ionic_Z1*Cw_Hydrogen_Ion*g_ionic_Z1*Cw_Bicarbonate)/(g_ionic_Z1
...
                                *Cw_Propionate(1)/(1E6)));
one_minus_expGRT_Propionate(1) = 1-exp((delta_G_rxn_Propionate(1)-
delta_G_critical_Propionate_to_Acetate)/(R*Temp));
if one_minus_expGRT_Propionate(1) >= 0
      Thermo_Factor_Propionate(1) = one_minus_expGRT_Propionate(1);
else
      Thermo_Factor_Propionate(1) = 0.00000001;
end

delta_G_rxn_Ace_to_BHB = zeros(1,length(t));
one_minus_expGRT_Ace_to_BHB = zeros(1,length(t));
Thermo_Factor_Ace_to_BHB = zeros(1,length(t));
delta_G_rxn_Ace_to_BHB(1) =
delta_G_zero_Ace_to_BHB+(R*Temp*log((g_ionic_Z1*Cw_BHB)/ ...

((g_ionic_Z1*Cw_Acetate(1)/(1E6))^2*Cw_Hydrogen_Ion*g_H2*Cw_H2(1))));

one_minus_expGRT_Ace_to_BHB(1) = 1-exp((delta_G_rxn_Ace_to_BHB(1)-
delta_G_critical_Ace_to_BHB)/(R*Temp));
   if one_minus_expGRT_Ace_to_BHB(1)>=0
       Thermo_Factor_Ace_to_BHB(1) = one_minus_expGRT_Ace_to_BHB(1);
   else
       Thermo_Factor_Ace_to_BHB(1) = 0;
   end

Pulse_Control_Waste = zeros(1,length(t));
Pulse_Control_Feed_EA = zeros(1,length(t));

Butyrate_Fermented_to_Acetate = zeros(1,length(t));
Butyrate_Fermented_to_Acetate(1) =
(k_Butyrate*X_Mt_Butyrate_Fermenters(1)*Cw_Butyrate(1)*Thermo_Factor_Butyrate
(1))/ ...
                                    (Ks_Butyrate+Cw_Butyrate(1));

Propionate_Fermented_to_Acetate = zeros(1,length(t));
Propionate_Fermented_to_Acetate(1) =
(k_Propionate*X_Mt_Butyrate_Fermenters(1)*Cw_Propionate(1)*Thermo_Factor_Prop
ionate(1))/ ...
                                      (Ks_Propionate+Cw_Propionate(1));
Acetate_Conversion_to_Methane = zeros(1,length(t));
Acetate_Conversion_to_Methane(1) =
(k_Acetate*X_Mt_Acetotrophs(1)*Cw_Acetate(1))/(Ks_Acetate+Cw_Acetate(1)+Ac_In
```

```
hibition*(Cw_Acetate(1)^2)/KI_Ac+PCE_Inhibition_to_CH4*Cw_PCE(1)^2/K_HI_PCE_o
n_CH4_Acetate);

H2_For_Methanogenesis = zeros(1,length(t));
H2_For_Methanogenesis(1) =
(k_H2_methane*X_Mt_Hydrogenotrophic_Methanogens(1)*(Cw_H2(1)-
H2_Threshold_meth))/(Ks_H2_methane+(Cw_H2(1)-
H2_Threshold_meth+PCE_Inhibition_to_CH4*Cw_PCE(1)^2/K_HI_PCE_on_CH4_H2));


PCE_Competitive_Inhibition_Term = zeros(1,length(t));
if  PCE_to_TCE_Competitive_Inhibition == 0;
        PCE_Competitive_Inhibition_Term(1) = 1;
    else
        PCE_Competitive_Inhibition_Term(1) = 1+(Cw_TCE(1)/K_CI_TCE_on_PCE);
end

TCE_Competitive_Inhibition_Term = zeros(1,length(t));
    if  TCE_to_DCE_Competitive_Inhibition == 0;
        TCE_Competitive_Inhibition_Term(1) = 1;
    else
        TCE_Competitive_Inhibition_Term(1) = 1+(Cw_DCE(1)/K_CI_DCE_on_TCE);
    end

DCE_Competitive_Inhibition_Term = zeros(1,length(t));
    if  DCE_to_VC_Competitive_Inhibition == 0;
        DCE_Competitive_Inhibition_Term(1) = 1;
    else
        DCE_Competitive_Inhibition_Term(1) =
(1+(Cw_TCE(1)/K_CI_TCE_on_DCE+Cw_PCE(1)/K_CI_PCE_on_DCE));
    end

VC_Competitive_Inhibition_Term = zeros(1,length(t));
    if  VC_to_ETH_Competitive_Inhibition == 0;
        VC_Competitive_Inhibition_Term(1) = 1;
    else
        VC_Competitive_Inhibition_Term(1) =
(1+(Cw_TCE(1)/K_CI_TCE_on_VC+Cw_DCE(1)/K_CI_DCE_on_VC));
    end

PCE_Dechlorination_to_TCE = zeros(1,length(t));
PCE_Dechlorination_to_TCE(1) =
((k_PCE*X_Mt_Dechlorinators(1)*Cw_PCE(1))/(Ks_PCE*PCE_Competitive_Inhibition_
Term(1)+Cw_PCE(1)+PCE_Inhibition*(Cw_PCE(1)^2)/K_HI_PCE_on_PCE)) ...
                                *((Cw_H2(1)-
H2_Threshold_dechlor)/(Ks_H2_Dechlor+(Cw_H2(1)-H2_Threshold_dechlor)));

TCE_Dechlorination_to_DCE = zeros(1,length(t));
TCE_Dechlorination_to_DCE(1) =
((k_TCE*X_Mt_Dechlorinators(1)*Cw_TCE(1))/(Ks_TCE*TCE_Competitive_Inhibition_
Term(1)+Cw_TCE(1)+PCE_Inhibition*(Cw_PCE(1)^2)/K_HI_PCE_on_TCE)) ...
                               *((Cw_H2(1)-
H2_Threshold_dechlor)/(Ks_H2_Dechlor+(Cw_H2(1)-H2_Threshold_dechlor)));

DCE_Dechlorination_to_VC = zeros(1,length(t));
```

```
DCE_Dechlorination_to_VC(1) =
((k_DCE*X_Mt_Dechlorinators(1)*Cw_DCE(1))/(Ks_DCE*DCE_Competitive_Inhibition_
Term(1)+Cw_DCE(1)+PCE_Inhibition*(Cw_PCE(1)^2)/K_HI_PCE_on_DCE)) ...
                              *((Cw_H2(1)-
H2_Threshold_dechlor)/(Ks_H2_Dechlor+(Cw_H2(1)-H2_Threshold_dechlor)));

VC_Dechlorination_to_ETH = zeros(1,length(t));
VC_Dechlorination_to_ETH(1) =
((k_VC*X_Mt_Dechlorinators(1)*Cw_VC(1))/(Ks_VC*VC_Competitive_Inhibition_Term
(1)+Cw_VC(1)+PCE_Inhibition*(Cw_PCE(1)^2)/K_HI_PCE_on_VC)) ...
                              *((Cw_H2(1)-
H2_Threshold_dechlor)/(Ks_H2_Dechlor+(Cw_H2(1)-H2_Threshold_dechlor)));

Biomass_Decay_Acetotrophs = zeros(1,length(t));
Biomass_Decay_Acetotrophs(1) = Decay_Acetotrophs*X_Acetotrophs(1);
Biomass_Decay_Butyrate_Fermenters = zeros(1,length(t));
Biomass_Decay_Butyrate_Fermenters(1) =
X_Butyrate_Fermenters(1)*Decay_Butyrate_Fermenters;
Biomass_Decay_Dechlorinators = zeros(1,length(t));
Biomass_Decay_Dechlorinators(1) = Decay_Dechlorinators*X_Dechlorinators(1);
Biomass_Decay_Hydrogenotrophic_Methanogens = zeros(1,length(t));
Biomass_Decay_Hydrogenotrophic_Methanogens(1) =
Decay_Hydrogenotrophic_Methanogens*X_Hydrogenotrophic_Methanogens(1);
Total_Biomass_Decay = zeros(1,length(t));
Total_Biomass_Decay(1) =
(Biomass_Decay_Acetotrophs(1)*Ac_Methanogens_mgVSS_per_cell+ ...

Biomass_Decay_Butyrate_Fermenters(1)*Fermenters_mgVSS_per_cell ...

+Biomass_Decay_Dechlorinators(1)*Dechlorinators_mgVSS_per_cell ...

+Biomass_Decay_Hydrogenotrophic_Methanogens(1)*H2_Methanogens_mgVSS_per_cell)
...

*Variable_Endognenous_Decay+Const_End_Decay*Constant_Endogenous_Decay;

Fermented_Myth_But = zeros(1,length(t));
Fermented_Myth_But(1) =
(k_Butyrate*X_Mt_Butyrate_Fermenters(1)*Cw_Myth_But(1)*Thermo_Factor_Butyrate
(1))/(Ks_Butyrate+Cw_Myth_But(1));
Myth_Lac_Fermented_to_Acetate = zeros(1,length(t));
Myth_Lac_Fermented_to_Acetate(1) =
k_Lactate_to_Acetate*X_Mt_Butyrate_Fermenters(1)*Cw_Myth_Lac(1)*Thermo_Factor
_Lac_to_Acetate(1)/(Ks_Lactate_to_Acetate+Cw_Myth_Lac(1));
Myth_Lac_Fermented_to_Propionate = zeros(1,length(t));
Myth_Lac_Fermented_to_Propionate(1) =
(k_Lactate_to_Propionate*X_Mt_Butyrate_Fermenters(1)*Cw_Myth_Lac(1)*Thermo_Fa
ctor_Lac_to_Propionate(1))/ ...

(Ks_Lactate_to_Propionate+Cw_Myth_Lac(1));

MYTHBUT =
@(t,Thermo_Factor_BHB,Thermo_Factor_Butyrate,Total_Biomass_Decay,X_Mt_Butyrat
e_Fermenters,Cw_Myth_But,Mythical_Fermentable_Butyrate) ...

((Total_Biomass_Decay)*fraction_decaying_biomass_to_mythical_pools*1000 ...
```

```
/mg_VSS_per_mmol_VSS*Endog_Decay*Fraction_of_ED_pool_treated_as_butyrate) ...
       -
(k_Butyrate*X_Mt_Butyrate_Fermenters*Cw_Myth_But*Thermo_Factor_Butyrate) ...
       /(Ks_Butyrate+Cw_Myth_But) ...
       -(k_BHB*X_Mt_Butyrate_Fermenters*Cw_Myth_But ...
       *max(0,(Thermo_Factor_BHB-Thermo_Factor_Butyrate))) ...
       /(Ks_BHB+Cw_Myth_But);

MYTHLAC =
@(t,Thermo_Factor_Lac_to_Acetate,Thermo_Factor_Lac_to_Propionate,Total_Biomas
s_Decay, ...
       X_Mt_Butyrate_Fermenters,Cw_Myth_Lac,Mythical_Fermentable_Lactate) ...

((Total_Biomass_Decay)*fraction_decaying_biomass_to_mythical_pools*1000 ...

/mg_VSS_per_mmol_VSS*Endog_Decay*Fraction_of_ED_pool_treated_as_lactate) ...
       -(k_Lactate_to_Acetate*X_Mt_Butyrate_Fermenters*Cw_Myth_Lac* ...
       Thermo_Factor_Lac_to_Acetate)/(Ks_Lactate_to_Acetate+Cw_Myth_Lac) ...
       -(k_Lactate_to_Propionate*X_Mt_Butyrate_Fermenters*Cw_Myth_Lac* ...

Thermo_Factor_Lac_to_Propionate)/(Ks_Lactate_to_Propionate+Cw_Myth_Lac);


BUTYRIC =
@(t,Thermo_Factor_BHB,Thermo_Factor_Butyrate,X_Mt_Butyrate_Fermenters,Cw_Buty
rate,Mt_Butyrate) ...
          (-(k_Butyrate*X_Mt_Butyrate_Fermenters*Cw_Butyrate...
          *Thermo_Factor_Butyrate)/(Ks_Butyrate+Cw_Butyrate)) ...
          -(k_BHB*X_Mt_Butyrate_Fermenters*Cw_Butyrate ...
          *max(0,(Thermo_Factor_BHB-Thermo_Factor_Butyrate))) ...
          /(Ks_BHB+Cw_Butyrate) ...
          +Constant_Butyrate_Feed*Step_Value_Butyric_Acid;

PROP =
@(t,Thermo_Factor_Propionate,X_Mt_Butyrate_Fermenters,Myth_Lac_Fermented_to_P
ropionate,Cw_Propionate,Mt_Propionate) ...

(fe_Lactate*Myth_Lac_Fermented_to_Propionate*Propionate_Formed_per_Lactate)
...
       -
(k_Propionate*X_Mt_Butyrate_Fermenters*Cw_Propionate*Thermo_Factor_Propionate
) ...
       /(Ks_Propionate+Cw_Propionate);
%umol/h

BIODONOR = @(t,Butyrate_Fermented_to_Acetate,X_Butyrate_Fermenters) ...
             (Y_Butyrate_Fermenters*Butyrate_Fermented_to_Acetate) ...
             -(X_Butyrate_Fermenters*Decay_Butyrate_Fermenters);

HYDROGEN =
@(t,H2_For_Methanogenesis,X_Mt_Butyrate_Fermenters,Cw_Acetate,Thermo_Factor_A
ce_to_BHB, ...

Cw_Myth_But,Thermo_Factor_BHB,Thermo_Factor_Butyrate,Cw_Butyrate, ...
```

```
Cw_H2,PCE_Dechlorination_to_TCE,TCE_Dechlorination_to_DCE,DCE_Dechlorination_
to_VC, ...

VC_Dechlorination_to_ETH,Butyrate_Fermented_to_Acetate,Propionate_Fermented_t
o_Acetate, ...

X_Mt_Hydrogenotrophic_Methanogens,Fermented_Myth_But,Myth_Lac_Fermented_to_Ac
etate, ...
             Mt_Hydrogen) ...
            ((fe_Butyrate*(Butyrate_Fermented_to_Acetate+Fermented_Myth_But)
...

*H2_per_Butyrate_Fermented_to_Acetate)+(fe_Lactate*Myth_Lac_Fermented_to_Acet
ate ...

*H2_per_Lactate_Fermented_to_Acetate)+(fe_Propionate*Propionate_Fermented_to_
Acetate ...
            *H2_per_Propionate_Fermented_to_Acetate)) ...
%Hydrogen Production
            -
((PCE_Dechlorination_to_TCE*H2_per_PCE_Dechlorinated+TCE_Dechlorination_to_DC
E* ...

H2_per_TCE_Dechlorinated+DCE_Dechlorination_to_VC*H2_per_DCE_Dechlorinated
...

+VC_Dechlorination_to_ETH*H2_per_VC_Dechlorinated)/fe_H2_to_Dechlorination)
...%H2 for Dechlorination
            - H2_For_Methanogenesis ...
            -(k_BHB*X_Mt_Butyrate_Fermenters*Cw_Myth_But ...
            *max(0,(Thermo_Factor_BHB-
Thermo_Factor_Butyrate)))/(Ks_BHB+Cw_Butyrate) ...
            -(k_BHB*X_Mt_Butyrate_Fermenters*Cw_Butyrate ...
            *max(0,(Thermo_Factor_BHB-
Thermo_Factor_Butyrate)))/(Ks_BHB+Cw_Butyrate) ...

+(k_Ace_to_BHB*X_Mt_Butyrate_Fermenters*Cw_Acetate*Thermo_Factor_Ace_to_BHB/(
Ks_Ace_to_BHB+Cw_Acetate)) ...
            +(Constant_Hydrogen_Feed*Step_Value_Hydrogen);

DHC_BIO =
@(t,PCE_Dechlorination_to_TCE,TCE_Dechlorination_to_DCE,DCE_Dechlorination_to
_VC, ...
           X_Dechlorinators) ...

Y_Dechlorinators*(PCE_Dechlorination_to_TCE*H2_per_PCE_Dechlorinated ...
           +TCE_Dechlorination_to_DCE*H2_per_TCE_Dechlorinated ...
           +DCE_Dechlorination_to_VC*H2_per_DCE_Dechlorinated) ...
           -Decay_Dechlorinators*X_Dechlorinators;

RATEPCE =
@(t,X_Mt_Dechlorinators,Cw_H2,Cw_PCE,Cg_PCE,PCE_Competitive_Inhibition_Term,M
w_PCE) ...
           PCE_Feed_Rate_in_umol_per_hr*Constant_EA_Feed ...
```

```
          -
((k_PCE*X_Mt_Dechlorinators*Cw_PCE)/(Ks_PCE*PCE_Competitive_Inhibition_Term+C
w_PCE+PCE_Inhibition*(Cw_PCE^2)/K_HI_PCE_on_PCE)) ...
          *((Cw_H2-H2_Threshold_dechlor)/(Ks_H2_Dechlor+(Cw_H2-
H2_Threshold_dechlor))) ...
          -Vw*Kla_PCE*(Cw_PCE-(Cg_PCE/Hc_PCE));
EXCHANGEPCE = @(t,Cg_PCE,Cw_PCE,Mg_PCE) ...
              Vw*Kla_PCE*(Cw_PCE-(Cg_PCE/Hc_PCE));

RATETCE =
@(t,X_Mt_Dechlorinators,Cw_H2,Cw_TCE,Cg_TCE,TCE_Competitive_Inhibition_Term,C
w_PCE,PCE_Competitive_Inhibition_Term,Mw_TCE) ...
          TCE_Feed_Rate_in_umol_per_hr*Constant_EA_Feed ...

+((k_PCE*X_Mt_Dechlorinators*Cw_PCE)/(Ks_PCE*PCE_Competitive_Inhibition_Term+
Cw_PCE+PCE_Inhibition*(Cw_PCE^2)/K_HI_PCE_on_PCE)) ...
          *((Cw_H2-H2_Threshold_dechlor)/(Ks_H2_Dechlor+(Cw_H2-
H2_Threshold_dechlor))) ...
          -
((k_TCE*X_Mt_Dechlorinators*Cw_TCE)/(Ks_TCE*TCE_Competitive_Inhibition_Term+C
w_TCE+Cw_PCE^2/K_HI_PCE_on_TCE))*((Cw_H2-H2_Threshold_dechlor)/ ...
          (Ks_H2_Dechlor+(Cw_H2-H2_Threshold_dechlor))) ...
          -Vw*Kla_TCE*(Cw_TCE-(Cg_TCE/Hc_TCE));
EXCHANGETCE = @(t,Cg_TCE,Cw_TCE,Mg_TCE) ...
              Vw*Kla_TCE*(Cw_TCE-(Cg_TCE/Hc_TCE));

RATEDCE =
@(t,Cw_PCE,X_Mt_Dechlorinators,Cw_H2,Cw_DCE,Cg_DCE,DCE_Competitive_Inhibition
_Term,Cw_TCE,TCE_Competitive_Inhibition_Term,Mw_DCE) ...
          cDCE_Feed_Rate_in_umol_per_hr*Constant_EA_Feed ...

+((k_TCE*X_Mt_Dechlorinators*Cw_TCE)/(Ks_TCE*TCE_Competitive_Inhibition_Term+
Cw_TCE+(Cw_PCE)^2/K_HI_PCE_on_TCE))*((Cw_H2-H2_Threshold_dechlor)/ ...
          (Ks_H2_Dechlor+(Cw_H2-H2_Threshold_dechlor))) ...
          -
((k_DCE*X_Mt_Dechlorinators*Cw_DCE)/(Ks_DCE*DCE_Competitive_Inhibition_Term+C
w_DCE+Cw_PCE^2/K_HI_PCE_on_DCE))*((Cw_H2-H2_Threshold_dechlor)/ ...
          (Ks_H2_Dechlor+(Cw_H2-H2_Threshold_dechlor))) ...
          -Vw*Kla_DCE*(Cw_DCE-(Cg_DCE/Hc_DCE));
EXCHANGEDCE = @(t,Cg_DCE,Cw_DCE,Mg_DCE) ...
              Vw*Kla_DCE*(Cw_DCE-(Cg_DCE/Hc_DCE));

RATEVC =
@(t,Cw_PCE,X_Mt_Dechlorinators,Cw_H2,Cw_VC,Cg_VC,VC_Competitive_Inhibition_Te
rm,Cw_DCE,DCE_Competitive_Inhibition_Term,Mw_VC) ...

((k_DCE*X_Mt_Dechlorinators*Cw_DCE)/(Ks_DCE*DCE_Competitive_Inhibition_Term+C
w_DCE+Cw_PCE^2/K_HI_PCE_on_DCE))*((Cw_H2-H2_Threshold_dechlor)/ ...
          (Ks_H2_Dechlor+(Cw_H2-H2_Threshold_dechlor))) ...
          -
((k_VC*X_Mt_Dechlorinators*Cw_VC)/(Ks_VC*VC_Competitive_Inhibition_Term+Cw_VC
+Cw_PCE^2/K_HI_PCE_on_VC))*((Cw_H2-H2_Threshold_dechlor)/ ...
          (Ks_H2_Dechlor+(Cw_H2-H2_Threshold_dechlor))) ...
          -Vw*Kla_VC*(Cw_VC-(Cg_VC/Hc_VC));
EXCHANGEVC = @(t,Cg_VC,Cw_VC,Mg_VC) ...
             Vw*Kla_VC*(Cw_VC-(Cg_VC/Hc_VC));
```

```
RATEETH =
@(t,Cw_PCE,X_Mt_Dechlorinators,Cw_H2,Cw_ETH,Cg_ETH,Cw_VC,VC_Competitive_Inhib
ition_Term,Mw_ETH) ...

((k_VC*X_Mt_Dechlorinators*Cw_VC)/(Ks_VC*VC_Competitive_Inhibition_Term+Cw_VC
+Cw_PCE^2/K_HI_PCE_on_VC))*((Cw_H2-H2_Threshold_dechlor)/ ...
          (Ks_H2_Dechlor+(Cw_H2-H2_Threshold_dechlor))) ...
          -Vw*Kla_ETH*(Cw_ETH-(Cg_ETH/Hc_ETH));
EXCHANGEETH = @(t,Cg_ETH,Cw_ETH,Mg_ETH) ...
              Vw*Kla_ETH*(Cw_ETH-(Cg_ETH/Hc_ETH));

ACETATE =
@(t,Acetate_Conversion_to_Methane,X_Mt_Butyrate_Fermenters,Thermo_Factor_Ace_
to_BHB,...

X_Mt_Acetotrophs,Butyrate_Fermented_to_Acetate,Propionate_Fermented_to_Acetat
e, ...

Fermented_Myth_But,Myth_Lac_Fermented_to_Acetate,Myth_Lac_Fermented_to_Propio
nate,Cw_Acetate,Mt_Acetate) ...
          (fe_Butyrate*(Butyrate_Fermented_to_Acetate+Fermented_Myth_But) ...

*Acetate_Formed_per_Butyrate)+(fe_Lactate*Myth_Lac_Fermented_to_Acetate ...

*Acetate_Formed_per_Lactate)+(fe_Propionate*Propionate_Fermented_to_Acetate
...

*Acetate_Formed_per_Propionate)+(fe_Lactate*Myth_Lac_Fermented_to_Propionate
...
          *Acetate_Formed_per_Lactate_to_Propionate)- ...

(k_Ace_to_BHB*X_Mt_Butyrate_Fermenters*Cw_Acetate*Thermo_Factor_Ace_to_BHB/(K
s_Ace_to_BHB+Cw_Acetate)) ...
          - Acetate_Conversion_to_Methane;

ACETOTROPHS = @(t,Acetate_Conversion_to_Methane,X_Acetotrophs) ...
              Y_Acetotrophs*Acetate_Conversion_to_Methane ...
              -Decay_Acetotrophs*X_Acetotrophs;
%cells/h

HYDROMETHAN = @(t,H2_For_Methanogenesis,X_Hydrogenotrophic_Methanogens) ...
              Y_Hydrogenotrophic_Methanogens*H2_For_Methanogenesis ...
              -
Decay_Hydrogenotrophic_Methanogens*X_Hydrogenotrophic_Methanogens;%cells/h

METHANE1 = @(t,Acetate_Conversion_to_Methane,Mt_Methane_From_Acetate) ...
             Acetate_Conversion_to_Methane*fe_Acetate;

METHANE2 = @(t,H2_For_Methanogenesis,Mt_Methane_From_H2) ...
              fe_H2*H2_For_Methanogenesis*H2_to_CH4_Molar_Conversion_Factor;
%umol/h

for i=1:(length(t)-1)
```

```
    Pulse_Control_Feed_EA(i) =
PULSE(t(i),Feed_Pulse_Time_EA,Feed_Increment_Time_EA);
    Pulse_Control_Waste(i) =
PULSE(t(i),Waste_Pulse_Time,Waste_Increment_Time);
    Pulse_Control_Feed_H2(i) =
PULSE(t(i),Feed_Time_Donor,Feed_Increment_Time_Donor);

    Pulse_Control_Feed_Butyrate(i) =
PULSE(t(i),Feed_Time_Donor,Feed_Increment_Time_Donor);
    Pulse_Control_Feed_YE(i) =
PULSE(t(i),Feed_Time_Donor,Feed_Increment_Time_Donor);
    Pulse_Control_Feed_Propionate(i) =
PULSE(t(i),Feed_Pulse_Time_Donor,Feed_Increment_Time);

    Purge_Control(i) = PULSE(t(i),Purge_Pulse_Time,Purge_Increment_Time);

    if Purge_Control(i) == 1

    Mt_Hydrogen(i) = 0;
    Cw_H2(i) = Mt_Hydrogen(i)/(Vw+(Hc_H2*Vg));
    Cg_H2(i) = Mt_Hydrogen(i)/((Vw/Hc_H2)+Vg);
    H2_atm(i) = Cg_H2(i)*R2*Temp/1E6;

    Mw_PCE(i) = 0;
    Mg_PCE(i) = 0;
    Cw_PCE(i) = Mw_PCE(i)/Vw;
    Cg_PCE(i) = Mg_PCE(i)/Vg;

    Mw_TCE(i) = 0;
    Mg_TCE(i) = 0;
    Cw_TCE(i) = Mw_TCE(i)/Vw;
    Cg_TCE(i) = Mg_TCE(i)/Vg;

    Mw_DCE(i) = 0;
    Mg_DCE(i) = 0;
    Cw_DCE(i) = Mw_DCE(i)/Vw;
    Cg_DCE(i) = Mg_DCE(i)/Vg;

    Mw_VC(i) = 0;
    Mg_VC(i) = 0;
    Cw_VC(i) = Mw_VC(i)/Vw;
    Cg_VC(i) = Mg_VC(i)/Vg;

    Mw_ETH(i) = 0;
    Mg_ETH(i) = 0;
    Cw_ETH(i) = Mw_ETH(i)/Vw;
    Cg_ETH(i) = Mg_ETH(i)/Vg;

    Mt_Methane_From_Acetate(i) = 0;
    Cw_Methane_From_Acetate(i) = Mt_Methane_From_Acetate(i)/(Vw+(Hc_CH4*Vg));
    Cg_Methane_From_Acetate(i) = Mt_Methane_From_Acetate(i)/((Vw/Hc_CH4)+Vg);

    Mt_Methane_From_H2(i) = 0;
    Cw_Methane_From_H2(i) = Mt_Methane_From_H2(i)/(Vw+(Hc_CH4*Vg));
    Cg_Methane_From_H2(i) = Mt_Methane_From_H2(i)/((Vw/Hc_CH4)+Vg);
```

```
    Mt_Total_Methane(i) = 0;
    Cw_Total_Methane(i) = 0;
    Cg_Total_Methane(i) = 0;

    else
    if Pulse_Control_Waste(i) == 1

    Mythical_Fermentable_Butyrate(i) = Mythical_Fermentable_Butyrate(i)*(1-
Liquid_Waste_Rate);
    Cw_Myth_But(i) = Mythical_Fermentable_Butyrate(i)/Vw;

    Mythical_Fermentable_Lactate(i) = Mythical_Fermentable_Lactate(i)*(1-
Liquid_Waste_Rate);
    Cw_Myth_Lac(i) = Mythical_Fermentable_Lactate(i)/Vw;

    Mt_Butyrate(i) = Mt_Butyrate(i)*(1-Liquid_Waste_Rate);
    Cw_Butyrate(i) = Mt_Butyrate(i)/Vw;

    Mt_Propionate(i) = Mt_Propionate(i)*(1-Liquid_Waste_Rate);
    Cw_Propionate(i) = Mt_Propionate(i)/Vw;

    X_Butyrate_Fermenters(i) = X_Butyrate_Fermenters(i)*(1-
Liquid_Waste_Rate);
    X_Mt_Butyrate_Fermenters(i) = X_Butyrate_Fermenters(i);
    X_Cw_Butyrate_Fermenters(i) = X_Butyrate_Fermenters(i)/Vw;

    Mt_Hydrogen(i) = Mt_Hydrogen(i)*(1-Liquid_Waste_Rate);
    Cw_H2(i) = Mt_Hydrogen(i)/(Vw+(Hc_H2*Vg));
    Cg_H2(i) = Mt_Hydrogen(i)/((Vw/Hc_H2)+Vg);
    H2_atm(i) = Cg_H2(i)*R2*Temp/1E6;

    X_Dechlorinators(i) = X_Dechlorinators(i)*(1-Liquid_Waste_Rate);
    X_Mt_Dechlorinators(i) = X_Dechlorinators(i);
    X_Cw_Dechlorinators(i) = X_Dechlorinators(i)/Vw;

    Mw_PCE(i) = Mw_PCE(i)*(1-Liquid_Waste_Rate);
    Mg_PCE(i) = Mg_PCE(i)*(1-Liquid_Waste_Rate);
    Cw_PCE(i) = Mw_PCE(i)/Vw;
    Cg_PCE(i) = Mg_PCE(i)/Vg;

    Mw_TCE(i) = Mw_TCE(i)*(1-Liquid_Waste_Rate);
    Mg_TCE(i) = Mg_TCE(i)*(1-Liquid_Waste_Rate);
    Cw_TCE(i) = Mw_TCE(i)/Vw;
    Cg_TCE(i) = Mg_TCE(i)/Vg;

    Mw_DCE(i) = Mw_DCE(i)*(1-Liquid_Waste_Rate);
    Mg_DCE(i) = Mg_DCE(i)*(1-Liquid_Waste_Rate);
    Cw_DCE(i) = Mw_DCE(i)/Vw;
    Cg_DCE(i) = Mg_DCE(i)/Vg;

    Mw_VC(i) = Mw_VC(i)*(1-Liquid_Waste_Rate);
    Mg_VC(i) = Mg_VC(i)*(1-Liquid_Waste_Rate);
    Cw_VC(i) = Mw_VC(i)/Vw;
```

```
    Cg_VC(i) = Mg_VC(i)/Vg;

    Mw_ETH(i) = Mw_ETH(i)*(1-Liquid_Waste_Rate);
    Mg_ETH(i) = Mg_ETH(i)*(1-Liquid_Waste_Rate);
    Cw_ETH(i) = Mw_ETH(i)/Vw;
    Cg_ETH(i) = Mg_ETH(i)/Vg;

    Mt_Acetate(i) = Mt_Acetate(i)*(1-Liquid_Waste_Rate);
    Cw_Acetate(i) = Mt_Acetate(i)/Vw;

    X_Acetotrophs(i) = X_Acetotrophs(i)*(1-Liquid_Waste_Rate);
    X_Mt_Acetotrophs(i) = X_Acetotrophs(i);
    X_Cw_Acetotrophs(i) = X_Acetotrophs(i)/Vw;                          %mg
VSS/L

    X_Hydrogenotrophic_Methanogens(i) = X_Hydrogenotrophic_Methanogens(i)*(1-
Liquid_Waste_Rate);
    X_Mt_Hydrogenotrophic_Methanogens(i) = X_Hydrogenotrophic_Methanogens(i);
    X_Cw_Hydrogenotrophic_Methanogens(i) =
X_Hydrogenotrophic_Methanogens(i)/Vw;

    Mt_Methane_From_Acetate(i) = Mt_Methane_From_Acetate(i)*(1-
Liquid_Waste_Rate);
    Cw_Methane_From_Acetate(i) = Mt_Methane_From_Acetate(i)/(Vw+(Hc_CH4*Vg));
    Cg_Methane_From_Acetate(i) = Mt_Methane_From_Acetate(i)/((Vw/Hc_CH4)+Vg);

    Mt_Methane_From_H2(i) = Mt_Methane_From_H2(i)*(1-Liquid_Waste_Rate);
    Cw_Methane_From_H2(i) = Mt_Methane_From_H2(i)/(Vw+(Hc_CH4*Vg));
    Cg_Methane_From_H2(i) = Mt_Methane_From_H2(i)/((Vw/Hc_CH4)+Vg);

    Mt_Total_Methane(i) = Mt_Total_Methane(i)*(1-Liquid_Waste_Rate);
    Cw_Total_Methane(i) = Mt_Total_Methane(i)/(Vw+(Hc_CH4*Vg));
    Cg_Total_Methane(i) = Mt_Total_Methane(i)/((Vw/Hc_CH4)+Vg);
    else
    end
    end

    Mt_Hydrogen(i) =
Mt_Hydrogen(i)+Pulse_Value_Hydrogen*Pulse_Control_Feed_H2(i);
    Cw_H2(i) = Mt_Hydrogen(i)/(Vw+(Hc_H2*Vg));
    Cg_H2(i) = Mt_Hydrogen(i)/((Vw/Hc_H2)+Vg);
    H2_atm(i) = Cg_H2(i)*R2*Temp/1E6;

    Mt_Butyrate(i) =
Mt_Butyrate(i)+Pulse_Control_Feed_Butyrate(i)*Pulse_Value_Butyric_Acid*Pulse_
Butyrate_Feed ...
                    + Pulse_Control_Feed_YE(i)*YE_Butyrate;
    Cw_Butyrate(i) = Mt_Butyrate(i)/Vw;

    Mythical_Fermentable_Butyrate(i) = Mythical_Fermentable_Butyrate(i) ...
                                       +
Pulse_Control_Feed_YE(i)*Fraction_of_YE_pool_treated_as_butyrate ...
                                      *YE_Unknown/Butyrate_ueq_per_umol;
    Cw_Myth_But(i) = Mythical_Fermentable_Butyrate(i)/Vw;
```

```
    Mythical_Fermentable_Lactate(i) = Mythical_Fermentable_Lactate(i) ...
                                +
Pulse_Control_Feed_YE(i)*Fraction_of_YE_pool_treated_as_lactate ...
                                *YE_Unknown/Lactate_ueq_per_umol;
    Cw_Myth_Lac(i) = Mythical_Fermentable_Lactate(i)/Vw;

    Mt_Propionate(i) = Mt_Propionate(i) ...
                               +
Pulse_Control_Feed_Propionate(i)*(YE_Propionate+Pulse_Value_Propionate_Acid);
    Cw_Propionate(i) = Mt_Propionate(i)/Vw;

    Mt_Hydrogen(i) = Mt_Hydrogen(i) +
Pulse_Control_Feed_H2(i)*Pulse_Value_Hydrogen;
    Cw_H2(i) = Mt_Hydrogen(i)/(Vw+(Hc_H2*Vg));
    Cg_H2(i) = Mt_Hydrogen(i+1)/((Vw/Hc_H2)+Vg);
    H2_atm(i) = Cg_H2(i)*R2*Temp/1E6;

    Mw_PCE(i) =
Mw_PCE(i)+Pulse_Control_Feed_EA(i)*Pulse_Value_PCE*Pulse_EA_Feed;
    Cw_PCE(i) = Mw_PCE(i)/Vw;

    Mw_TCE(i) =
Mw_TCE(i)+Pulse_Control_Feed_EA(i)*Pulse_Value_TCE*Pulse_EA_Feed;
    Cw_TCE(i) = Mw_TCE(i)/Vw;

    Mw_DCE(i) =
Mw_DCE(i)+Pulse_Control_Feed_EA(i)*Pulse_Value_DCE*Pulse_EA_Feed;
    Cw_DCE(i) = Mw_DCE(i)/Vw;

    Mt_Acetate(i) = Mt_Acetate(i) + Pulse_Control_Feed_YE(i)*YE_Acetate;
    Cw_Acetate(i) = Mt_Acetate(i)/Vw;


    delta_G_rxn_Butyrate(i) =
delta_G_zero_Butyrate+(R*Temp*log((g_ionic_Z1*Cw_Hydrogen_Ion* ...

(g_ionic_Z1*Cw_Acetate(i)/(1E6))^2*(g_H2*Cw_H2(i)/(1E6))^2)/(g_ionic_Z1* ...
                          (Cw_Butyrate(i)+Cw_Myth_But(i))/(1E6))));
   one_minus_expGRT_Butyrate(i) = 1-exp((delta_G_rxn_Butyrate(i)-
delta_G_critical_Butyrate)/(R*Temp));
   if one_minus_expGRT_Butyrate(i)>=0
      Thermo_Factor_Butyrate(i) = one_minus_expGRT_Butyrate(i);
   else
      Thermo_Factor_Butyrate(i) = 0;
   end

delta_G_rxn_BHB(i) =
delta_G_zero_BHB+(R*Temp*log((g_ionic_Z1*Cw_BHB)*(g_H2*Cw_H2(i)/(1E6))/ ...
                       (g_ionic_Z1*(Cw_Butyrate(i)+Cw_Myth_But(i))/(1E6))));
one_minus_expGRT_BHB(i) = 1-exp((delta_G_rxn_BHB(i)-
delta_G_critical_Butyrate)/(R*Temp));
   if one_minus_expGRT_BHB(i)>=0
       Thermo_Factor_BHB(i) = one_minus_expGRT_BHB(i);
   else
       Thermo_Factor_BHB(i) = 0;
```

```
   end

delta_G_rxn_Lac_to_Acetate(i) =
delta_G_zero_Lac_to_Acetate+R*Temp*log((g_ionic_Z1 ...

*Cw_Hydrogen_Ion*g_ionic_Z1*Cw_Bicarbonate*g_ionic_Z1*Cw_Acetate(i) ...

/(1E6)*(g_H2*Cw_H2(i)/(1E6))^2)/(g_ionic_Z1*Cw_Myth_Lac(i)/(1E6)));

one_minus_expGRT_Lac(i) = 1-exp((delta_G_rxn_Lac_to_Acetate(i)-
delta_G_critical_Lac_to_Acetate) ...
                               /(R*Temp));
if one_minus_expGRT_Lac(i)>=0
      Thermo_Factor_Lac_to_Acetate(i) = one_minus_expGRT_Lac(i);
else
      Thermo_Factor_Lac_to_Acetate(i) = 0;
end

delta_G_rxn_Lac_to_Propionate(i) =
delta_G_zero_Lac_to_Propionate+R*Temp*log(((g_ionic_Z1 ...

*Cw_Hydrogen_Ion)^(1/3)*(g_ionic_Z1*Cw_Acetate(i)/(1E6))^(1/3)*(g_ionic_Z1
...

*Cw_Bicarbonate)^(1/3)*(g_ionic_Z1*Cw_Propionate(i)/(1E6))^(2/3))/(g_ionic_Z1
* ...
                                (Cw_Myth_Lac(i))/(1E6)));
one_minus_expGRT_Lac_to_Propionate(i) = 1-
exp((delta_G_rxn_Lac_to_Propionate(i)- ...
                               delta_G_critical_Lac_to_Propionate)/(R*Temp));
if one_minus_expGRT_Lac_to_Propionate(i)>=0
      Thermo_Factor_Lac_to_Propionate(i) =
one_minus_expGRT_Lac_to_Propionate(i);
else
      Thermo_Factor_Lac_to_Propionate(i) = 0;
end

delta_G_rxn_Propionate(i) =
delta_G_zero_Propionate+R*Temp*log((g_ionic_Z1*Cw_Acetate(i)/(1E6)*(g_H2*Cw_H
2(i) ...

/(1E6))^3*g_ionic_Z1*Cw_Hydrogen_Ion*g_ionic_Z1*Cw_Bicarbonate)/(g_ionic_Z1
...
                                *Cw_Propionate(i)/(1E6)));
one_minus_expGRT_Propionate(i) = 1-exp((delta_G_rxn_Propionate(i)-
delta_G_critical_Propionate_to_Acetate)/(R*Temp));
if one_minus_expGRT_Propionate(i) >= 0
      Thermo_Factor_Propionate(i) = one_minus_expGRT_Propionate(i);
else
      Thermo_Factor_Propionate(i) = 0.00000001;
end

delta_G_rxn_Ace_to_BHB(i) =
delta_G_zero_Ace_to_BHB+(R*Temp*log((g_ionic_Z1*Cw_BHB)/ ...

((g_ionic_Z1*Cw_Acetate(i)/(1E6))^2*Cw_Hydrogen_Ion*g_H2*Cw_H2(i))));
```

```
one_minus_expGRT_Ace_to_BHB(i) = 1-exp((delta_G_rxn_Ace_to_BHB(i)-
delta_G_critical_Ace_to_BHB)/(R*Temp));
   if one_minus_expGRT_Ace_to_BHB(i)>=0
       Thermo_Factor_Ace_to_BHB(i) = one_minus_expGRT_Ace_to_BHB(i);
   else
       Thermo_Factor_Ace_to_BHB(i) = 0;
   end

    Butyrate_Fermented_to_Acetate(i) =
(k_Butyrate*X_Mt_Butyrate_Fermenters(i)*Cw_Butyrate(i)*Thermo_Factor_Butyrate
(i))/ ...
                                          (Ks_Butyrate+Cw_Butyrate(i));
    Propionate_Fermented_to_Acetate(i) =
(k_Propionate*X_Mt_Butyrate_Fermenters(i)*Cw_Propionate(i)*Thermo_Factor_Prop
ionate(i))/ ...
                                          (Ks_Propionate+Cw_Propionate(i));
    Acetate_Conversion_to_Methane(i) =
(k_Acetate*X_Mt_Acetotrophs(i)*Cw_Acetate(i))/(Ks_Acetate+Cw_Acetate(i)+ ...

Ac_Inhibition*(Cw_Acetate(i)^2)/KI_Ac+PCE_Inhibition_to_CH4*(Cw_PCE(i)^2)/K_H
I_PCE_on_CH4_Acetate);
    H2_For_Methanogenesis(i) =
(k_H2_methane*X_Mt_Hydrogenotrophic_Methanogens(i)*(Cw_H2(i)-
H2_Threshold_meth))/ ...
                                          (Ks_H2_methane+(Cw_H2(i)-
H2_Threshold_meth)+PCE_Inhibition_to_CH4*(Cw_PCE(i)^2)/K_HI_PCE_on_CH4_H2);

    if  PCE_to_TCE_Competitive_Inhibition == 0;
        PCE_Competitive_Inhibition_Term(i) = 1;
    else
        PCE_Competitive_Inhibition_Term(i) = 1+(Cw_TCE(i)/K_CI_TCE_on_PCE);
    end
    if  TCE_to_DCE_Competitive_Inhibition == 0;
        TCE_Competitive_Inhibition_Term(i) = 1;
    else
        TCE_Competitive_Inhibition_Term(i) = 1+(Cw_DCE(i)/K_CI_DCE_on_TCE);
    end
    if  DCE_to_VC_Competitive_Inhibition == 0;
        DCE_Competitive_Inhibition_Term(i) = 1;
    else
        DCE_Competitive_Inhibition_Term(i) =
(1+(Cw_TCE(i)/K_CI_TCE_on_DCE)+(Cw_PCE(i)/K_CI_PCE_on_DCE));
    end
    if  VC_to_ETH_Competitive_Inhibition == 0;
        VC_Competitive_Inhibition_Term(i) = 1;
    else
        VC_Competitive_Inhibition_Term(i) =
(1+(Cw_TCE(i)/K_CI_TCE_on_VC)+(Cw_DCE(i)/K_CI_DCE_on_VC));
    end

    PCE_Dechlorination_to_TCE(i) =
((k_PCE*X_Mt_Dechlorinators(i)*Cw_PCE(i))/(Ks_PCE*PCE_Competitive_Inhibition_
Term(i)+Cw_PCE(i)+PCE_Inhibition*(Cw_PCE(i)^2)/K_HI_PCE_on_PCE)) ...
                                    *((Cw_H2(i)-
H2_Threshold_dechlor)/(Ks_H2_Dechlor+(Cw_H2(i)-H2_Threshold_dechlor)));
```

```
    TCE_Dechlorination_to_DCE(i) =
((k_TCE*X_Mt_Dechlorinators(i)*Cw_TCE(i))/(Ks_TCE*TCE_Competitive_Inhibition_
Term(i)+Cw_TCE(i)+(Cw_PCE(i))^2/K_HI_PCE_on_TCE))*((Cw_H2(i)-
H2_Threshold_dechlor)/ ...
                                  (Ks_H2_Dechlor+(Cw_H2(i)-
H2_Threshold_dechlor)));

    DCE_Dechlorination_to_VC(i) =
((k_DCE*X_Mt_Dechlorinators(i)*Cw_DCE(i))/(Ks_DCE*DCE_Competitive_Inhibition_
Term(i)+Cw_DCE(i)+Cw_PCE(i)^2/K_HI_PCE_on_DCE))*((Cw_H2(i)-
H2_Threshold_dechlor)/ ...
                                 (Ks_H2_Dechlor+(Cw_H2(i)-
H2_Threshold_dechlor)));

    VC_Dechlorination_to_ETH(i) =
((k_VC*X_Mt_Dechlorinators(i)*Cw_VC(i))/(Ks_VC*VC_Competitive_Inhibition_Term
(i)+Cw_VC(i)+Cw_PCE(i)^2/K_HI_PCE_on_VC))*((Cw_H2(i)-H2_Threshold_dechlor)/
...
                                  (Ks_H2_Dechlor+(Cw_H2(i)-
H2_Threshold_dechlor)));

    Biomass_Decay_Acetotrophs(i) = Decay_Acetotrophs*X_Acetotrophs(i);
    Biomass_Decay_Butyrate_Fermenters(i) =
X_Butyrate_Fermenters(i)*Decay_Butyrate_Fermenters;
    Biomass_Decay_Dechlorinators(i) =
Decay_Dechlorinators*X_Dechlorinators(i);
    Biomass_Decay_Hydrogenotrophic_Methanogens(i) =
Decay_Hydrogenotrophic_Methanogens*X_Hydrogenotrophic_Methanogens(i);
    Total_Biomass_Decay(i) =
(Biomass_Decay_Acetotrophs(i)*Ac_Methanogens_mgVSS_per_cell+ ...

Biomass_Decay_Butyrate_Fermenters(i)*Fermenters_mgVSS_per_cell ...

+Biomass_Decay_Dechlorinators(i)*Dechlorinators_mgVSS_per_cell ...

+Biomass_Decay_Hydrogenotrophic_Methanogens(i)*H2_Methanogens_mgVSS_per_cell)
...

*Variable_Endognenous_Decay+Const_End_Decay*Constant_Endogenous_Decay;

    Fermented_Myth_But(i) =
(k_Butyrate*X_Mt_Butyrate_Fermenters(i)*Cw_Myth_But(i)*Thermo_Factor_Butyrate
(i))/(Ks_Butyrate+Cw_Myth_But(i));
    Myth_Lac_Fermented_to_Acetate(i) =
(k_Lactate_to_Acetate*X_Mt_Butyrate_Fermenters(i)*Cw_Myth_Lac(i)*Thermo_Facto
r_Lac_to_Acetate(i))/(Ks_Lactate_to_Acetate+Cw_Myth_Lac(i));
    Myth_Lac_Fermented_to_Propionate(i) =
(k_Lactate_to_Propionate*X_Mt_Butyrate_Fermenters(i)*Cw_Myth_Lac(i)*Thermo_Fa
ctor_Lac_to_Propionate(i))/ ...

(Ks_Lactate_to_Propionate+Cw_Myth_Lac(i));
```

```
        k_mythbut_1 =
MYTHBUT(t(i),Thermo_Factor_BHB(i),Thermo_Factor_Butyrate(i),Total_Biomass_Dec
ay(i),X_Mt_Butyrate_Fermenters(i),Cw_Myth_But(i),Mythical_Fermentable_Butyrat
e(i));
        k_mythbut_2 =
MYTHBUT(t(i)+0.5*dT,Thermo_Factor_BHB(i),Thermo_Factor_Butyrate(i),Total_Biom
ass_Decay(i),X_Mt_Butyrate_Fermenters(i),Cw_Myth_But(i),(Mythical_Fermentable
_Butyrate(i)+0.5*dT*k_mythbut_1));
        k_mythbut_3 =
MYTHBUT((t(i)+0.5*dT),Thermo_Factor_BHB(i),Thermo_Factor_Butyrate(i),Total_Bi
omass_Decay(i),X_Mt_Butyrate_Fermenters(i),Cw_Myth_But(i),(Mythical_Fermentab
le_Butyrate(i)+0.5*dT*k_mythbut_2));
        k_mythbut_4 =
MYTHBUT((t(i)+dT),Thermo_Factor_BHB(i),Thermo_Factor_Butyrate(i),Total_Biomas
s_Decay(i),X_Mt_Butyrate_Fermenters(i),Cw_Myth_But(i),(Mythical_Fermentable_B
utyrate(i)+k_mythbut_3*dT));
        Mythical_Fermentable_Butyrate(i+1) =
Mythical_Fermentable_Butyrate(i) +
(1/6)*(k_mythbut_1+2*k_mythbut_2+2*k_mythbut_3+k_mythbut_4)*dT;
        Cw_Myth_But(i+1) = Mythical_Fermentable_Butyrate(i+1)/Vw;

        k_mythlac_1 =
MYTHLAC(t(i),Thermo_Factor_Lac_to_Acetate(i),Thermo_Factor_Lac_to_Propionate(
i),Total_Biomass_Decay(i), ...

X_Mt_Butyrate_Fermenters(i),Cw_Myth_Lac(i),Mythical_Fermentable_Lactate(i));
        k_mythlac_2 =
MYTHLAC(t(i)+0.5*dT,Thermo_Factor_Lac_to_Acetate(i),Thermo_Factor_Lac_to_Prop
ionate(i),Total_Biomass_Decay(i), ...

X_Mt_Butyrate_Fermenters(i),Cw_Myth_Lac(i),(Mythical_Fermentable_Lactate(i)+0
.5*dT*k_mythlac_1));
        k_mythlac_3 =
MYTHLAC((t(i)+0.5*dT),Thermo_Factor_Lac_to_Acetate(i),Thermo_Factor_Lac_to_Pr
opionate(i),Total_Biomass_Decay(i), ...

X_Mt_Butyrate_Fermenters(i),Cw_Myth_Lac(i),(Mythical_Fermentable_Lactate(i)+0
.5*dT*k_mythlac_2));
        k_mythlac_4 =
MYTHLAC((t(i)+dT),Thermo_Factor_Lac_to_Acetate(i),Thermo_Factor_Lac_to_Propio
nate(i),Total_Biomass_Decay(i), ...

X_Mt_Butyrate_Fermenters(i),Cw_Myth_Lac(i),(Mythical_Fermentable_Lactate(i)+k
_mythlac_3*dT));
        Mythical_Fermentable_Lactate(i+1) = Mythical_Fermentable_Lactate(i)
+ (1/6)*(k_mythlac_1+2*k_mythlac_2+2*k_mythlac_3+k_mythlac_4)*dT;
        Cw_Myth_Lac(i+1) = Mythical_Fermentable_Lactate(i+1)/Vw;

       k_butyric_1 =
BUTYRIC(t(i),Thermo_Factor_BHB(i),Thermo_Factor_Butyrate(i),X_Mt_Butyrate_Fer
menters(i),Cw_Butyrate(i),Mt_Butyrate(i));
       k_butyric_2 =
BUTYRIC(t(i)+0.5*dT,Thermo_Factor_BHB(i),Thermo_Factor_Butyrate(i),X_Mt_Butyr
ate_Fermenters(i),Cw_Butyrate(i),(Mt_Butyrate(i)+0.5*dT*k_butyric_1));
```

```
        k_butyric_3 =
BUTYRIC((t(i)+0.5*dT),Thermo_Factor_BHB(i),Thermo_Factor_Butyrate(i),X_Mt_But
yrate_Fermenters(i),Cw_Butyrate(i),(Mt_Butyrate(i)+0.5*dT*k_butyric_2));
        k_butyric_4 =
BUTYRIC((t(i)+dT),Thermo_Factor_BHB(i),Thermo_Factor_Butyrate(i),X_Mt_Butyrat
e_Fermenters(i),Cw_Butyrate(i),(Mt_Butyrate(i)+k_butyric_3*dT));
        Mt_Butyrate(i+1) = Mt_Butyrate(i) +
(1/6)*(k_butyric_1+2*k_butyric_2+2*k_butyric_3+k_butyric_4)*dT;
        Cw_Butyrate(i+1) = Mt_Butyrate(i+1)/Vw;

        k_prop_1 =
PROP(t(i),Thermo_Factor_Propionate(i),X_Mt_Butyrate_Fermenters(i),Myth_Lac_Fe
rmented_to_Propionate(i),Cw_Propionate(i),Mt_Propionate(i));
        k_prop_2 =
PROP(t(i)+0.5*dT,Thermo_Factor_Propionate(i),X_Mt_Butyrate_Fermenters(i),Myth
_Lac_Fermented_to_Propionate(i),Cw_Propionate(i),(Mt_Propionate(i)+0.5*dT*k_p
rop_1));
        k_prop_3 =
PROP((t(i)+0.5*dT),Thermo_Factor_Propionate(i),X_Mt_Butyrate_Fermenters(i),My
th_Lac_Fermented_to_Propionate(i),Cw_Propionate(i),(Mt_Propionate(i)+0.5*dT*k
_prop_2));
        k_prop_4 =
PROP((t(i)+dT),Thermo_Factor_Propionate(i),X_Mt_Butyrate_Fermenters(i),Myth_L
ac_Fermented_to_Propionate(i),Cw_Propionate(i),(Mt_Propionate(i)+k_prop_3*dT)
);
        Mt_Propionate(i+1) = Mt_Propionate(i) +
(1/6)*(k_prop_1+2*k_prop_2+2*k_prop_3+k_prop_4)*dT;
        Cw_Propionate(i+1) = Mt_Propionate(i+1)/Vw;


        k_biodonor_1 =
BIODONOR(t(i),Butyrate_Fermented_to_Acetate(i),X_Butyrate_Fermenters(i));
        k_biodonor_2 =
BIODONOR(t(i)+0.5*dT,Butyrate_Fermented_to_Acetate(i),(X_Butyrate_Fermenters(
i)+0.5*dT*k_biodonor_1));
        k_biodonor_3 =
BIODONOR((t(i)+0.5*dT),Butyrate_Fermented_to_Acetate(i),(X_Butyrate_Fermenter
s(i)+0.5*dT*k_biodonor_2));
        k_biodonor_4 =
BIODONOR((t(i)+dT),Butyrate_Fermented_to_Acetate(i),(X_Butyrate_Fermenters(i)
+k_biodonor_3*dT));
        X_Butyrate_Fermenters(i+1) = X_Butyrate_Fermenters(i) +
(1/6)*(k_biodonor_1+2*k_biodonor_2+2*k_biodonor_3+k_biodonor_4)*dT;
        X_Mt_Butyrate_Fermenters(i+1) = X_Butyrate_Fermenters(i+1);
        X_Cw_Butyrate_Fermenters(i+1) = X_Butyrate_Fermenters(i+1)/Vw;


        k_h2_1 =
HYDROGEN(t(i),H2_For_Methanogenesis(i),X_Mt_Butyrate_Fermenters(i),Cw_Acetate
(i),Thermo_Factor_Ace_to_BHB(i), ...

Cw_Myth_But(i),Thermo_Factor_BHB(i),Thermo_Factor_Butyrate(i),Cw_Butyrate(i),
...

Cw_H2(i),PCE_Dechlorination_to_TCE(i),TCE_Dechlorination_to_DCE(i),DCE_Dechlo
rination_to_VC(i), ...
```

```
VC_Dechlorination_to_ETH(i),Butyrate_Fermented_to_Acetate(i),Propionate_Ferme
nted_to_Acetate(i), ...

X_Mt_Hydrogenotrophic_Methanogens(i),Fermented_Myth_But(i),Myth_Lac_Fermented
_to_Acetate(i), ...
                 Mt_Hydrogen(i));
        k_h2_2 =
HYDROGEN(t(i)+0.5*dT,H2_For_Methanogenesis(i),X_Mt_Butyrate_Fermenters(i),Cw_
Acetate(i),Thermo_Factor_Ace_to_BHB(i), ...

Cw_Myth_But(i),Thermo_Factor_BHB(i),Thermo_Factor_Butyrate(i),Cw_Butyrate(i),
...

Cw_H2(i),PCE_Dechlorination_to_TCE(i),TCE_Dechlorination_to_DCE(i),DCE_Dechlo
rination_to_VC(i), ...

VC_Dechlorination_to_ETH(i),Butyrate_Fermented_to_Acetate(i),Propionate_Ferme
nted_to_Acetate(i), ...

X_Mt_Hydrogenotrophic_Methanogens(i),Fermented_Myth_But(i),Myth_Lac_Fermented
_to_Acetate(i), ...
                 (Mt_Hydrogen(i)+0.5*dT*k_h2_1));
        k_h2_3 =
HYDROGEN((t(i)+0.5*dT),H2_For_Methanogenesis(i),X_Mt_Butyrate_Fermenters(i),C
w_Acetate(i),Thermo_Factor_Ace_to_BHB(i), ...

Cw_Myth_But(i),Thermo_Factor_BHB(i),Thermo_Factor_Butyrate(i),Cw_Butyrate(i),
...

Cw_H2(i),PCE_Dechlorination_to_TCE(i),TCE_Dechlorination_to_DCE(i),DCE_Dechlo
rination_to_VC(i), ...

VC_Dechlorination_to_ETH(i),Butyrate_Fermented_to_Acetate(i),Propionate_Ferme
nted_to_Acetate(i), ...

X_Mt_Hydrogenotrophic_Methanogens(i),Fermented_Myth_But(i),Myth_Lac_Fermented
_to_Acetate(i), ...
                 (Mt_Hydrogen(i)+0.5*dT*k_h2_2));
        k_h2_4 =
HYDROGEN((t(i)+dT),H2_For_Methanogenesis(i),X_Mt_Butyrate_Fermenters(i),Cw_Ac
etate(i),Thermo_Factor_Ace_to_BHB(i), ...

Cw_Myth_But(i),Thermo_Factor_BHB(i),Thermo_Factor_Butyrate(i),Cw_Butyrate(i),
...

Cw_H2(i),PCE_Dechlorination_to_TCE(i),TCE_Dechlorination_to_DCE(i),DCE_Dechlo
rination_to_VC(i), ...

VC_Dechlorination_to_ETH(i),Butyrate_Fermented_to_Acetate(i),Propionate_Ferme
nted_to_Acetate(i), ...

X_Mt_Hydrogenotrophic_Methanogens(i),Fermented_Myth_But(i),Myth_Lac_Fermented
_to_Acetate(i), ...
                 (Mt_Hydrogen(i)+k_h2_3*dT));
        Mt_Hydrogen(i+1) = Mt_Hydrogen(i) +
(1/6)*(k_h2_1+2*k_h2_2+2*k_h2_3+k_h2_4)*dT;
```

```
        Cw_H2(i+1) = Mt_Hydrogen(i+1)/(Vw+(Hc_H2*Vg));
        Cg_H2(i+1) = Mt_Hydrogen(i+1)/((Vw/Hc_H2)+Vg);
        H2_atm(i+1) = Cg_H2(i+1)*R2*Temp/1E6;

        k_dhcbio_1 =
DHC_BIO(t(i),PCE_Dechlorination_to_TCE(i),TCE_Dechlorination_to_DCE(i),DCE_De
chlorination_to_VC(i), ...
                    X_Dechlorinators(i));
        k_dhcbio_2 =
DHC_BIO(t(i)+0.5*dT,PCE_Dechlorination_to_TCE(i),TCE_Dechlorination_to_DCE(i)
,DCE_Dechlorination_to_VC(i), ...
                    (X_Dechlorinators(i)+0.5*dT*k_dhcbio_1));
        k_dhcbio_3 =
DHC_BIO((t(i)+0.5*dT),PCE_Dechlorination_to_TCE(i),TCE_Dechlorination_to_DCE(
i),DCE_Dechlorination_to_VC(i), ...
                    (X_Dechlorinators(i)+0.5*dT*k_dhcbio_2));
        k_dhcbio_4 =
DHC_BIO((t(i)+dT),PCE_Dechlorination_to_TCE(i),TCE_Dechlorination_to_DCE(i),D
CE_Dechlorination_to_VC(i), ...
                    (X_Dechlorinators(i)+k_dhcbio_3*dT));
        X_Dechlorinators(i+1) = X_Dechlorinators(i) +
(1/6)*(k_dhcbio_1+2*k_dhcbio_2+2*k_dhcbio_3+k_dhcbio_4)*dT;
        X_Mt_Dechlorinators(i+1) = X_Dechlorinators(i+1);
        X_Cw_Dechlorinators(i+1) = X_Dechlorinators(i+1)/Vw;

        k_PCE_w1 =
RATEPCE(t(i),X_Mt_Dechlorinators(i),Cw_H2(i),Cw_PCE(i),Cg_PCE(i),PCE_Competit
ive_Inhibition_Term(i),Mw_PCE(i));
        k_PCE_w2 =
RATEPCE(t(i)+0.5*dT,X_Mt_Dechlorinators(i),Cw_H2(i),Cw_PCE(i),Cg_PCE(i),PCE_C
ompetitive_Inhibition_Term(i),Mw_PCE(i)+0.5*dT*k_PCE_w1);
        k_PCE_w3 =
RATEPCE(t(i)+0.5*dT,X_Mt_Dechlorinators(i),Cw_H2(i),Cw_PCE(i),Cg_PCE(i),PCE_C
ompetitive_Inhibition_Term(i),Mw_PCE(i)+0.5*dT*k_PCE_w2);
        k_PCE_w4 =
RATEPCE(t(i)+dT,X_Mt_Dechlorinators(i),Cw_H2(i),Cw_PCE(i),Cg_PCE(i),PCE_Compe
titive_Inhibition_Term(i),Mw_PCE(i)+k_PCE_w3*dT);
        Mw_PCE(i+1) =
Mw_PCE(i)+(1/6)*(k_PCE_w1+2*k_PCE_w2+2*k_PCE_w3+k_PCE_w4)*dT;

        k_PCE_g1 = EXCHANGEPCE(t(i),Cg_PCE(i),Cw_PCE(i),Mg_PCE);
        k_PCE_g2 =
EXCHANGEPCE(t(i)+0.5*dT,Cg_PCE(i),Cw_PCE(i),(Mg_PCE(i)+0.5*dT*k_PCE_g1));
        k_PCE_g3 =
EXCHANGEPCE((t(i)+0.5*dT),Cg_PCE(i),Cw_PCE(i),(Mg_PCE(i)+0.5*dT*k_PCE_g2));
        k_PCE_g4 =
EXCHANGEPCE((t(i)+dT),Cg_PCE(i),Cw_PCE(i),(Mg_PCE(i)+k_PCE_g3*dT));
        Mg_PCE(i+1) = Mg_PCE(i) +
(1/6)*(k_PCE_g1+2*k_PCE_g2+2*k_PCE_g3+k_PCE_g4)*dT;

        Cw_PCE(i+1) = Mw_PCE(i+1)/Vw;
        Cg_PCE(i+1) = Mg_PCE(i+1)/Vg;
        Mt_PCE(i+1) = Mw_PCE(i+1)+Mg_PCE(i+1);
```

```
        k_TCE_w1 =
RATETCE(t(i),X_Mt_Dechlorinators(i),Cw_H2(i),Cw_TCE(i),Cg_TCE(i),TCE_Competit
ive_Inhibition_Term(i),Cw_PCE(i),PCE_Competitive_Inhibition_Term(i),Mw_TCE(i)
);
        k_TCE_w2 =
RATETCE(t(i)+0.5*dT,X_Mt_Dechlorinators(i),Cw_H2(i),Cw_TCE(i),Cg_TCE(i),TCE_C
ompetitive_Inhibition_Term(i),Cw_PCE(i),PCE_Competitive_Inhibition_Term(i),Mw
_TCE(i)+0.5*dT*k_TCE_w1);
        k_TCE_w3 =
RATETCE(t(i)+0.5*dT,X_Mt_Dechlorinators(i),Cw_H2(i),Cw_TCE(i),Cg_TCE(i),TCE_C
ompetitive_Inhibition_Term(i),Cw_PCE(i),PCE_Competitive_Inhibition_Term(i),Mw
_TCE(i)+0.5*dT*k_TCE_w2);
        k_TCE_w4 =
RATETCE(t(i)+dT,X_Mt_Dechlorinators(i),Cw_H2(i),Cw_TCE(i),Cg_TCE(i),TCE_Compe
titive_Inhibition_Term(i),Cw_PCE(i),PCE_Competitive_Inhibition_Term(i),Mw_TCE
(i)+k_TCE_w3*dT);
        Mw_TCE(i+1) =
Mw_TCE(i)+(1/6)*(k_TCE_w1+2*k_TCE_w2+2*k_TCE_w3+k_TCE_w4)*dT;

        k_TCE_g1 = EXCHANGETCE(t(i),Cg_TCE(i),Cw_TCE(i),Mg_TCE);
        k_TCE_g2 =
EXCHANGETCE(t(i)+0.5*dT,Cg_TCE(i),Cw_TCE(i),(Mg_TCE(i)+0.5*dT*k_TCE_g1));
        k_TCE_g3 =
EXCHANGETCE((t(i)+0.5*dT),Cg_TCE(i),Cw_TCE(i),(Mg_TCE(i)+0.5*dT*k_TCE_g2));
        k_TCE_g4 =
EXCHANGETCE((t(i)+dT),Cg_TCE(i),Cw_TCE(i),(Mg_TCE(i)+k_TCE_g3*dT));
        Mg_TCE(i+1) = Mg_TCE(i) +
(1/6)*(k_TCE_g1+2*k_TCE_g2+2*k_TCE_g3+k_TCE_g4)*dT;

        Cw_TCE(i+1) = Mw_TCE(i+1)/Vw;
        Cg_TCE(i+1) = Mg_TCE(i+1)/Vg;
        Mt_TCE(i+1) = Mw_TCE(i+1)+Mg_TCE(i+1);

        k_DCE_w1 =
RATEDCE(t(i),Cw_PCE(i),X_Mt_Dechlorinators(i),Cw_H2(i),Cw_DCE(i),Cg_DCE(i),DC
E_Competitive_Inhibition_Term(i),Cw_TCE(i),TCE_Competitive_Inhibition_Term(i)
,Mw_DCE(i));
        k_DCE_w2 =
RATEDCE(t(i)+0.5*dT,Cw_PCE(i),X_Mt_Dechlorinators(i),Cw_H2(i),Cw_DCE(i),Cg_DC
E(i),DCE_Competitive_Inhibition_Term(i),Cw_TCE(i),TCE_Competitive_Inhibition_
Term(i),Mw_DCE(i)+0.5*dT*k_DCE_w1);
        k_DCE_w3 =
RATEDCE(t(i)+0.5*dT,Cw_PCE(i),X_Mt_Dechlorinators(i),Cw_H2(i),Cw_DCE(i),Cg_DC
E(i),DCE_Competitive_Inhibition_Term(i),Cw_TCE(i),TCE_Competitive_Inhibition_
Term(i),Mw_DCE(i)+0.5*dT*k_DCE_w2);
        k_DCE_w4 =
RATEDCE(t(i)+dT,Cw_PCE(i),X_Mt_Dechlorinators(i),Cw_H2(i),Cw_DCE(i),Cg_DCE(i)
,DCE_Competitive_Inhibition_Term(i),Cw_TCE(i),TCE_Competitive_Inhibition_Term
(i),Mw_DCE(i)+k_DCE_w3*dT);
        Mw_DCE(i+1) =
Mw_DCE(i)+(1/6)*(k_DCE_w1+2*k_DCE_w2+2*k_DCE_w3+k_DCE_w4)*dT;

        k_DCE_g1 = EXCHANGEDCE(t(i),Cg_DCE(i),Cw_DCE(i),Mg_DCE);
        k_DCE_g2 =
EXCHANGEDCE(t(i)+0.5*dT,Cg_DCE(i),Cw_DCE(i),Mg_DCE(i)+0.5*dT*k_DCE_g1);
```

```
        k_DCE_g3 =
EXCHANGEDCE(t(i)+0.5*dT,Cg_DCE(i),Cw_DCE(i),Mg_DCE(i)+0.5*dT*k_DCE_g2);
        k_DCE_g4 =
EXCHANGEDCE(t(i)+dT,Cg_DCE(i),Cw_DCE(i),Mg_DCE(i)+k_DCE_g3*dT);
        Mg_DCE(i+1) = Mg_DCE(i) +
(1/6)*(k_DCE_g1+2*k_DCE_g2+2*k_DCE_g3+k_DCE_g4)*dT;

        Cw_DCE(i+1) = Mw_DCE(i+1)/Vw;
        Cg_DCE(i+1) = Mg_DCE(i+1)/Vg;
        Mt_DCE(i+1) = Mw_DCE(i+1)+Mg_DCE(i+1);

        k_VC_w1 =
RATEVC(t(i),Cw_PCE(i),X_Mt_Dechlorinators(i),Cw_H2(i),Cw_VC(i),Cg_VC(i),VC_Co
mpetitive_Inhibition_Term(i),Cw_DCE(i),DCE_Competitive_Inhibition_Term(i),Mw_
VC(i));
        k_VC_w2 =
RATEVC(t(i)+0.5*dT,Cw_PCE(i),X_Mt_Dechlorinators(i),Cw_H2(i),Cw_VC(i),Cg_VC(i
),VC_Competitive_Inhibition_Term(i),Cw_DCE(i),DCE_Competitive_Inhibition_Term
(i),Mw_VC(i)+0.5*dT*k_VC_w1);
        k_VC_w3 =
RATEVC(t(i)+0.5*dT,Cw_PCE(i),X_Mt_Dechlorinators(i),Cw_H2(i),Cw_VC(i),Cg_VC(i
),VC_Competitive_Inhibition_Term(i),Cw_DCE(i),DCE_Competitive_Inhibition_Term
(i),Mw_VC(i)+0.5*dT*k_VC_w2);
        k_VC_w4 =
RATEVC(t(i)+dT,Cw_PCE(i),X_Mt_Dechlorinators(i),Cw_H2(i),Cw_VC(i),Cg_VC(i),VC
_Competitive_Inhibition_Term(i),Cw_DCE(i),DCE_Competitive_Inhibition_Term(i),
Mw_VC(i)+k_VC_w3*dT);
        Mw_VC(i+1) = Mw_VC(i)+(1/6)*(k_VC_w1+2*k_VC_w2+2*k_VC_w3+k_VC_w4)*dT;

        k_VC_g1 = EXCHANGEVC(t(i),Cg_VC(i),Cw_VC(i),Mg_VC);
        k_VC_g2 =
EXCHANGEVC(t(i)+0.5*dT,Cg_VC(i),Cw_VC(i),(Mg_VC(i)+0.5*dT*k_VC_g1));
        k_VC_g3 =
EXCHANGEVC((t(i)+0.5*dT),Cg_VC(i),Cw_VC(i),(Mg_VC(i)+0.5*dT*k_VC_g2));
        k_VC_g4 =
EXCHANGEVC((t(i)+dT),Cg_VC(i),Cw_VC(i),(Mg_VC(i)+k_VC_g3*dT));
        Mg_VC(i+1) = Mg_VC(i) +
(1/6)*(k_VC_g1+2*k_VC_g2+2*k_VC_g3+k_VC_g4)*dT;

        Cw_VC(i+1) = Mw_VC(i+1)/Vw;
        Cg_VC(i+1) = Mg_VC(i+1)/Vg;
        Mt_VC(i+1) = Mw_VC(i+1)+Mg_VC(i+1);

        k_ETH_w1 =
RATEETH(t(i),Cw_PCE(i),X_Mt_Dechlorinators(i),Cw_H2(i),Cw_ETH(i),Cg_ETH(i),Cw
_VC(i),VC_Competitive_Inhibition_Term(i),Mw_ETH(i));
        k_ETH_w2 =
RATEETH(t(i)+0.5*dT,Cw_PCE(i),X_Mt_Dechlorinators(i),Cw_H2(i),Cw_ETH(i),Cg_ET
H(i),Cw_VC(i),VC_Competitive_Inhibition_Term(i),Mw_ETH(i)+0.5*dT*k_ETH_w1);
        k_ETH_w3 =
RATEETH(t(i)+0.5*dT,Cw_PCE(i),X_Mt_Dechlorinators(i),Cw_H2(i),Cw_ETH(i),Cg_ET
H(i),Cw_VC(i),VC_Competitive_Inhibition_Term(i),Mw_ETH(i)+0.5*dT*k_ETH_w2);
        k_ETH_w4 =
RATEETH(t(i)+dT,Cw_PCE(i),X_Mt_Dechlorinators(i),Cw_H2(i),Cw_ETH(i),Cg_ETH(i)
,Cw_VC(i),VC_Competitive_Inhibition_Term(i),Mw_ETH(i)+k_ETH_w3*dT);
```

```
        Mw_ETH(i+1) =
Mw_ETH(i)+(1/6)*(k_ETH_w1+2*k_ETH_w2+2*k_ETH_w3+k_ETH_w4)*dT;

        k_ETH_g1 = EXCHANGEETH(t(i),Cg_ETH(i),Cw_ETH(i),Mg_ETH);
        k_ETH_g2 =
EXCHANGEETH(t(i)+0.5*dT,Cg_ETH(i),Cw_ETH(i),(Mg_ETH(i)+0.5*dT*k_ETH_g1));
        k_ETH_g3 =
EXCHANGEETH((t(i)+0.5*dT),Cg_ETH(i),Cw_ETH(i),(Mg_ETH(i)+0.5*dT*k_ETH_g2));
        k_ETH_g4 =
EXCHANGEETH((t(i)+dT),Cg_ETH(i),Cw_ETH(i),(Mg_ETH(i)+k_ETH_g3*dT));
        Mg_ETH(i+1) = Mg_ETH(i) +
(1/6)*(k_ETH_g1+2*k_ETH_g2+2*k_ETH_g3+k_ETH_g4)*dT;

        Cw_ETH(i+1) = Mw_ETH(i+1)/Vw;
        Cg_ETH(i+1) = Mg_ETH(i+1)/Vg;
        Mt_ETH(i+1) = Mw_ETH(i+1)+Mg_ETH(i+1);
        Mt_VC_ETH(i+1) = Mt_VC(i+1)+Mt_ETH(i+1);

        k_ace_1 =
ACETATE(t(i),Acetate_Conversion_to_Methane(i),X_Mt_Butyrate_Fermenters(i),The
rmo_Factor_Ace_to_BHB(i), ...

X_Mt_Acetotrophs(i),Butyrate_Fermented_to_Acetate(i),Propionate_Fermented_to_
Acetate(i), ...

Fermented_Myth_But(i),Myth_Lac_Fermented_to_Acetate(i),Myth_Lac_Fermented_to_
Propionate(i),Cw_Acetate(i),Mt_Acetate(i));
        k_ace_2 =
ACETATE(t(i)+0.5*dT,Acetate_Conversion_to_Methane(i),X_Mt_Butyrate_Fermenters
(i),Thermo_Factor_Ace_to_BHB(i), ...

X_Mt_Acetotrophs(i),Butyrate_Fermented_to_Acetate(i),Propionate_Fermented_to_
Acetate(i), ...

Fermented_Myth_But(i),Myth_Lac_Fermented_to_Acetate(i),Myth_Lac_Fermented_to_
Propionate(i),Cw_Acetate(i),(Mt_Acetate(i)+0.5*dT*k_ace_1));
        k_ace_3 =
ACETATE((t(i)+0.5*dT),Acetate_Conversion_to_Methane(i),X_Mt_Butyrate_Fermente
rs(i),Thermo_Factor_Ace_to_BHB(i), ...

X_Mt_Acetotrophs(i),Butyrate_Fermented_to_Acetate(i),Propionate_Fermented_to_
Acetate(i), ...

Fermented_Myth_But(i),Myth_Lac_Fermented_to_Acetate(i),Myth_Lac_Fermented_to_
Propionate(i),Cw_Acetate(i),(Mt_Acetate(i)+0.5*dT*k_ace_2));
        k_ace_4 =
ACETATE((t(i)+dT),Acetate_Conversion_to_Methane(i),X_Mt_Butyrate_Fermenters(i
),Thermo_Factor_Ace_to_BHB(i), ...

X_Mt_Acetotrophs(i),Butyrate_Fermented_to_Acetate(i),Propionate_Fermented_to_
Acetate(i), ...

Fermented_Myth_But(i),Myth_Lac_Fermented_to_Acetate(i),Myth_Lac_Fermented_to_
Propionate(i),Cw_Acetate(i),(Mt_Acetate(i)+k_ace_3*dT));
        Mt_Acetate(i+1) = Mt_Acetate(i) +
(1/6)*(k_ace_1+2*k_ace_2+2*k_ace_3+k_ace_4)*dT;
```

```
        Cw_Acetate(i+1) = Mt_Acetate(i+1)/Vw;

        k_acebio_1 =
ACETOTROPHS(t(i),Acetate_Conversion_to_Methane(i),X_Acetotrophs(i));
        k_acebio_2 =
ACETOTROPHS(t(i)+0.5*dT,Acetate_Conversion_to_Methane(i),(X_Acetotrophs(i)+0.
5*dT*k_acebio_1));
        k_acebio_3 =
ACETOTROPHS((t(i)+0.5*dT),Acetate_Conversion_to_Methane(i),(X_Acetotrophs(i)+
0.5*dT*k_acebio_2));
        k_acebio_4 =
ACETOTROPHS((t(i)+dT),Acetate_Conversion_to_Methane(i),(X_Acetotrophs(i)+k_ac
ebio_3*dT));
        X_Acetotrophs(i+1) = X_Acetotrophs(i) +
(1/6)*(k_acebio_1+2*k_acebio_2+2*k_acebio_3+k_acebio_4)*dT;

        X_Mt_Acetotrophs(i+1) = X_Acetotrophs(i+1);
        X_Cw_Acetotrophs(i+1) = X_Acetotrophs(i+1)/Vw;


        k_h2ch4bio_1 =
HYDROMETHAN(t(i),H2_For_Methanogenesis(i),X_Hydrogenotrophic_Methanogens(i));
        k_h2ch4bio_2 =
HYDROMETHAN(t(i)+0.5*dT,H2_For_Methanogenesis(i),(X_Hydrogenotrophic_Methanog
ens(i)+0.5*dT*k_h2ch4bio_1));
        k_h2ch4bio_3 =
HYDROMETHAN((t(i)+0.5*dT),H2_For_Methanogenesis(i),(X_Hydrogenotrophic_Methan
ogens(i)+0.5*dT*k_h2ch4bio_2));
        k_h2ch4bio_4 =
HYDROMETHAN((t(i)+dT),H2_For_Methanogenesis(i),(X_Hydrogenotrophic_Methanogen
s(i)+k_h2ch4bio_3*dT));
        X_Hydrogenotrophic_Methanogens(i+1) =
X_Hydrogenotrophic_Methanogens(i) +
(1/6)*(k_h2ch4bio_1+2*k_h2ch4bio_2+2*k_h2ch4bio_3+k_h2ch4bio_4)*dT;

        X_Mt_Hydrogenotrophic_Methanogens(i+1) =
X_Hydrogenotrophic_Methanogens(i+1);
        X_Cw_Hydrogenotrophic_Methanogens(i+1) =
X_Hydrogenotrophic_Methanogens(i+1)/Vw;

        k_CH4_11 =
METHANE1(t(i),Acetate_Conversion_to_Methane(i),Mt_Methane_From_Acetate(i));
        k_CH4_12 =
METHANE1(t(i)+0.5*dT,Acetate_Conversion_to_Methane(i),(Mt_Methane_From_Acetat
e(i)+0.5*dT*k_CH4_11));
        k_CH4_13 =
METHANE1((t(i)+0.5*dT),Acetate_Conversion_to_Methane(i),(Mt_Methane_From_Acet
ate(i)+0.5*dT*k_CH4_12));
        k_CH4_14 =
METHANE1((t(i)+dT),Acetate_Conversion_to_Methane(i),(Mt_Methane_From_Acetate(
i)+k_CH4_13*dT));
        Mt_Methane_From_Acetate(i+1) = Mt_Methane_From_Acetate(i) +
(1/6)*(k_CH4_11+2*k_CH4_12+2*k_CH4_13+k_CH4_14)*dT;
```

```
        Cw_Methane_From_Acetate(i+1) =
Mt_Methane_From_Acetate(i+1)/(Vw+(Hc_CH4*Vg));
        Cg_Methane_From_Acetate(i+1) =
Mt_Methane_From_Acetate(i+1)/((Vw/Hc_CH4)+Vg);

        k_CH4_21 =
METHANE2(t(i),H2_For_Methanogenesis(i),Mt_Methane_From_H2(i));
        k_CH4_22 =
METHANE2(t(i)+0.5*dT,H2_For_Methanogenesis(i),(Mt_Methane_From_H2(i)+0.5*dT*k
_CH4_21));
        k_CH4_23 =
METHANE2((t(i)+0.5*dT),H2_For_Methanogenesis(i),(Mt_Methane_From_H2(i)+0.5*dT
*k_CH4_22));
        k_CH4_24 =
METHANE2((t(i)+dT),H2_For_Methanogenesis(i),(Mt_Methane_From_H2(i)+k_CH4_23*d
T));
        Mt_Methane_From_H2(i+1) = Mt_Methane_From_H2(i) +
(1/6)*(k_CH4_21+2*k_CH4_22+2*k_CH4_23+k_CH4_24)*dT;

        Cw_Methane_From_H2(i+1) = Mt_Methane_From_H2(i+1)/(Vw+(Hc_CH4*Vg));
        Cg_Methane_From_H2(i+1) = Mt_Methane_From_H2(i+1)/((Vw/Hc_CH4)+Vg);

        Mt_Total_Methane(i+1) =
Mt_Methane_From_Acetate(i+1)+Mt_Methane_From_H2(i+1);
        Cw_Total_Methane(i+1) =
Cw_Methane_From_Acetate(i+1)+Cw_Methane_From_H2(i+1);
        Cg_Total_Methane(i+1) =
Cg_Methane_From_Acetate(i+1)+Cg_Methane_From_H2(i+1);
end
```

REFERENCES

Aggazzotti, G., Fantuzzi, G., Righi, E., Predieri, G., Gobba, F.M., Paltrinieri, M., & Cavalleri, A. (1994). Occupational and environmental exposure to perchloroethylene (PCE) in dry cleaners and their family members. *Archives of Environmental Health: An International Journal*, 49(6), 487-493.

Amos, B.K., Christ, J.A., Abriola, L.M., Pennell, K.D., & Löffler, F.E. (2007). Experimental evaluation and mathematical modeling of microbially enhanced tetrachloroethene (PCE) dissolution. *Environ. Sci. Technol.*, 41(3), 963–970.

Beun, J.J., Paletta, F., Van Loosdrecht., M.C.M., & Heijnen, J.J. (2000). Stoichiometry and kinetics of poly-β-hydroxybutyrate metabolism in aerobic, slow growing, activated sludge cultures. *Biotechnol. Bioeng.*, 67(4), 379-389.

Beun, J.J., Dircks, D., Van Loosdrecht, M.C.M., & Heijnen, J.J. (2002). Poly-β-hydroxybutyrate metabolism in dynamically fed mixed microbial cultures. *Water Research*, 36, 1167-1180.

Bouwer, E.J., & McCarty, P.L. (1983). Transformation of 1- and 2-carbon halogenated aliphatic organic compounds under methanogenic conditions. *Appl. Environ. Microbiol.*, 45(4), 1286–1294.

Bradley, P.M. (2003). History and ecology of chloroethene bioremediation: A review. *Bioremediation Journal*, 7(2), 81-109.

Braunegg, G., Sonnleitner, B., & Lafferty, R.M. (1978). A rapid gas chromatographic method for the determination of poly-β-hydroxybutyric acid in microbial biomass. *Eur. J. Appl. Microbiol. Biotechnol.*, 6, 29– 37.

Comeau, Y., Hall, K.J., & Oldham, W.K. (1988). Determination of poly-hhydroxybutyrate and Poly-β-hydroxyvalerate in activated sludge by gas-liquid chromatography. Appl Environ Microbiol 54:2323–2327.

Cupples, A.M., Spormann, A.M., & McCarty, P.L. (2004). Vinyl chloride and *cis*-dichloroethene dechlorination kinetics and microorganism growth under substrate limiting conditions. *Enviro. Sci. Technol*, 38, 1102-1107.

Dionisi, D., Majone, M., Tandoi, V., & Beccari, M. (2001) Sequencing batch reactor: influence of periodic operation on performance of activated sludge in biological wastewater treatment. *Ind. Eng. Chem. Res.*, 40, 5110-5119.

DiStefano, T.D., Gossett, J.M., & Zinder, S.H. (1991). Reductive dechlorination of high concentrations of tetrachloroethene to ethene by an anaerobic enrichment culture in the absence of methanogenesis. *Appl. Environ. Microbiol.*, 57(8), 2287–2292.

DiStefano, T.D., Gossett, J.M., & Zinder, S.H. (1992). Hydrogen as an electron donor for dechlorination of tetrachloroethene by an anaerobic mixed culture. *Appl. Environ. Microbiol.*, 58,3622–3629.

Doherty, R. E. (2000). A history of the production and use of carbon tetrachloride, tetrachloroethylene, trichloroethylene and 1,1,1-trichloroethane in the United States: Part 1--Historical background; Carbon tetrachloride and tetrachloroethylene. *Environmental Forensics*, 1(2), 69–81.

Duhamel, M., Wehr, S.D., Yu, L., Rizvi, H., Seepersad, D., Dworatzek, S., Cox, E.E., & Edwards, E.A. (2002). Comparison of anaerobic dechlorinating enrichment cultures maintained on tetrachloroethene, trichloroethene, *cis*-dichloroethene and vinyl chloride. *Water Research*, 36 (17), 4193–4202.

Fathepure, B.Z., Nengu, J.P., & Boyd, S.A. (1987). Anaerobic bacteria that dechlorinate perchloroethene. *Appl. Environ. Microbiol.*, 53(11), 2671–2674.

Fennell. D.E. (1998). Comparison of alternative hydrogen donors for anaerobic reductive dechlorination of tetrachlroethene. PhD dissertation, Cornell University.

Fennell, D.E., Gossett, J.M., Zinder, S.H. (1997). Comparison of butyric acid, ethanol, lactic acid, and propionic acid as hydrogen donors for the reductive dechlorination of tetrachloroethene. *Environ. Sci. Technol.*, 31, 918–926.

Fennell, D.E., & Gossett, J.M. (1998). Modeling the production of and competition for hydrogen in a dechlorinating culture. *Environ. Sci. Technol.*, 32, 2450-2460.

Freedman, D.L., & Gossett, J.M. (1989). Biological reductive dechlorination of tetrachloroethylene and trichloroethylene to ethylene under methanogenic conditions. *Appl. Environ. Microbiol.*, 55(9), 2144–2151.

Gantzer, C.J., & Wackett, L.P. (1991). Reductive dechlorination catalyzed by bacterial transition-metal coenzymes. *Environ. Sci. Technol.*, 25(4),715–722.

Garant, H., & Lynd, L., (1998). Applicability of competitive and noncompetitive kinetics to the reductive dechlorination of chlorinated ethenes. *Biotechnol. Bioeng.*, 57(6), 751–755.

Haston, Z.C., & McCarty, P.L., (1999). Chlorinated ethene half-velocity coefficients (K–S) for reductive dehalogenation. *Environ. Sci. & Technol.*, 33 (2), 223–226.

Haest, P.J., Ruymen, S., Springael, D., Smolders, E. (2006). Reductive dechlorination at high aqueous TCE concentrations. *Communications in Applied and Biological Sciences*, 71 (1), 165–169.

Haest, P.J.,Sprinael, D., & Smolders, E. (2010). Dechlorination kinetics of TCE at toxic TCE concentrations: Assessment if different models. *Water Research*, 44, 331-339.

He, J., Ritalahti, K.M., Yang, K-L., Koenigsberg, S.S., Löffler, F.E. (2003). Detoxification of vinyl chloride to ethene coupled to growth of an anaerobic bacterium. *Nature*, 424, 62–65.

Heavner, G.L. (2013). Biokinetic modeling, laboratory examination and field analysis of DNA, RNA and protein as robust molecular biomarkers of chloroethene reductive dechlorination in *Dehalococcoides mccartyi*. PhD Dissertation, Cornell University.

Heavner, G.L, Rowe, A.R., Mansfeldt, C.B., Pan, J. K., Gossett, J.M., & Richardson, R.E. (2013). Molecular biomarker-based biokinetic modeling of a PCE-dechlorinating and methanogenic mixed culture. *Environ. Sci. Technol.*, 47(8), 3724-3733.

Henry, B. M. In *In Situ Remediation of Chlorinated Solvent Plumes*; Stroos, H. F.; Ward, C. H., Eds.; Springer, 2010; pp. 357–423.

Holliger, C., Schraa, G., Stams, A.J., & Zehnder, A.J. (1993). A highly purified enrichment culture couples the reductive dechlorination of tetrachloroethene to growth. *Appl. Environ. Microbiol.*, 59(9), 2991–2997.

Holliger, C., Hahn, D., Harmsen, H., Ludwig, W., Schumacher, W., Tindall, B., Vazquez, F., Weiss, N., & Zehnder, A.J.B. (1998). *Dehalobacter restrictus* gen. nov. and sp. nov., a strictly anaerobic bacterium that reductively dechlorinates tetra- and trichloroethene in an anaerobic respiration. *Arch. Microbiol.*, 169, 313–321.

Huang, D., & Becker, J.G. (2011). Dehalorespiration model that incorporates the self-inhibition and biomass inactivation effects of high tetrachloroethene concentrations. *Environ. Sci. Technol.*, 45, 1093-1099.

IARC (International Agency for Research on Cancer). (1995). Dry-Cleaning, Some Chlorinated Solvents and Other Industrial Chemicals. World Health Organization IARC Monographs on the Evaluation of Carcinogenic Risks to Humans, Vol 63.

ITRC (Interstate Technology & Regulatory Council). (2005). *Overview of In Situ bioremediation of chlorinated ethene DNAPL source zones*. *BIODNAPL-1*. Washington, D.C.: Interstate Technology & Regulatory Council, Bioremediation of Dense Nonaqueous Phase Liquids (Bio DNAPL) Team. Retrieved from http://www.itrcweb.org.

Kielhorn, J., Melber, C., Wahnschaffe, U., Aitio, A., & Mangelsdof, I. (2000). Vinyl chloride: Still a cause for concern. *Environ Health Perspect*, 108(7), 579–588.

Krumholz, L.R., Sharp, R., & Fishbain, S.S. (1996). A freshwater anaerobe coupling acetate oxidation to tetrachloroethene dehalogenation. *Appl. Environ. Microbiol.*, 62(11), 4108–4113.

Lee, I-S., Bae, J-H., Yang, Y., & McCarty, P.L. (2004). Simulated and experimental evaluation of factors affecting the rate and extent of reductive dehalogenation of chloroethenes with glucose. *J. Contam. Hydrol.*, 74, 313-331.

Lemos, P.L., Serafim, L.S., & Reis, M.A.M. (2006). Synthesis of polyhydroxyalkanoates from

different short-chain fatty acids by mixed cultures submitted to aerobic dynamic feeding. *Journal of Biotechnology*, 122, 226-238.

Löffler, F. E. & Edwards, E. A. (2006). Harnessing microbial activities for environmental cleanup. *Current Opinion in Biotechnology*, 17, 274–284.

Löffler, F. E. Ritalahti, K.M., & Zinder, S.H. (2013a). *Dehalococoides* and reductive dechlorination of chlorinated solvents. In H.F. Stroo, A. Leeson and C.H. Ward (Eds,), *Bioaugmentation for groundwater remediation* (pp.39-88), Springer Science+Business Media, LLC, New York, NY.

Löffler, F.E., Yan, J., Ritalahti, K.M., Adrian, L., Edwards, E.A., Konstantinidis, K.T., Müller, J.A., Fullerton, H., Zinder, S.H., & Spormann, A.M. (2013b). *Dehalococcoides mccartyi* gen. nov., sp. nov., obligately organohalide-respiring anaerobic bacteria relevant to halogen cycling and bioremediation, belong to a novel bacterial class, *Dehalococcoidia* classis nov., order *Dehalococcoidales* ord. nov. and family *Dehalococcoidaceae* fam. nov., within the phylum *Chloroflexi*. *International Journal of Systematic and Evolutionary Microbiology*, 63, 625-635.

Luong, J.H.T. (1987). Generalization of Monod kinetics for analysis of growth data with substrate inhibition. *Biotechnol. Bioeng.*, 29, 242-248.

Lyon, D.Y., & Vogel, T.M. (2013). Bioaugmentation for groundwater remediation: An overview. In H.F. Stroo, A. Leeson and C.H. Ward (Eds,), *Bioaugmentation for groundwater remediation* (pp.1-37), Springer Science+Business Media, LLC, New York, NY.

Mackay, D.M., & Cherry, J.A. (1989). Groundwater contamination: Pump-and-treat remediation. *Environ. Sci. Technol.*, 23(6), 630–636.

Magnuson, J.K., Stern, R.V., Gossett, J.M., Zinder, S.H., & Burris, D.R. (1998). Reductive dechlorination of tetrachloroethene to ethene by a two-component enzyme pathway. *Appl. Environ. Microbiol.*, 64(4), 1270-1275.

Magnuson, J.K., Romine, M.F., Burris, D.R., & Kingsley, M.T. (2000). Trichloroethene reductive dehalogenase from Dehalococcoides ethenogenes: Sequence of tceA and substrate range characterization. *Appl. Environ. Microbiol.*, 66, 5141–5147.

MathWorks. (2014). *MATLAB The language of technical computing*. Retrieved June 21, 2014, from http://www.mathworks.com/products/matlab/.

Maymó-Gatell, X., Chien, Y-T., Gossett, J.M., & Zinder, S.H. (1997). Isolation of a bacterium that reductively dechlorinates tetrachloroethene to ethene. *Science*, 276(5318), 1568–1571.

Maymó-Gatell, X., Anguish, T., & Zinder, S.H. (1999). Reductive dechlorination of chlorinated ethenes and 1,2-dichloroethane by Dehalococcoides ethenogenes 195. *Appl. and Environ. Microbiol.*, 65, 3108-3113.

Maymó-Gatell, X., Nijenhuis, I., & Zinder, S.H. (2001). Reductive dechlorination of cis-dichloroethene and vinyl chloride by "*Dehalococcoides ethenogenes*". *Environ. Sci. Technol.*, 35, 516–521.

McCarty, P.L. (2010) Groundwater contamination by chlorinated solvents: History, remediation technologies and strategies. In H.F. Stroo & C.H. Ward (Eds), *In Situ remediation of chlorinated sovent plumes* (pp.1-28), Springer Science+Business Media, LLC, New York, NY.

Moran, M.J. (2006). Occurrence and implications of selected chlorinated solvents in ground water and source water in the United States and in drinking water in 12 Northeast and Mid-Atlantic States, 1993–2002: U.S. Geological Survey Scientific Investigations Report 2005–5268, 70 p.

Müller, J.A., Rosner, B.M., Von Abendroth, G., Meshulam-Simon, G., McCarty, P.L., & Spormann, A.M. (2004). Molecular identification of the catabolic vinyl chloride reductase from *Dehalococcoides* sp. strain VS and its environmental distribution. *Appl. Environ. Microbiol.*, 70(8), 4880–4888.

Neumann, A., Scholz-Muramatsu, H., & Diekert, G. (1994). Tetrachloroethene metabolism of Dehalospirillum multivorans. *Arch. Microbiol.*, 162, 295–301.

Richardson, R.E., Bhupathiraju, V.K., Song, D.L., Goulet, T.A., & Alvarez-Cohen, L. (2002). Phylogenetic characterization of microbial communities that reductively dechlorinate TCE based upon a combination of molecular techniques. *Environ. Sci. Technol.*, 36(12), 2652–2662.

Rowe, A. R., Lazar, B. J., Morris, R. M., & Richardson, R. E. (2008). Characterization of the Community Structure of a Dechlorinating Mixed Culture and Comparisons of Gene Expression in Planktonic and Biofloc-Associated *Dehalococcoides* and *Methanospirillum* Species. *Appl. Environ. Microb*, 74, 6709–6719.

Russell, H. H., Matthews, J. E., & Sewell, G. W. (1992). *EPA Ground water issue: TCE removal from contaminated soil and ground water*. EPA/540/S-92/002. Washingtong, D.C.: Technology Innovation Office, Office of Solid Waste and Emergency Response, US EPA.

Satoh, H., Mino, T., & Matsuo, T. (1992). Uptake of organic substrates and accumulation of polyhydroxyalkanoates linked with glycolysis of intracellular carbohydrates under anaerobic conditions in the biological excess phosphate removal processes. *Water Sci. Technol.,* 26, 933–942.

Serafim, L.S., Lemos, P.C., Oliveira, R., & Reis, M.A.M. (2004) Optimization of polyhydroxybutyrate production by mixed cultures submitted to aerobic dynamic feeding conditions. *Biotechnol. Bioeng*., 87(2), 145-160.

Seshadri, R., Adrian, L., Fouts, D.E., Eisen, J.A., Phillippy, A.M., Methe, B.A., Ward, N.L., Nelson, W.C., Deboy,R.T., Khouri, H.M., Kolonay, J.F., Dodson, R.J., Daugherty, S.C., Brinkac, L.M., Sullivan, S.A., Madupu, R., Nelson, K.E., Kang, K.H., Impraim, M., Tran, K., Robinson,

J.M., Forberger, H.A., Fraser, C.M., Zinder, S.H., & Heidelberg, H.F. (2005). Genome sequence of the PCE-dechlorinating bacterium Dehalococcoides ethenogenes. *Science*, 307, 105-108.

Shampine, L.F. (2005). Solving ODEs and DDEs with residual control. *Applied Numerical Methmatics*, 52, 113-127.

Sung, Y., Ritalahti, K.M., Apkarian, R.P., & Löffler F.E. (2006). Quantitative PCR confirms purity of strain GT, a novel trichloroethene (TCE)-to-ethene respiring *Dehalococcoides* isolate. *Appl. Environ. Microbiol.*, 72(3), 1980–1987.

Tandoi, V., Distefano, T.D., Bowser, P.A., Gossett, J.M., Zinder, S. H., (1994). Reductive dehalogenation of chlorinated ethenes and halogenated ethanes by a high-rate anaerobic enrichment culture. *Environ. Sci. Technol.*, 28(5), 973–979.

Thauer, R. K., Jungermann, K. & Decker, D. (1977). Energy conservation in chemotrophic anaerobic bacteria. *Bacteriol. Rev.* 1977, 41(1), 100-180.

Tonnaer, H., Alphenaar, A., Wit, H.D., Grutters, M., Spuij, F., Gerritse, J., & Gottschal, J.C. (1997). Modelling of anaerobic dechlorination of chloroethenes for *in-situ* bioremediation. In: B.C. Alleman, A. Leeson (Eds), *Proceedings of the Fourth International Conference on In Situ and On-Site Bio- remediation* (pp. 591-596). Battelle Press, Columbus, OH.

U.S. EPA (Environmental Protection Agency). (2001). Groundwater pump and treat systems: Summary of selected cost and performance information at Superfund-financed sites. EPA 542-R-01-02b.

U.S. EPA (Environmental Protection Agency). (2004a). 2004 Edition of the drinking water standards and health advisories. 822-R-04-005. Washington, DC: Office of Water.

U.S. EPA (Environmental Protection Agency). (2004b). *In-Situ* thermal treatment of chlorinated solvents: Fundamentals and Field Applications. EPA 542-R-04-010. Washington, DC: Office of Solid Waste and Emergency Response, Office of Superfund Remediation and Technology Innovation.

U.S. EPA (Environmental Protection Agency). (2007). Treatment technologies for site cleanup: Annual status report (Twelfth edition). EPA-542-R-07-012. Washington, DC: Solid Waste and Emergency Response.

U.S. EPA (Environmental Protection Agency). (2011). Toxicological review of trichloroethylene: In support of summary information on the integrated risk information system (IRIS). EPA/635/R-09/011F. Washington, DC: U.S. Environmental Protection Agency.

Vainberg, S., Condee, C.W., Steffan, R.J. (2009). Large-scale production of bacterial consortia for remediation of chlorinated solvent-contaminated groundwater. *J Ind Microbiol Biotechnol*, 36, 1189–1197.

Vogel, T.M., & McCarty, P.L. (1985). Biotransformation of tetrachloroethylene to trichloroethylene, dichloroethylene, vinyl chloride, and carbon dioxide under methanogenic conditions. *Appl. Environ. Microbiol.*, 49(5), 1080–1083.

Westrick, J. J., Mello, J.W., & Thomas, R.F. (1984). The Groundwater Supply Survey. *Journal - American Water Works Association*, 76(5), 52-59.

WHO (World Health Organization). (1999). International programme on chemical safety. Vinyl chloride. Environmental health criteria 215. Geneva: World Health Organization.

Wilson, J.T., & Wilson, B.H. (1985). Biotransformation of trichloroethylene in soil. *Appl. Environ. Microbiol.*, 49(1), 242-243.

Yang, Y., & McCarty, P.L. (2000). Biologically enhanced dissolution of tetrachloroethene DNAPL. *Environ. Sci. Technol*., 34,2979–2984.

Yu, S. (2003). Kinetics and modeling investigations of the anaerobic reductive dechlorination of chlorinated ethylenes using single and binary mixed cultures and silicon-based organic compounds as slow-release substrates. Ph.D. thesis, Oregon State University, Corvallis.

Yu, S., & Semprini, L. (2004). Kinetics and modeling of reductive dechlorination at high PCE and TCE concentrations. *Biotechnol. Bioeng.*, 88 (4), 451–464.